UNIVERSITY OF CALGARY

The Promotion of Peripheral Nerve Regeneration by PAR_2 Activation Following Induction of Acute Nerve Injury

by

Cathy Nguyen

A THESIS

SUBMITTED TO THE FACULTY OF GRADUATE STUDIES

IN PARTIAL FULFILMENT OF THE REQUIREMENTS FOR THE

DEGREE OF MASTER OF SCIENCE

DEPARTMENT OF MEDICAL SCIENCE

CALGARY, ALBERTA

JANUARY, 2007

UNIVERSITY OF
CALGARY

Abstract

The main finding of this study indicates that Proteinase Activated Receptor-2 (PAR_2) is pro-regenerative in the peripheral nervous system. Activation of PAR_2 at the site of injury with the PAR_2 activating peptide (PAR_2-AP), SLIGRL-NH_2, increased the rate of peripheral nerve regeneration, which was demonstrated by a faster recovery of neuronal functions (thermal nociception, mechanical nociception and muscle strength) and increased distal stump myelinated fibre calibre in wild-type (WT) mice. In PAR_2-deficient mice ($PAR_2^{-/-}$) mice with nerve crush injury, increased hyperalgesic responses showed the neuroprotective properties of PAR_2; however, in $PAR_2^{-/-}$ mice with nerve section injury, the rate of peripheral nerve regeneration was improved. PAR_2 was confirmed to mediate neurite outgrowth as media supplemented with SLIGRL-NH_2 increased neurite outgrowth in WT primary neurons whereas, media supplemented with PAR_2-AP outgrowth did not increase neurite outgrowth in $PAR_2^{-/-}$ primary neurons. In the presence of nerve growth factor (NGF), media supplemented with SLIGRL-NH_2 decreased the average neurite length of PC12 neuronal cells, indicating that PAR_2-induced neurite outgrowth was not mediated through a mechanism of direct activation on neuronal cells. Indeed, reverse transcriptase polymerase chain reaction (RT-PCR), immunohistochemistry, and immunocytochemistry have linked PAR_2 expression to Schwann cells. Furthermore, sciatic nerve conditioned media supplemented with NGF and SLIGRL did increase neurite outgrowth in PC12 cells, which suggests that PAR_2-induced neurite outgrowth is mediated through an indirect mechanism involving neuronal support cells.

First and foremost, I would like send my utmost gratitude to my supervisor Dr. Nathalie Vergnolle. As her first graduate student, I have not only learned many lessons in science, but I have also learned many lessons in life. I truly could not ask for much more in a supervisor. Her ability to grant me freedom alongside her guidance has taught me invaluable skills that I will use no matter where life takes me. She has shown me the importance of asking the right questions, believing in yourself, and using unexpected outcomes to your advantage. Her passion for science and love of her career has shown me the importance and advantages of loving your work.

I would like to thank my committee members, Dr. Morley D. Hollenberg and Dr. Doug W. Zochodne for their time, support, kindness, and advice. A student's work is always easier when wiser scholars believe in it too.

I would like to thank Dr. Valentine Brussee and Dr. M. D'Andrea for their scientific contributions to the study.

I would like to thank all of the past and present lab members of the Vergnolle lab for their advice, their assistance, and their antics. You all have made my time in the lab quite memorable. A special thank you goes to my two favourite lab technicians Kevin Chapman and Laurie Cellars.

I would like to thank my family and friends for their support, their patience, and their comfort, especially, my sister, who kept me company and fed while writing my thesis.

Finally, I would like to thank my love, MDP. Your strength has made every step easier. Your laughter has kept my spirits high. Your belief in me has kept my goals in sight.

To My Parents,

For their example of hard work and perseverance has inspired me to strive for my own dreams.

Table of Contents

List of Tables

List of Figures and Illustrations

List of Symbols, Abbreviations and Nomenclature

Symbol	Definition
ABC	Avidin: Biotinylated enzyme Complex
ANOVA	Analysis of Variance
BDNF	Brain-Derived Neurotrophic Factor
BSA	Bovine Serum Albumin
Ca^{2+}	Calcium
cDNA	Complementary Deoxyribonucleic Acid
CGRP	Calcitonin Gene-Related Peptide
CM	Conditioned Media
CNS	Central Nervous System
CNTF	Ciliary Neurotrophic Factor
DAB	3,3'-diaminobenzidine
DAG	Diacylglycerol
DEPC	Diethyl Pyrocarbonate
DMEM	Dulbecco's Modified Eagle's Medium
dNTP	Deoxynucleotide Triphosphate
DRG	Dorsal Root Ganglion
ERK	Extracellular Signal Related Kinase
ERK1/2	Extracellular Signal-Regulated Kinase ½
FBS	Fetal Bovine Serum
GADPH	Glyceraldehyde-3-phosphate dehydrogenase

GFAP	Glial Fibrillary Acidic Protein
GPCRs	Guanine Nucleotide-Binding Protein-Coupled Receptor
HBSS	Hank’s Buffered Saline Solution
HBSS	Hank’s Balanced Salt Solution
HIV	Human Immunodeficiency Virus
HUVECs	Human Umbilical Vein Endothelial Cells
i.m.	Intramuscular
IGF	Insulin-like Growth Factor
IL-1	Interleukin-1
IL-6	Interleukin-6
IP3	Inositol Triphosphate
MAPK	Mitogen-Activated Protein Kinase
MEK	ERK kinase
mRNA	Messenger Ribonucleic Acid
MSM	Muscle Strength Meter
NGF	Nerve Growth Factor
NK1	Neurokinin Receptor 1
NT-3	Neurotrophin-3
NT-4/5	Neurotrophin-4/5
NT-6	Neurotrophin-6
PAR-AP	Proteinase Activated Receptor-Activating Peptide
PARs	Proteinase Activated Receptor
PBS	Phosphate Buffered Saline

PC12	Rat Pheochromocytoma cell line
PKC	Protein Kinase C
PLCβ	Phospholipase C
PNS	Peripheral Nervous System
RT-PCR	Reverse Transcriptase Polymerase Chain Reaction
RNA	Ribonucleic Acid
RSK	Ribosomal Protein S6 Kinase
SCs	Schwann Cells
SNCM	Sciatic Nerve Conditioned Media
SEM	Standard Error of the Means
SP	Substance P
TNFα	Tumour Necrosis Factor α
trkA	Tyrosine Receptor Kinase A
trkB	Tyrosine Receptor Kinase B
trkC	Tyrosine Receptor Kinase C
WD	Wallerian Degeneration
WT	Wild-type

Epigraph

Science may set limits to knowledge,

but should not set limits to imagination.

Bertrand Russell (1872-1970)

Chapter One: **General Introduction**

According to the 2005 Canadian National Trauma Registry Report, nerve and spinal cord injuries are relatively frequent in patients entering the emergency room. Between the 2003-2004 year period, 539 Canadians were afflicted by nerve or spinal cord injuries, resulting in a total of 6.3% emergency room trauma patients each year [1]. By increasing the research and funding into studying nerve injury and repair, the costly burden of nerve injury treatment and rehabilitation may be alleviated.

The intricate relationship between nerves and their target organs complicate the efficiency and effectiveness of repair and regeneration. The outcome of peripheral nerve repair is not only influenced by the nature, location and degree of the injury, it is also affected by the level of repair and the timing between nerve injury and repair [2]. Presently, surgical nerve repair, which is aimed at directing the regenerating nerves into the proximity of the distal nerve stump, is the most commonly used technique for facilitating peripheral nerve repair. By bringing the severed ends into close proximity with one another, surgical repair simply reconnects the detached ends of the connective tissue thus, reinstating the appropriate anatomical environment for optimal regeneration [2]. Although current surgical repair, which incorporates advanced microsurgical techniques, is quite progressive from procedures developed in the early 20^{th} century; its shortcomings are attributable to the lack of cellular repair and neurite induction at the cellular level. As successful peripheral nerve repair is dependent on the proximal axon fibres making appropriate connections with the distal target organs, this study has been

implemented to investigate the potential role of PAR_2 activation in the promotion of peripheral nerve regeneration at the cellular level.

1.1 Types of Peripheral Nerve Injury

The 3 main categories of nerve fibre injury include neurapraxia, axonotmesis, and neurotmesis (Figure 1-1) [3-5]. The mildest form of nerve injury is classified as neuropraxia. It is described as an acute insult to the peripheral nerve resulting in an interruption of impulse transmission continuity between the neuron and the target organ. Upon clinical evaluation, partial function may be noted, but sensory and motor deficits will be apparent in the region that is innervated by the injured nerve. Histologically, evaluation of the tissue reveals only minor morphologic alterations that are of a reversible nature, and recovery is accomplished with conservative therapy. Possible causes of neurapraxia include microvascular alteration resulting in transient ischemia, concussion/shock-like injury to the fibre brought about by blunt trauma, mild compression or axon demyelination.

If there is physical disruption of one or more axons without injury to the stromal tissue, the injury is classified as axonotmesis, the second degree of nerve injury. In this type of injury, the axoplasm and cell membranes are damaged; however, the Schwann cell and connective tissue elements are conserved. Here, clinical evaluation will show evident functional deficits in the areas that are innervated by the damaged axons. The loss of sensory and motor function will be dependent upon the number and type of injured axons. Diagnosis for recovery will vary depending on the degree of lesion severity and

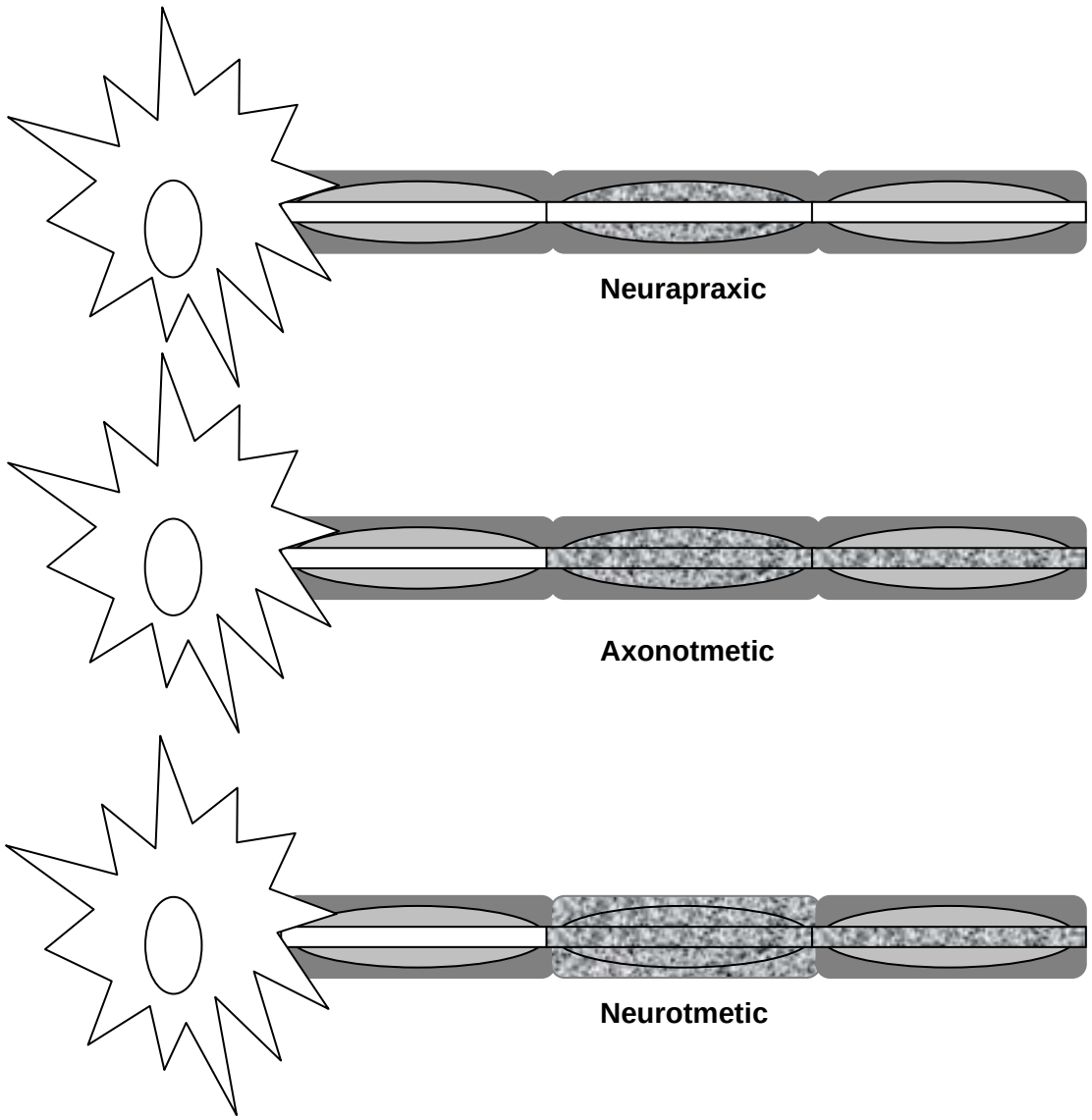

Figure 1-1. Three Categories of Nerve Injury

The 3 categories of nerve injuries, neurapraxia, axonotmesis, and neurotomesis were described by Seddon [3]. The speckled regions represent the areas afflicted by injury.

the evaluation of clinical and diagnostic outcomes. This type of injury is similar to the experimental model of the nerve crush [6].

The last class of peripheral nerve injury is termed neurotmesis and refers to the complete severance of the peripheral nerve trunk, which includes both the axon and the surrounding stromal tissue. Sensory and motor innervation to all autonomous branches of the injured nerve is lost, which results in complete loss of clinical function. This type of injury is similar to the experimental model of the nerve transection [6].

1.2 Peripheral Nerve Regeneration

The first step towards regeneration begins with the degenerative phase commonly known as Wallerian Degeneration (WD) (Figure 1-2). Following axonotomesis or neurotmesis, the nerve segment distal to the lesion site undergoes WD, a process characterized by the activation of peripheral oligodendrocytes, or Schwann cells (SCs), and the inflammatory cells, namely the macrophages [7]. Within 24 hours of injury, SCs present signs of nucleus and cytoplasm enlargement in addition to, an amplification of their mitotic rate. Macrophages appear on site by passing through capillary walls, which have become permeable from the trauma [8]. SCs and macrophages then work together to phagocytose and clear the axonal and myelin debris. Both cell types also secrete growth and mitogenic factors, which diffuse from the distal stump across the injury area to exert a trophic influence on the axons regenerating from the proximal stump[9-11]. Additionally, SC proliferation in the distal stump provides the sprouting axons with a guide to the target site thereby producing and directing reinnervation [12]. At the proximal end of the

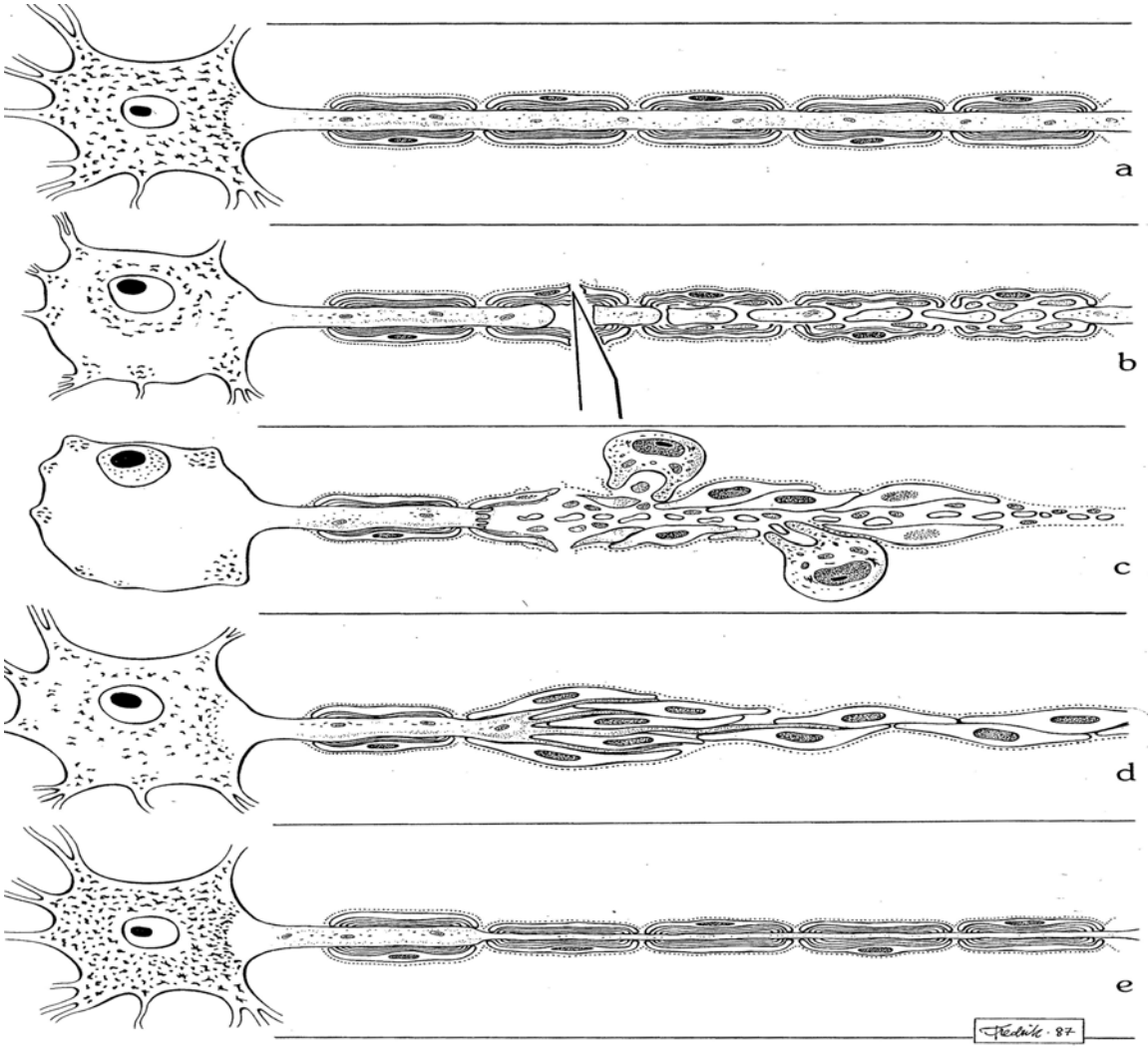

Figure 1-2. Wallerian Degeneration Divided Into Five Stages

a) Un-injured state, b) Axotomy accompanied by distal fragmentation of axon and myelin and swelling of the cell body, c) Proliferation of SC in the distal segment, phagocytosis of debris by both macrophages and SC, migration of the nucleus to the periphery, and chromatolysis, d) SC form continuous longitudinal columns along the basal lamina termed bands of Büngner, axonal sprouting and advancement of the axon proceed along the SCs toward the target organ for reinnervation, e) Axonal reinnervation with the periphery, restoration of the connective tissue, atrophy, and pruning of misdirected axonal sprouts, which do not reconnect to the periphery. (From Lundborg 1988. [4])

transected axon, the axons degenerate in a retrograde fashion to the first node of Ranvier. Following this short period of degeneration, the regenerative phase begins and the injured axon produces several neuronal sprouts [13], which will eventually form the growth cone. The growth cone responds to contact guidance cues and actively seeks a suitable matrix and environment to support the axonal growth [12, 14]. At the neuronal cell body, structural and functional changes occur, which include swelling of the cell body, displacement of the nucleus to the periphery, and disappearance of basophilic material from the cytoplasm, a process termed chromatolysis [15, 16]. Chromatolysis is a phenomenon that is attributed to the reorganization of the rough endoplasmic reticulum, which includes chemical changes in RNA and protein metabolism. These changes are aimed at halting the synaptic function of the neuron and increasing the regeneration potential of the neuron.

In the absence of nerve injury, it is now recognized that the neuronal cell body continues to rely on a supply of trophic factors from the peripheral target cells to maintain normal function. Studies have shown that a common trophic factor, nerve growth factor (NGF), is transmitted by retrograde axonal transport along the axon in low concentrations to sustain survival and essential activities of the nerve cell body [17-21]. Therefore, it is believed that the interruption of the trophic factor transport between the neuron cell bodies and the target organ is the basis for initiating chromatolysis following severe nerve injury [22]. Additionally, various neurotrophic factors have been found to be upregulated to avert cell death. Some of the neurotrophic factors that prevent cell death may include: NGF, brain derived neurotrophic factor (BDNF), neurotrophin-3,-4/5,-6

(NT-3, NT-4/5, NT-6), ciliary neurotrophic factor (CNTF), and insulin-like growth factor (IGF) [23-27].

1.3 Proteinase Activated Receptors (PARs)

Proteinase Activated Receptors (PARs) are a novel subclass of seven transmembrane domain G-protein coupled receptors (GPCRs) that are recognized for their roles in inflammation, pain, and tissue repair [28-33]. The discovery of the PAR family initially began with the search for a new thrombin receptor by using direct expression cloning in xenopus oocytes [34]. Thrombin induced responses found in the exogenous mRNA expressing oocytes led researchers to identify a functional human thrombin receptor, which had a thrombin cleavage site within the extracellular N-terminal of this receptor. Following its discovery on xenopus oocytes, the receptor was found to be endogenously expressed on both human platelets and endothelial cells. The discovery of this new receptor, led to the discovery of a novel sub-family of the seven transmembrane domain GPCR super-family; this new group of receptors was named the PAR family. To date, four PARs have been cloned and identified in this family, $PAR_{1,}$ PAR_2, PAR_3, and $PAR_{4.}$

1.4 Proteinase Activated Receptor-2 (PAR_2)

1.4.1 PAR_2 Discovery and Structure

Following the discovery of PAR_1 researchers revealed pharmacological evidence for the presence of other PAR receptor subtypes even prior to the cloning of PAR_2. In a 1993 study looking at the role of thrombin receptor derived polypeptides in different bioassay

systems, researchers found support for the existence of unique thrombin receptor subtypes. The evidence included specific differences in potency orders of thrombin receptor polypeptides in different bioassay systems, distinct intracellular signaling pathways activated by the thrombin receptor polypeptides in different tissues, and the selectivity of the Nleu-P6 peptide [35].

The successful cloning of PAR_2 shortly followed as a result of diligent investigation and screening of a mouse genomic library in search for novel GPCRs [36]. What researchers found was a sequence encoding a protein with 395 amino acids having a hydrophobicity plot revealing seven segments likely to span a membrane surface. Additional features found in this sequence included a hydrophobic amino-terminal likely representing a signal peptide, various amino acid resides generally conserved among GPCRs, two potential sites for extracellular N-linked glycosylation, and several prospective sites for phosphorylation.

How the researchers linked PAR_2 to the PAR_1 receptor entailed the careful analysis and comparison of protein sequences from the European Molecular Biology Laboratory database. When compared, the mouse PAR_2 clone sequence revealed a 30% likeness to the human thrombin receptor, and a 28% resemblance to the mouse thrombin receptor. However, there were dissimilarities in the PAR_2 sequence that uncovers its uniqueness in the PAR family. First, excluding the region where thrombin cleaves PAR_1, there is a lack of homology to the PAR_1 receptor in the N-terminal portion of the PAR_2 receptor. Second, the PAR_2 receptor does not contain the important acidic residues found in the

PAR_1 receptor that are perceived to mediate thrombin binding. Third, there is little analogy in the intracellular C-terminal sequence between the PAR_1 and PAR_2 receptors.

1.4.2 PAR_2 Activation and Signaling

The novelty of the PAR receptor family stems from their mode of activation through proteolytic cleavage by specific proteases. PAR activation (Figure 1-3) begins with proteolytic cleavage of the extracellular N-terminus by a protease. The newly exposed N-terminal tethered ligand domain then binds to specific conserved regions of the second extracellular loop resulting in intracellular signalling mediated by guanine nucleotide-binding proteins (G-proteins; subunits $\alpha\beta\gamma$). Additionally, PARs can be activated pharmacologically with the addition of synthetic hexapeptides (PAR-APs) specific to each PAR. Specifically, each PAR-AP consists of an approximate six amino acid sequence that resembles the amino acid sequence of the newly exposed N-terminus following proteolytic cleavage of their respective PAR.

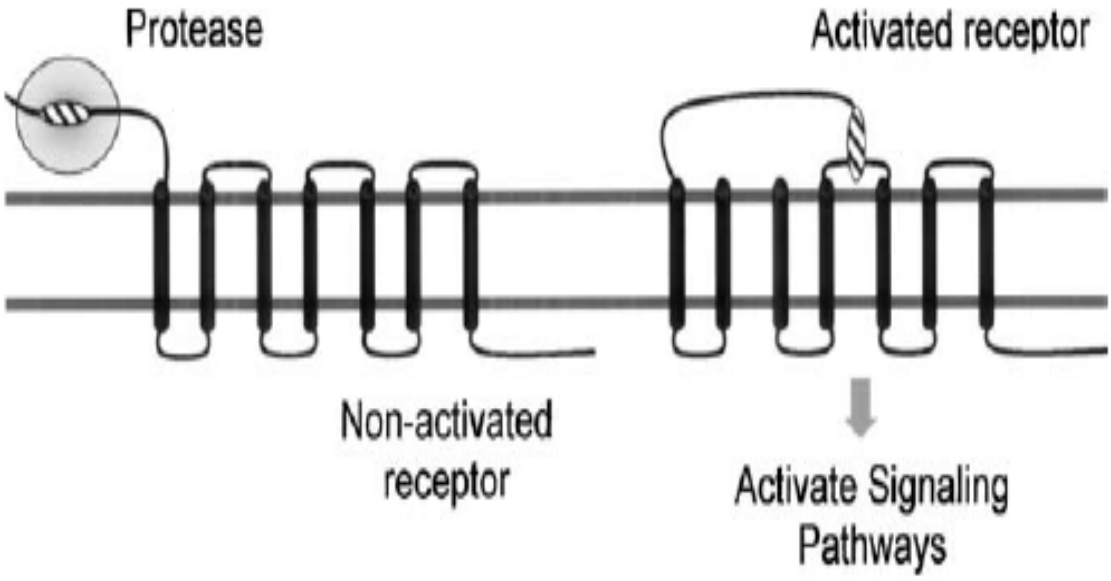

Figure 1-3. Schematic Diagram of PAR Activation

PAR activation begins with protease recognition of the cleavage sequences of the N-terminus of the receptor. Following recognition, the N-terminus is cleaved by the protease and newly revealed sequence self-binds to an extracellular site on the receptor. (From Barnes [37])

Similar to the other PAR family members, PAR_2 is a seven transmembrane G-protein coupled receptor that can be activated by proteases and synthetic peptides that resemble the tethered ligand post-cleavage. However, what makes PAR_2 unique is the fact that unlike the other PAR family members, PAR_2 cannot be activated by the coagulation protease thrombin. Instead, the tethered extracellular N-terminus contains a trypsin cleavage site between arginine^{34} and serine^{35}, SKGR^{34}↓S^{35}LIGR (Figure 1-4). Thus, the primary activators of PAR_2 include serine or serine-like proteases such as trypsin [36], mast cell tryptase [38], neutrophil proteinase 3 [39], tissue factor/factorVIIa/factor Xa [40], and membrane tethered serine protease-1 [41]. Additionally, as it was previously mentioned, its synthetic hexapeptide (PAR_2-AP) specific to its newly exposed tethered ligand post-cleavage is also capable of activating PAR_2 in the absence of proteolytic cleavage. In the case of the rodent, the synthetic hexapeptide has the amino acid sequence SLIGRL-NH_2, whereas the human hexapeptide has the amino acid sequence SLIGKV-NH_2. For a more complete list of PAR_2 agonists see Table 1.

Currently, the knowledge of intracellular signaling down stream from PAR_2 is quite limited. However, it is commonly accepted that PAR_2 activation increases intracellular calcium release and couples to $G_{\alpha q/11}$ (Figure 1-5) to activate phospholipase Cβ (PLCβ). This results in the cleavage of phosphatidylinositol 4,5-bisphosphate [$PI(4,5)P_2$] and leads to the production of 1,4,5-trisphosphate (IP_3) and 1,2-diacylglycerol (DAG) in a variety of cell types including myocytes [42], enterocytes [43] epithelial cells and endothelial cells [36]. Moreover, PAR_2 has also been linked to the extracellular signal-

regulated kinases 1 and 2 (ERK 1/2) cytoplasmic restricted pathway (Figure 1-5) through a β-arrestin-dependent mechanism mediated by protein kinase C (PKC) [44].

Table 1. PAR_2 Agonists

PAR_2 Agonist	Source	Reference
Brain derived trypsin-like protease (P22)	Brain	[45]
Der p3	Dust mite allergen	[46]
Der p9	Dust mite allergen	[46]
Gingipain-R	Porphyromonas gingivalis	[47]
Human Airway Trypsin-like Protease	Airway epithelial cells	[48]
Tryptase	Human mast cells	[38]
Membrane Tethered Serine Proteinase-1	High levels in GI tract, prostate; Low levels in kidney, liver, lung, and spleen	[41]
Human Kallikrein-6 (Neurosin)	Central Nervous System	[49, 50]
Neutrophil Proteinase 3	Activated neutrophils	[39]
Pancreatic Trypsin	Pancreatic acinar cells	[51]
Acrosin	Sperm	[52]
Coagulation Factor VIIa-Xa-Tissue Factor Complex	Circulatory system	[40]
Trypsin-II	Lung epithelium	[53]
Trypsin-IV	Nervous system, epithelial cells from the colon/lung/prostate	[54]
SLIGRL-NH_2, SLIGKV-NH_2	Rodent synthetic peptide Human synthetic peptide	[36]
Furoyl-LIGRLO-NH_2	Synthetic peptide	[55]

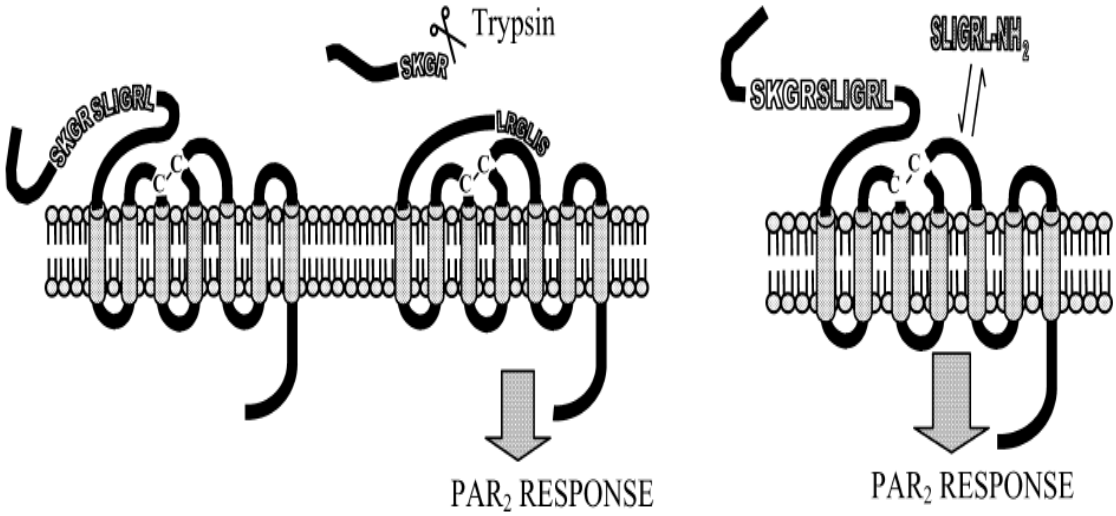

Figure 1-4. Schematic Diagram of PAR-2 Activation

This figure demonstrates the mechanism of PAR_2 activation. The far left receptor represents the PAR_2 receptor in an unactivated form. The centre receptor represents the activation of PAR_2 by the serine protease trypsin. The far right receptor represents the activation of the receptor with its synthetic peptide ligand, which resembles the amino acid sequence of the newly revealed ligand if the receptor was cleaved with trypsin. (From Hollenberg 2005. [56])

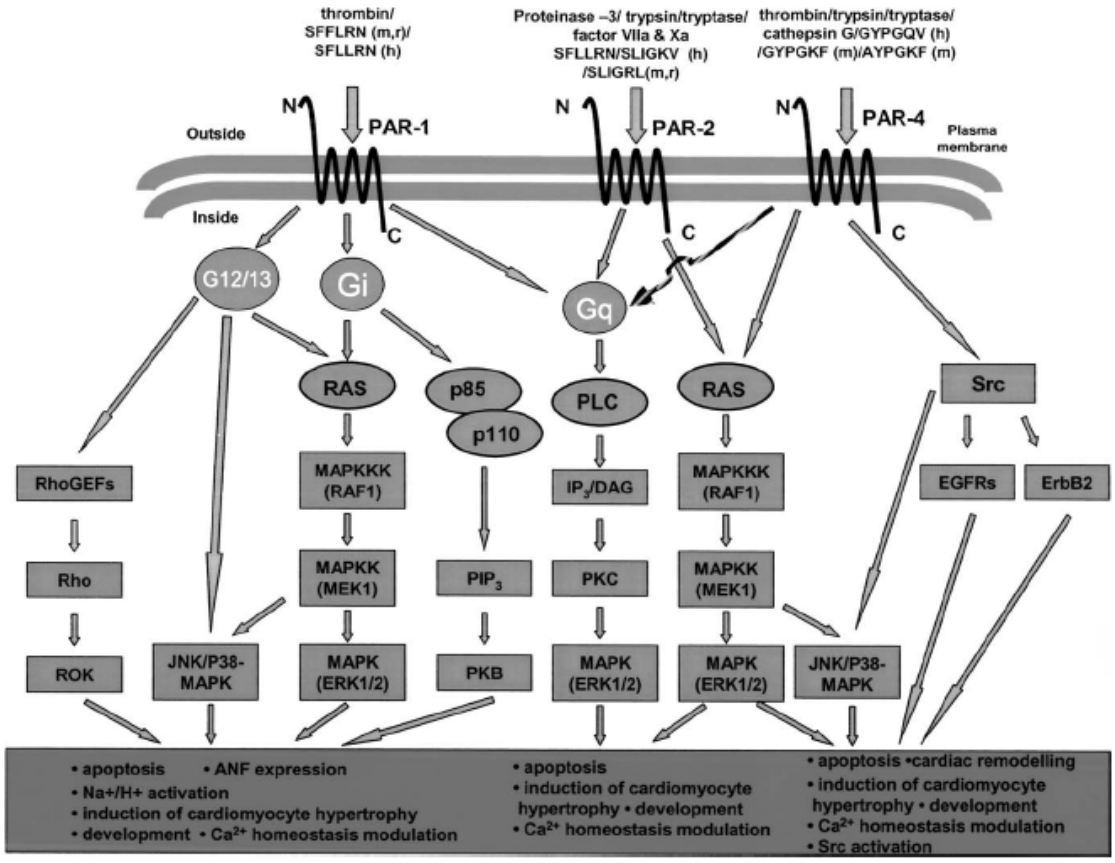

Figure 1-5. Intracellular signaling diagrams of PAR-1, PAR-2, and PAR-4

Little is still known about the intracellular signaling pathways involved downstream of PAR_2 activation. However, as seen in the above diagram, PAR_2 is suggested to couple with G_q to activate signaling pathways involving PLC, IP_3/DAG, PKC, RAS and ERK1/2. (From Barnes 2004. [37])

1.4.3 PAR_2 Distribution and Function

PAR_2 distribution in the different organ systems is quite astounding. It has been detected in the cardiovascular system in the heart [57], the male reproductive system in the prostate [57], the renal system including the kidney [57] and bladder [58], the digestive system including the pancreas, the colon, the small intestine [57] and the stomach [36], the respiratory system including the lung and trachea [57], the skin [59], and the central [60] and peripheral nervous systems [61].

Investigations of PAR_2 functionality in these various systems are still on going; however, to date, the role of PAR_2 is largely prominent in the area of inflammation. The first evidence linking PAR_2 and inflammation was in 1996. Using human umbilical vein endothelial derived cells (HUVECs), investigators found that PAR_2 expression was elevated in a dose-dependent manner when stimulated with the two inflammatory cytokines tumour necrosis factor alpha (TNFα) or interleukin-1 (IL-1) [62]. Additionally, this dose-dependent up-regulation of PAR_2 was also observed when stimulated with bacterial lipopolysaccharide isolated from gram-negative bacteria. These results suggest a role of PAR_2 in the development of acute inflammatory responses, but it was in 1999 that the effects of PAR_2 activation on inflammatory parameters were defined.

Researchers explored the effects of PAR_2 activation in leukocyte rolling, and adhesion, which are steps required for the recruitment of inflammatory cells. Evidence from this study suggested a major role for PAR_2 activation in the early events of the inflammatory reaction, which include leukocyte recruitment [63]. Additional studies have documented

a role for PAR_2 in tissue oedema [64], granulocyte infiltration [64, 65], vascular permeability [66], and vessel relaxation [67]. What is interesting and of particular importance to this study is the fact that several of the pro-inflammatory effects mediated by PAR_2 are dependent on a neurogenic mechanism [61, 68], which opens that gate to the possibilities of PAR_2's role in the nervous system. Thus, a more extensive discussion of PAR_2's role in the nervous system will follow.

1.4.4 PAR_2 in the Central Nervous System (CNS)

In the CNS, the PAR_2 protein has been identified in the rodent hippocampus, cortex, amygdala, thalamus, hypothalamus, and striatum [69]. In a study done by Smith-Swintosky [60], it was suggested that PAR_2 had a neurotoxic effect in the CNS. Exposure of hippocampal cultures to the PAR_2 activating peptide, SLIGRL (> 100μM) caused a concentration-dependent decrease in neuron survival, which correlated with significant increases in Ca^{2+}. Interestingly, independent studies have demonstrated that sustained increases in $[Ca^{2+}]$ can be lethal to neural cells [70, 71].

Conversely, PAR_2 has also been reported to be involved in CNS neuroprotection. In a study looking at PAR_2, neuroinflammation and HIV-1-associated dementia [72], it was observed that up-regulated expression of PAR_2 coincided with the occurrence of neuroinflammation in the brain tissue of HIV-1-associated dementia patients. However, it was discovered that this enhanced PAR-2 expression and subsequent activation prevented neuronal cell death and induction of the tumour suppressor, p53, caused by the HIV-

encoded protein, Tat. Furthermore, $PAR_2^{(-/-)}$ deficient animals showed more severe neuroinflammation and neuronal loss caused by Tat neurotoxicity.

1.4.5 PAR_2 in the Peripheral Nervous System (PNS)

In the PNS, PAR_2 has been detected on rodent primary spinal afferents [61] and guinea pig myenteric and submucosal neurons [73, 74]. Physiologically, PAR_2 has been linked to inflammation [61, 68, 75], and hyperalgesia [76, 77]. In 2000, it was revealed that the PAR_2 protein co-expressed on primary spinal afferents with the inflammatory neuropeptides calcitonin gene related peptide (CGRP) and substance P (SP) [61]. In fact, it was shown that in the presence of trypsin or tryptase, PAR_2 activation on dorsal horn slices could stimulate the release of the inflammatory peptides CGRP and SP from the central and peripheral projections of spinal afferent neurons in a Ca^{2+}-dependent manner. This same study demonstrated that intraplantar injection of the PAR_2-AP results in a markedly significant increase in paw oedema, an oedema that has been attributed to a neurogenic mechanism. Specifically, a significant reduction of PAR_2-induced paw oedema was observed in animals with capsaicin ablated spinal afferent C-fibres. There was also a marked decrease in PAR_2-induced paw oedema when the animals were pre-treated with either the CGRP-1 receptor antagonist or the NK1 antagonist, SR140333 [61]

Similar results have been observed in the rodent colon. In 2002, PAR_2 activation was discovered to induce colonic inflammation following intracolonic administration of the PAR_2-AP [75], but at this point the mechanism by which inflammation was induced in

the colon was still unknown. PAR_2 had already been immunolocalized on rat primary sensory afferent neurons, and its activation is known to cause the release of neuropeptides [61]. Therefore we hypothesized that PAR_2 agonists administered intracolonically in mice induces inflammation through a neurogenic mechanism. Using CGRP and neurokinin-1 antagonists and capsaicin, PAR_2-agonist-induced colitis was alleviated; thus, inferring that PAR_2-agonist-induced intestinal inflammation involves the release of inflammatory neuropeptides [68].

Further studies have examined the involvement of PAR_2 activation in pain and nociception. In a 2001 peripheral nociceptive study, it was revealed that intraplantar injection of the PAR_2 agonist, at sub-inflammatory doses, stimulated nociceptive neurons and resulted in hyperalgesic responses [76]. A significant increase in Fos expression was detected in the spinal cord dorsal horn at the L4/L5 level in the laminae I and II areas, which indicates activity in nociceptive neurons. In a separate study looking at PAR_2-induced visceral hypersensitivity, it was found that intracolonic infusion of the PAR_2 agonists at sub-inflammatory doses could activate spinal afferent neurons. Furthermore, activation of these neurons were found to produce a delayed rectal hyperalgesia involving the activation of NK1 receptors [77].

Up until this point little has been known about PAR_2 activation and direct afferent impulse generation. However, in a 2002 study looking at the sensitivity of jejunal afferent nerves to the PAR_2-AP, SLIGRL-NH_2 [78], it was discovered that intravenous administration of SLIGRL-NH_2 evokes complex activation of predominantly spinally

projecting extrinsic intestinal afferent nerves, which involves both direct and indirect mechanisms.

1.5 Hypothesis

The presence of PAR_2 on sensory afferents nerves and the involvement of PAR_2 in nociception and inflammation led to the hypothesis that PAR_2 activation may modulate other nerve functions. Because inflammatory cells and inflammatory mediators are known to contribute to neuronal survival and axonal regeneration after injury [6, 79-82], the goal of this study is to investigate the role of PAR_2 activation following peripheral nerve injury with a direct focus on peripheral nerve regeneration and/or degeneration.

Thus, it is our hypothesis that **PAR_2 activation promotes peripheral nerve regeneration and neuronal repair following nerve injury.**

1.6 Specific Aims and Objectives

While the pharmacology of PAR_2 has been well established, no study has explored the role of PAR_2 in peripheral nerve regeneration. Thus, the objective of this study is to identify the possible role of PAR_2 activation in peripheral nerve regeneration or degeneration with the following aims:

I. Use behavioural nociceptive techniques in wild-type mice and $PAR_2^{(-/-)}$ deficient mice to study the role of local *in vivo* PAR_2 activation and peripheral nerve

recovery in two different models of sciatic nerve injury, the sciatic nerve crush model and the sciatic nerve transection model.

II. Use morphometrical evaluation in wild-type mice to examine the effects of local *in vivo* PAR_2 activation and peripheral nerve recovery in the sciatic nerve crush model

III. Isolate and use a primary neuronal culture isolated from the dorsal root ganglion of wild-type and PAR_2 deficient mice to examine the role of PAR_2 activation and nerve regeneration/degeneration *in vitro*.

IV. Use reverse transcriptase polymerase chain reaction (RT-PCR), calcium signaling, and immunocytochemistry techniques to characterize the PC12 cell line a cell line commonly used to study nerve regeneration, with respect to PAR_2 presence and distribution.

V. Use the PC12 cell line to study the effects of PAR_2 activation and neurite outgrowth in the absence of other cell types.

VI. Isolate a primary Schwann cell culture and probe for PAR_2 expression using RT-PCR and immunocytochemistry techniques.

VII. Use the PC12 cell line as a neurite outgrowth indicator cell line to study the effects of PAR_2 activation on PNS support cells.

Chapter Two: **Experimental Procedures**

2.1 Animals

Male C57Bl6 mice 4-6 weeks old were obtained from Charles River Laboratories (Montreal, QC, Canada). Four to six week old PAR_2-deficient ($PAR_2^{-/-}$) mice and their wild-type littermates ($PAR_2^{+/+}$) originally obtained from Johnson and Johnson Pharmaceutical Research Institute (Spring House, PA), were bred at the University of Calgary Animal Resource Centre breeding facility. Animals were contained in transparent plastic cages with bedding and housed in a temperature controlled room at the University of Calgary Animal Resource Centre. Animals were exposed to a 12hr light/12hr dark cycle, fed standard laboratory chow, and tap water *ad libitum*. All experiments performed have been approved by the Animal Care Committee of the University of Calgary and have been performed in accordance with the Canadian Council on Animal Care guidelines.

2.2 Nerve Injury Models

2.2.1 Sciatic Nerve Crush

Mice were anesthetized with a ketalean/xylazine mixture (ketalean 1.6 mL of 100mg/mL, xylazine 0.08mL of 100 mg/mL, saline 2.32mL) injected i.p. at a dose of 0.1mL/25g. Under anaesthetic, the right sciatic nerve was exposed at the mid-thigh level by blunt dissection. The nerve crush was completed by pinching the nerve approximately 10 mm proximal to the knee joint with jeweller's forceps for 2 ×10 seconds. Following the

sciatic nerve crush, the muscle was loosely sutured with dissolvable vicryl thread and the skin was sutured with silk thread.

2.2.2 Sciatic Nerve Transection

Under a ketalean/xylazine anesthetic mentioned above, the right sciatic nerve was exposed at the mid-thigh level by blunt dissection. The right sciatic nerve was exposed and completely transected with fine surgical scissors approximately 10 mm proximal to the knee joint. After nerve section, the muscle was loosely sutured with dissolvable vicryl thread and the skin was sutured with silk thread.

2.3 Peptide Dose and Evaluation of Peripheral Nerve Injury and Regeneration

2.3.1 Peptide Dose

Following surgery animals were treated daily with the PAR_2 activating peptide (PAR_2-AP): SLIGRL-NH_2, the reverse peptide: LRGILS-NH_2, or the vehicle control: saline. A sub-inflammatory dose of the PAR_2-AP (1ng/50µL/animal) was injected daily intramuscularly (i.m.) at the site of the nerve injury for the duration of the study. The SLIGRL-NH_2 and LRGILS-NH_2 peptides were synthesized and obtained from the Peptide Synthesis Facility, University of Calgary.

2.3.2 Thermal Nociception

Thermal nociception was used as one of the indicators for measuring peripheral nerve regeneration. Thermal nociception was measured in withdrawal latency. Withdrawal

latency was based on the time (seconds) it takes for the animal to feel the heat stimulus and withdrawal its hind limb from the stimulus. Recovery of thermal sensation was defined as a return of withdrawal latency values post-surgery comparable to baseline values.

Prior to the induction of the peripheral nerve injury, the mice were assessed for nociceptive responses to a thermal stimulus using a plantar test apparatus (Stoelting, Chicago, Illinois, USA). Each mouse was placed individually on a clear glass floor and contained under an inverted clear plastic testing cup. Each animal was allowed to acclimatize to the new environment for 5 minutes. A source of radiant heat was then placed underneath the floor of the testing box, directly below the mouse's right hind paw. The withdrawal reflex latency of the right hind paw was measured in seconds by means of a timer connected to the heat source. The testing box was thoroughly cleaned between each animal. Following training, initial readings were taken to establish a comparable baseline. Five readings were recorded for each animal with a 5 minute rest time between each reading. One week following the sciatic nerve crush or transection, paw withdrawal latency to the radiant heat stimulus was measured weekly using the plantar test apparatus (Stoelting, Chicago, Illinois, USA) for a period of 4 weeks and 12 weeks respectively.

2.3.3 Mechanical Nociception

Mechanical nociception was the second parameter used for measuring peripheral nerve regeneration. Mechanical nociception was evaluated using the von Frey filament test. The von Frey filament test measures the response to mechanical stimuli using a series of

different filament sizes. When applied correctly to the hind paw, each filament size delivers a specific stroke pressure to the plantar surface depending on the filament size. The 3 different von Frey filament sizes used thinnest to thickest were 3.61, 3.84, and 4.08, which corresponded to 3 different applied forces, 0.4g, 0.6g, and 1.0g.

Prior to the induction of peripheral nerve injury, mice were assessed for cutaneous sensitivity to mechanical stimuli using the von Frey filament test. Each mouse was placed individually on a plastic grid floor and contained under an inverted clear plastic testing cup. Each animal was allowed to acclimatize to the new environment for 5 minutes. Three von Frey filaments with marking forces of 0.4g, 0.6g, and 1.0g were applied onto right hind plantar in sequential order of size. The filaments were applied three times and a score out of a possible total of 6 was assigned based on the animal's response: 0 = no movement, 1 = removal of the paw; 2 = removal of the paw and licking or holding of the paw. The nociceptive score was totalled from the three applications and expressed as a percentage of maximal response with the lowest score 0 = 0% and the highest score 6 = 100%. One week following sciatic nerve crush or transection, response to mechanical stimuli was measured weekly using the von Frey filaments for a period of 4 weeks and 12 weeks respectively. Recovery of cutaneous sensitivity to mechanical stimuli was defined as a return of nociceptive score values post-injury comparable to basal values.

2.3.4 Muscle Strength

Prior to the induction of peripheral nerve injury, mice motor nerve function was evaluated using the muscle strength meter (MSM), which measures the maximal force applied by the animal's right hind paw before releasing the bar. Each animal was thoroughly trained and handled prior to recording the baseline readings, in order to obtain a reliable and consistent reading. The animal was manually positioned to face the handle of the MSM. The left hind leg was restrained by the experimenter and the right hind limb was left to freely grip the MSM. As the unrestrained hind paw was brought into contact with the handle, the reflex of the animal is to grip the bar. Once the bar is gripped, the animal is then gently pulled away from the device and the reading is recorded. Three complete grip attempts were recorded and the average of the three attempts was used to establish a baseline. One week following sciatic nerve crush or transection, motor nerve function was measured weekly using the MSM for a period of 4 weeks and 12 weeks respectively. Recovery of motor nerve function was defined as a return of grip force values post injury, comparable to basal values.

2.3.5 Evaluation of Nerve Fibre Morphology Using Epon Embedded Sciatic Nerve Tissues

Four weeks after sciatic nerve crush, Dr. Valentine Brussee harvested the proximal and distal stumps of the sciatic nerves from PAR_2 agonist-treated group and the control peptide-treated group. Tissue was fixed overnight with 2.5% glutaraldehyde in 0.025 M cacodylate buffer. Following the overnight incubation, tissue was washed in 0.15M cacodylate buffer, postfixed with osmium tetroxide (2% in 0.12 M cacodylate),

dehydrated in alcohol, and then embedded in epon resin. Sciatic nerve segments were sectioned into 1 μm thick slices using an ultra microtome and stained with 0.5% toludine blue for visualization.

Myelinated calibre area (μm^2) was measured in proximal and distal sciatic nerve sections in both groups using a Zeiss Axioskop. Axonal calibre was measured on the surface area of the transverse face of the axon and did not include the myelin profile.

A total of 20 axons from each field were measured for axonal calibre, 15 large axons and 5 small. Large and small axonal calibre means were combined for each sample. For each sample, a minimum of five fields were imaged; however, six or more fields were counted for most samples. The five best fields, which contained minimal or no artifact were used for analysis. Samples were counted twice and all imaging and counting was done blinded.

2.3.6 Evaluation of PAR_2 Expression in Proximal and Distal Stumps Following Sciatic Nerve Crush

Four weeks after sciatic nerve crush, tissue samples were sent to Dr. M. D'Andrea from Johnson & Johnson to be processed for PAR_2 expression. Both proximal and distal stumps were evaluated for PAR_2 expression using fluorescent immunohistochemistry, in conjunction with the S-100 Schwann cell marker, the GFAP activated Schwann Cell Marker, and MAC-3 macrophage marker.

2.4 Primary Neuron, and PC12 Cell Culture and Maintenance

2.4.1 Isolation and Culture of Neurons from Mouse Dorsal Root Ganglion

Animals were humanely euthanized with an overdose of Euthanyl. DRG from thoracic and lumbar spinal cord of mice were isolated and minced in cold sterile HBSS and incubated for 60–90 min at 37°C in DMEM containing: 0.5mg/mL trypsin, 1mg/mL collagenase type IA, and 0.1mg/mL DNase type IV (Sigma, St. Louis,MO). Following incubation, soybean trypsin inhibitor (SBTI) (Sigma) was added to neutralize the enzymatic activity of the trypsin. Neurons were then centrifuged (10 minutes; 1000 rpm), the supernatant was removed and the pellet was resuspended in DMEM containing 10% fetal bovine serum, 10% horse serum, 100 U/ml penicillin, 0.1 mg/ml streptomycin, 2mM glutamine, and 2.5g/ml DNase type IV, and was plated on 35mm Petri dishes coated with collagen for 2–3days.

2.4.2 PC12 Cell Growth and Maintenance

PC12 cells obtained from ATCC® were maintained at 37^{o}C, 95% O_2, 5% CO_2, in Ham's F12K medium with 2 mM L-glutamine adjusted to contain 1.5 g/L sodium bicarbonate, 82.5%; horse serum, 15%; fetal bovine serum, 2.5%. Cells were sub-cultivated at a 1:4 ratio every 3-4 days.

2.5 Schwann Cell Isolation, Purification, and Culture

Left and right sciatic nerves removed from sacrificed animals were collected and placed in ice cold PBS. The thick vascular ectoneurium, rich in fibroblasts, vascular smooth

muscle and endothelial cells, was removed using a dissecting microscope and the remaining tissue was rinsed with sterile PBS. Tissue was then transferred to another Petri dish containing Ham's F10 media (2mL) supplemented with antibiotics (1% penicillin-streptomycin) and 1mL collagenase dissolved in Ham's F10 media (10mg collagenase /1mL Ham's F10 media). The plates were incubated for 90 minutes at $37^oC/O_2/CO_2$. Following incubation with collagenase, a trypsin solution (1mL; 150mg Trypsin, 15mg DNAse, 15mL PBS supplemented with Mg^{2+} (0.5 $MgSO_4$ in 100mL PBS), 90μL of 1M NaOH) was added to the Petri plates and incubated for another 7 minutes. Cells were then centrifuged at 150g for 3 minutes at 4^oC and the supernatant was removed. DNAse/DMEM (2mL; 7.5mg DNAse, 15mL DMEM) was added to the pellet and the solution was further disrupted by sending it through a sterile syringe with a 25G needle two times. After the last passage through the syringe, DMEM/10% FBS was added and the cells were centrifuged at 150g for 10 minutes at 4^oC. Again the supernatant was removed and the pellet was resuspended in 10mL DMEM/10%FBS and plated on T-75 flasks and incubated at $37^oC/O_2/CO_2$.

Once the Schwann cells reach confluence, they were washed three times with PBS and then lifted with 3mL of Versene (Gibco). Once the cells were in suspension, DMEM/10%FBS (9mL) was added to the flasks, the cells were transfer to a conical tube and centrifuged at 150g for 10 minutes at 4^oC. The supernatant was removed, the pellet was resuspended with anti-Thy 1.1 (1mL), which is an antibody against an antigen found on fibroblasts, and incubated on ice for 1 hour. Following incubation, the cells were centrifuged at 150g for 10 minutes at 4^oC, and the unbound antibody was removed by

replacing the medium containing the antibody with 3mL of DMEM media containing 1mL of complement for 1 hour at 37^{o}C. Subsequently, the complement was diluted with 10mL of DMEM and then centrifuged at 150g for 5 minutes at 4^{o}C. The media was replaced with new DMEM and centrifuged again. The washes were repeated for a total of 3 cycles. At the end of the washes the cells were resuspended in fresh DMEM, 10% FBS, plated on T-75 cell culture treated flasks and grown until confluence.

2.6 Detection of PAR_2 mRNA in PC12 Cells and Schwann Cells Using RT-PCR

2.6.1 RNA isolation

Cells grown to confluency on T-75 cell culture treated flasks were lysed with 3mLs of Trizol reagent, and scraped from the flasks. The homogenized samples were transferred to conical tubes, and incubated for 5 minutes at 15 to 30°C. Chloroform was then added to the samples (0.2 ml of chloroform / 1 ml of TRIZOL Reagent) and the tubes were manually shaken for 15 seconds. Cells were let to sit at room temperature for 2 to 3 minutes and then spun at 10,000 x g for 15 minutes at 2 to 8°C. Following centrifugation, the mixture is separated into a lower red, phenol-chloroform phase, an interphase, and a colorless, upper, RNA containing, aqueous phase. The aqueous phase is transferred to a fresh tube and the RNA is precipitated by mixing in isopropyl alcohol (0.5 ml of isopropyl alcohol per 1 ml of TRIZOL Reagent used for the initial homogenization) at room temperature for 10 minutes. Following incubation, the RNA is collected into a pellet by centrifuging the tubes at 10,000 × g for 10 minutes at 2 to 8°C. The supernatant was removed, and the RNA pellet was washed with 75% ethanol (1mL 75% ethanol per

1mL initial TRIZOL Reagent used for the initial homogenization). The samples were centrifuged again at 7,000 × g for 5 minutes at 2 to 8°C, the ethanol was removed, the RNA pellet was air-dried and the pellet was resuspended in RNase-free water.

2.6.2 cDNA Synthesis from mRNA using Reverse Transcriptase (RT)

The mRNA concentration of each sample was quantified with a spectrophotometer calibrated to detect RNA absorbance. Samples were diluted with DEPC H2O (1:50) and quantified against a standard containing only DEPC H2O. Final RNA concentrations were used to synthesize cDNA.

For the reverse transcriptase reaction, which uses the RNA samples as a template to synthesize cDNA, the following items were combined: 1µL superscript RT, 1µL RNAse inhibitor, 2µL deoxynucleoside triphosphate dNTP (10µM), 2µL N_6 random hexamers, 2µL TE buffer (0.1X), 1µL RNA. RNA samples were heat cycled using a DNA Engine Thermal Cycler (MJ Research, Waltham, MA). First, samples were incubated at room temperature for 10 minutes, the reaction mixture was then heated to 42°C for 50 min and then to 95°C at 10 minutes to denature the Superscript enzyme. cDNA obtained from this reaction was then cooled to 4°C and stored at –20°C until use.

2.6.3 Polymerase Chain Reaction (PCR)

The PCR was performed on the cDNA with a DNA Engine Thermal Cycler (MJ Research, Waltham, MA). The reaction mixture contained 5µl of 10x PCR buffer, 2µl of 2mM dNTP, 2 µl of each of the 5' and 3' primers, 38 µl of DEP-treated H_2O, 2 µl of the cDNA template, and 0.5 µl of HotStartTaq DNA polymerase.

The primer sequences used for PAR_2 amplification in the rat PC12 cells were a follows:

Forward Primer: GGG ACA TGT TCA GTT ACT TCC TCT

Reverse Primer: ATA TCC TCA GAC CCA GCT CAG TAG

The final product size was expected to be 502bp.

The primer sequences used for PAR_2 amplification in the mouse Schwann cells were as follows:

Forward Primer: CAA GGT GCT CAT TGG CTT TT

Reverse Primer: CAG AGG GCG ACA AGG TAG AG

The final product size was expected to be 549bp.

The primer sequences used for NGF amplification in the mouse Schwann cells were a follows:

Forward Primer: AGC TTT CTA TAC TGG

Reverse Primer: TATCTCCAACCCACACACTGAC

The final product size was expected to be 480bp.

The primer sequences used for GADPH amplification in both the mouse Schwann cells and the rat PC12 cells were as follows:

Forward Primer: CGG AGT CAA CGG ATT TGG TCG TAT

Reverse Primer: AGC CTT CTC CAT GGT GGT GAA GAC

The final product size was expected to be 306bp.

The PAR_2 PCR for the rat PC12 cells was stopped after 32 cycles (denaturation for 1 minute at 95^{o}C, annealing for 30 seconds at 54^{o}C, and elongation for 1 minute at 72^{o}C). The GADPH PCR for the rat PC12 cells was performed under the same conditions.

The PAR_2 PCR for the mouse Schwann cells was stopped after 32 cycles (denaturation for 1 minute at 95^{o}C, annealing for 30 seconds at 54^{o}C, and elongation for 1 minute at 72^{o}C). The NGF PCR for the mouse Schwann cells was performed under the same conditions, but stopped after 25 cycles. The GADPH PCR for the mouse Schwann cells was performed under the same conditions, but stopped after 23 cycles.

PCR samples were separated on a 1% agarose gel containing ethidium bromide at 90 V for approximately 45 minutes. Bands were then photographed using a Gel Doc 2000 (Bio-Rad, Hercules, CA).

2.7 Detection of PAR_2 Protein in PC12 Cells Using Immunocytochemistry

Cells were rinsed with Hank's buffered saline solution (HBSS), fixed for 1hr with 4% paraformaldehyde in PBS and then blocked with 10% donkey serum diluted with PBS at room temperature for 1 hour in a humidity chamber. After blocking with the donkey serum, the cells were incubated with A5 primary antibody (1:500; courtesy of Dr. MD Hollenberg) in a humidity chamber for 1 hour. Subsequently, the primary antibody was removed and the cells underwent three, 5 minutes washes with PBS to remove any excess, unattached primary antibody. The cells were then incubated with a polyclonal

donkey anti-rabbit secondary antibody conjugated to a Cy3 fluorescent label (Santa Cruz Biotechnology, Inc., Santa Cruz, California) in the dark for 1 hour in a humidity chamber. The secondary was then removed and the cells were washed for three, 5 minute washes with PBS. Following the final washes, cells were protected with coverslips attached with fluorosave. Cells were visualized with a Leica DMR inverted fluorescence microscope and photomicrographs were taken on a Photometrics CoolSNAP digital camera (Roper Scientific, Tucson, Ariz.).

2.8 Detection of PAR_2 Protein in Schwann Cells Using Immunocytochemistry

Schwann cells were isolated, purified, and grown on collagen coated plates. Schwann cells grown overnight on 35mm collagen coated plates were washed three times with PBS to remove any residual media on the cells. Cells were fixed with 4% paraformaldehyde for 20 minutes then underwent three 5 minute washes with 0.05% Triton-X, 1% BSA, PBS solution. Following the washes with the detergent, the cells were rinsed with three 10 minute washes of 1% BSA in PBS and then incubated for 90 minutes with a goat polyclonal PAR-2 primary antibody (Santa Cruz Biotechnology) at a 1:50 dilution in a humid chamber. The primary antibody was then removed and the cells underwent three 10 minute washes with 1%BSA in PBS. Once the unbound primary antibody was removed with the washes, the cells were incubated with a fluorescent secondary (Alexa Fluor® 488 donkey anti-goat IgG, Molecular Probes) at a 1:1000 dilution for 45 minutes in a humid chamber protected from light. Following incubation with the secondary antibody, the cells were washed with 1%BSA in PBS for two 10 minute intervals. Schwann cells were visualized as described for the PC12 cells.

2.9 Calcium Signalling

PC12 cells grown to confluence on T-75 tissue culture treated flasks (Nunc, VWR Canada) were lifted, placed in a 15mL conical flask, and centrifuged using a bench top centrifuge at 900rpm for 10 minutes. The supernatant was decanted and the cells were resuspended in 1 ml of 1X HBSS pH 7.4. Once the cells were in suspension, sulfinpyrazone (2.5 µl; 100 mM stock solution), Pluronic F-127 (1 µl; 20 % solution), and Fluo-3 AM (5µl; 2.2 mM solution) were added and the cells were incubated under gentle agitation for 25 minutes at room temperature. Following incubation, 10 ml of the calcium assay HEPES buffer working solution was added to the tube; the cells were gently mixed, and then centrifuged at 900rpm for 10 minutes. This rinse and spin was repeated three times. After the last spin, the cell pellet was resuspended in 1 ml of the calcium assay HEPES buffer working solution and ready for the calcium signalling assay. Evaluation of peptide-stimulated Ca^{2+} release was represented by fluorescence emission. Measurements were conducted at 24°C using an AMINCO-Bowman® Series 2 Luminescence Spectrometer (Spectronic Unicam, Rochester, NY), with an excitation wavelength of 480 nm and an emission recorded at 530 nm.

2.10 Morphometric analysis of primary neuron neurite outgrowth and PC12 cell differentiation

2.10.1 Neurofilament Immunocytochemistry on Primary Neurons and PC12 Cells

Immunocytochemistry was used to visualize primary neurons isolated from mouse DRG and PC12 cells for the neurite outgrowth assay. Incubation media was removed from the

cells grown on collagen coated plates and the cells were rinsed with Hank's Balanced Salt Solution (HBSS). Cells were then fixed with 4% paraformaldehyde in phosphate buffered saline solution (PBS) for 90 minutes at 4^{o}C. Following fixation, cells were gently washed three times with PBS and then blocked at room temperature with blocking buffer (PBS, 0.01% Tween, 1.5% non-fat dry milk; pH 7.4) for 30 minutes under gentle agitation. After blocking, the cells were incubated overnight in a humid chamber at 4^{o}C with a monoclonal antibody against phosphorylated neurofilaments diluted in blocking buffer (1:1000). The next day the cells were washed once with Tween-20 Buffered Saline (TBS; 0.01% Tween-20 in PBS) and twice with PBS. The cells were then incubated for 90 minutes in a humid chamber with a biotin-labelled secondary antibody (ABC kit, Vector Labs, Burlington, Ontario). After incubation with the secondary antibody, the cells were washed three times with PBS, and incubated in the dark, in a humid chamber at room temperature with an avidin biotinylated enzyme complex (ABC), which binds to the biotinylated secondary antibody. In the last step of the procedure, the cells were washed with PBS three times and then visualized by developing the plates in the dark with 3,3'-diaminobenzidine (DAB Substrate Kit for peroxidise, Vector Labs, Burlington, Ontario) for 2-10 minutes. Cells were rinsed and stored with ddH_2O.

2.10.2 Primary Neuron and PC12 Cell Neurite Outgrowth Assay

Cells were analyzed with a Zeiss Axioskop 2 FS microscope connected to an ExwaveHAD SSC-DC50A color digital video camera (Sony), which transfers images to a video monitor (Sony). Cell number and neurite length were measured following incubation and immunocytochemistry. Two measurements were used to evaluate the rate

of nerve regeneration in the primary neuronal culture, and for the purpose of analysis, the cells were classified as differentiated and non-differentiated. First, the percentage of cells with neurite outgrowth was evaluated by measuring the ratio between the number of cells with neurite outgrowth and the number of neurons without neurite outgrowth. Second, average neurite length was evaluated by measuring the longest neurite extension on exactly 10 neurons per plate. The first 10 neurite measurements were combined together for an average value. In order to keep the measurements among the plates consistent, two guidelines were established. First, to keep the number of cells measured relatively consistent, 2 fixed areas were outlined on the 35mm Petri dishes. Initially, one fixed area was counted and the only cells that were included in the measurements were the cells in that designated area. A minimum of 50 and a maximum of 1000 cells were counted per Petri dish. The average number of cells that were counted ranged from 300-600 cells. However, if <50 cells were counted in the initial area, the second outlined area was added to the count. Second, to ensure that only true neurite extensions were assessed in the evaluation of average neurite length, only neurite extensions equal to or over 25μm were included in the measurements. However, in some cell conditions there was limited neurite outgrowth, but in order to keep the data collection consistent 10 values were combined for the average. Therefore the first criteria, neurite extensions equal to or over 24.6μm were included in the measurements was abided, but in addition to the first criteria, the second criteria was followed, 10 values were combined for the average. Thus, for example, in conditions that may have yielded only 6 neurons with neurite extensions equal to or over 25μm in the entire counted area, the remainder 4 values would have to be

defined with a 0μm value, which means that in some cases data showing average neurite length values will be less than 25μm.

2.11 Measuring Neurite Outgrowth in PC12 Cells incubated with Sciatic Nerve Conditioned Media

2.11.1 Production and Collection of Sciatic Nerve Conditioned Media

Sciatic nerve removed from C57Bl6 wild-type mice 6 weeks old were rinsed in ice cold PBS and cultured in 12-well plates containing 1mL DMEM without sera for 8 days at $37^{o}C/O_2/CO_2$. At the beginning of day 9, the nerves were transferred to new wells with fresh serum-free DMEM containing, NGF (1ng/mL), SLIGRL (20μM, 100 μM) & NGF (1ng/mL) or LRGILS (100μM & NGF 1ng/mL). This conditioned media (CM) was collected every 24 h, from the end of day 9 until day 11, and stored at $70^{o}C$ until use.

2.11.2 PC12 Cells in Culture with Sciatic Nerve Conditioned Media

For the neurite outgrowth assays, PC12 cells were plated overnight on 35mm collagen coated plates containing DMEM control media (DMEM, 10% FBS, 5% HS, and 1% penicillin/streptomycin). At the beginning of the assay, the old media was removed and replaced with new DMEM control media or by one of the CM samples collected from the sciatic nerve incubation (see section 2.11.1) equally supplemented with 10% FBS, 5% HS, and 1% penicillin/streptomycin. Media was change every 24 hours for 3 days and the cells were fixed, immunostained for neurofilaments (see section 2.5) and evaluated with the neurite outgrowth assay (see section 2.6).

2.12 Statistical Analysis

Data were expressed as means ± standard error of the mean (SEM), with statistical significance set at $p<0.05$ or less. Data were analyzed for Gaussian distribution using the D'Agostino and Pearson omnibus normality test. If the data set demonstrated Gaussian distribution, statistical analysis was performed with a one-way analysis of variance test (1-way ANOVA) followed by a Tukey's post test, which compared means. If the data set did not demonstrate Gaussian distribution, statistical analysis was performed with a Kruskal-Wallis test followed by a Dunn's post-test to compare means. All statistical analysis was performed using GraphPad Prism statistical software (GraphPad Software, Inc., San Diego, CA).

Chapter Three: **Effects of Local PAR_2 Activation on Peripheral Nerve Functional Recovery after Injury.**

3.1 Study Introduction, and Objectives

The study began with the goal to evaluate the effects of PAR_2 activation on nerve regeneration *in vivo* using a number of indirect parameters to measure nerve recovery. The measurements, which included thermal withdrawal latency, mechanical nociceptive score, and muscle strength, were used to evaluate peripheral nerve recovery. Following the *in vivo* measurements, sciatic nerve tissue was removed from the sciatic nerve crush group and processed to look at fibre number, size, and myelination differences between the groups at the end of the study. Two different nerve injury models were used to look at the effects of the PAR_2-AP SLIGRL, and two different approaches to evaluate the role of PAR_2 were taken. The first approach was to assess the effects of daily local administration of the PAR_2-AP, SLIGRL, on nociception and peripheral nerve functional recovery in wild type mice following either a sciatic nerve crush model or a sciatic nerve transection model. The second approach was to evaluate the endogenous role of PAR_2 activation in peripheral nerve functional recovery following peripheral nerve injury in PAR_2 deficient mice.

3.2 Experimental Methods

For techniques used in this chapter, see sections 2.1-2.3.

Study Design

Prior to sciatic nerve crush or transection surgery, thermal withdrawal latency, mechanical nociception, and muscle strength baseline measurements were recorded in 48 mice. At day 0, 24 mice underwent sciatic nerve crush surgery and 24 mice underwent transection surgery. In each surgery group mice were subsequently divided into 3 groups of 8. Each group of 8 was assigned a daily treatment regime of either saline, control peptide (LRGILS-NH_2), or PAR_2-AP (SLIGRL-NH_2) injected intramuscularly starting at day 0 and continued daily for the remainder of the study. Thermal withdrawal latency, mechanical nociception, and muscle strength measurements were started one week following the induction of nerve injury and measured weekly for 4 weeks in the sciatic nerve crush groups and 12 weeks in the sciatic nerve transection groups. Additionally, in the sciatic nerve crush groups, tissue was removed at the end of the 4 week period and processed for morphometrical analysis.

For the PAR_2 deficiency studies, thermal withdrawal latency, mechanical nociception, and muscle strength baselines were measured in 16 $PAR_2^{(-/-)}$ mice and 16 wild-type mice prior to sciatic nerve crush or transection. At day 0, 8 wild type and 8 $PAR_2^{(-/-)}$ mice underwent sciatic nerve crush surgery and 8 wild type and 8 $PAR_2^{(-/-)}$ mice under went sciatic nerve transection surgery. Thermal withdrawal latency, mechanical nociception, and muscle strength measurements resumed 1 week post-crush and 2 weeks post-transection for a period of 26 days and 7 weeks respectively.

3.3 Results

3.3.1 Effects of PAR_2 Agonist on Thermal Nociception Following Nerve Injury

Crush: At week 1 post-injury in both nerve injury models, all groups (SLIGRL-NH_2 1ng/day i.m, LRGILS 1ng/day i.m., and Saline) exhibited a delayed thermal withdrawal latency time, which was indicative of the loss of the thermal nociceptive function (Figure 3-1). Two weeks after sciatic nerve crush, the thermal withdrawal latencies of mice that received daily treatments with SLIGRL-NH_2 were back to normal levels, not significantly different from the basal measurements. In contrast, withdrawal latencies of LRGILS-NH_2 or saline treated mice were still significantly elevated 2 weeks after sciatic nerve crush, and returned to basal levels only 4 weeks after injury. **Transection**: Similar results were observed in the animals that had nerve transection (Figure 3-1). More specifically, animals treated with SLIGRL-NH_2, recovered to basal levels earlier (3 weeks post-section) in comparison to the control groups treated with LRGILS-NH_2 or saline (recovering to basal withdrawal latency values at 6 weeks post-section).

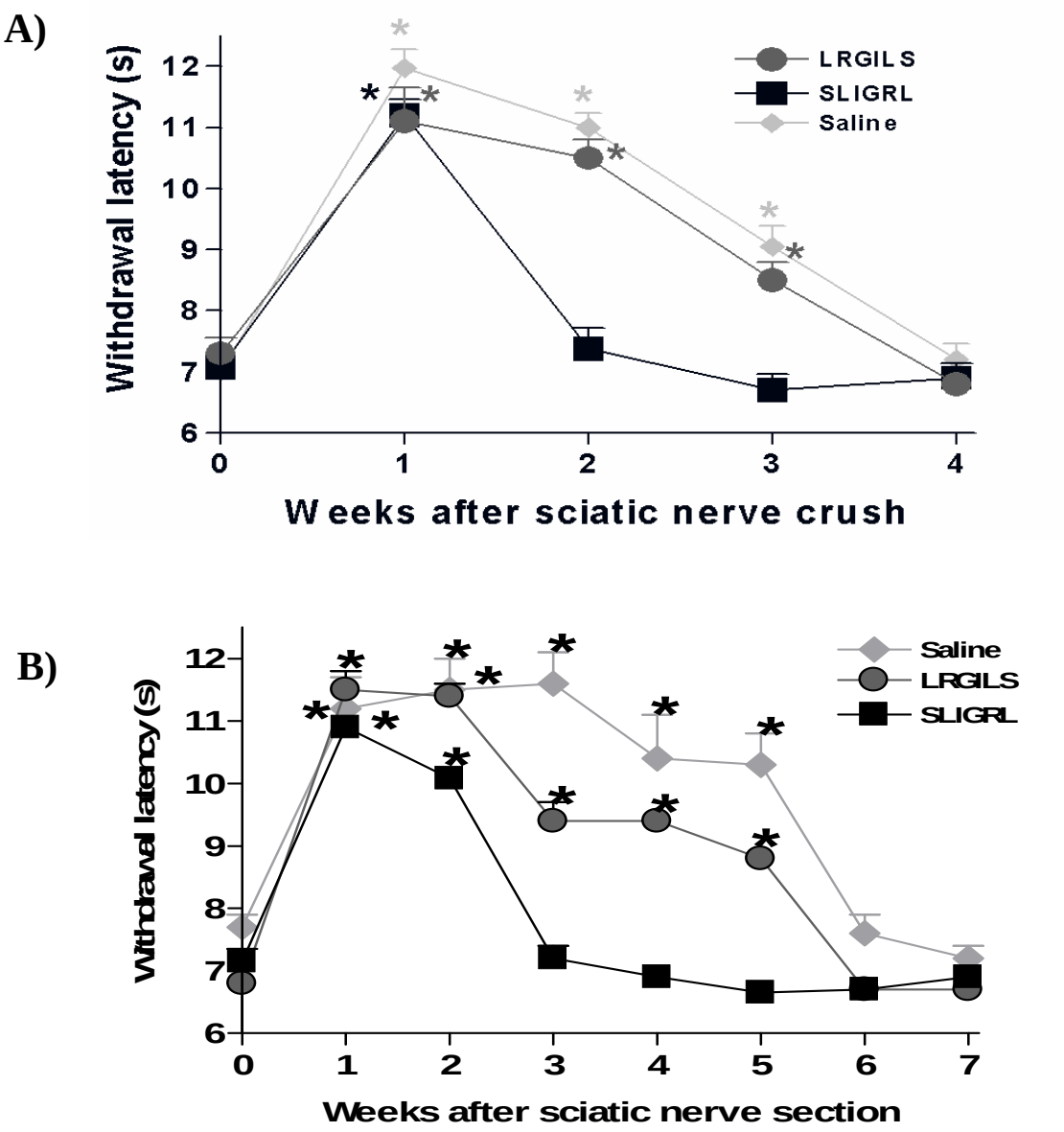

Figure 3-1. Thermal Withdrawal Latency Following Sciatic Nerve Crush (A) or Transection (B)

Thermal withdrawal latency over 4 and 7 weeks in wild-type mice following a sciatic nerve crush (A) or transection (B) respectively. Intramuscular (i.m.) injections at the site of injury of SLIGRL (1ng/mouse), LRGILS (1ng/mouse), or the vehicle saline were performed daily. Data were expressed as mean ± SEM; * means post-injury values were statistically different for $p < 0.05$ from basal values (week 0).

3.3.2 Effects of PAR_2 Agonist on Mechanical Nociception Following Nerve Injury

Crush: As shown in Figure 3-2, none of the filaments evoked a nociceptive response among any of the groups regardless of treatment one week post-crush injury. At week 2, with the allodynic filament 3.61, there was an increased nociceptive response in all of the treated groups; however, nociceptive responses were not significantly different from their respective baselines. At weeks 3 and 4, an allodynic response, which was reflected by significantly high nociceptive scores, was seen in the two control groups (LRGILS-NH_2 and saline). This result is in contrast to the SLIGRL-NH_2 treated group, which at weeks 3 and 4 has nociceptive scores comparable to the baseline values prior to nerve crush. With the higher filament sizes (3.84 and 4.08) the nociceptive score measured 2 weeks post-crush increased significantly and a hyperalgesic response was observed in all of the treated groups. By week 3, the SLIGRL-NH_2 treated mice showed a diminished nociceptive score with values that were no longer significantly different from baseline levels. Conversely, in the control mice (saline or LRGILS-NH_2) at weeks 3 and 4 post-crush, significantly higher nociceptive response scores with the higher filaments sizes, 3.84 and 4.08 indicated hyperalgesia.

Transection: In the animals that underwent sciatic nerve transection, which is a more severe form of nerve injury, no nociceptive response was observed for the first 4-6 weeks following nerve injury (Figure 3-3). At approximately 4 weeks post-nerve transection a significant increase in nociceptive score tested with the largest filament, 4.08, was observed in the animals that have been treated with SLIGRL-NH_2. The values observed for nociceptive score in SLIGRL-NH_2 treated mice at that time-point were in the same

range as basal values measured before the induction of injury. Six weeks post-injury, a significant increase in nociceptive response scores was seen in SLIGRL-NH_2 treated mice compared to saline or control peptide-treated mice when they were tested with the thinner filaments, 3.84 and 3.61. Nociceptive score 6 weeks post-injury reached values comparable to basal measures in the SLIGRL-treated group. In contrast, full recovery was never observed in either of the control groups (saline or LRGILS-NH_2 treated) for the entire length of the experiment (12 weeks).

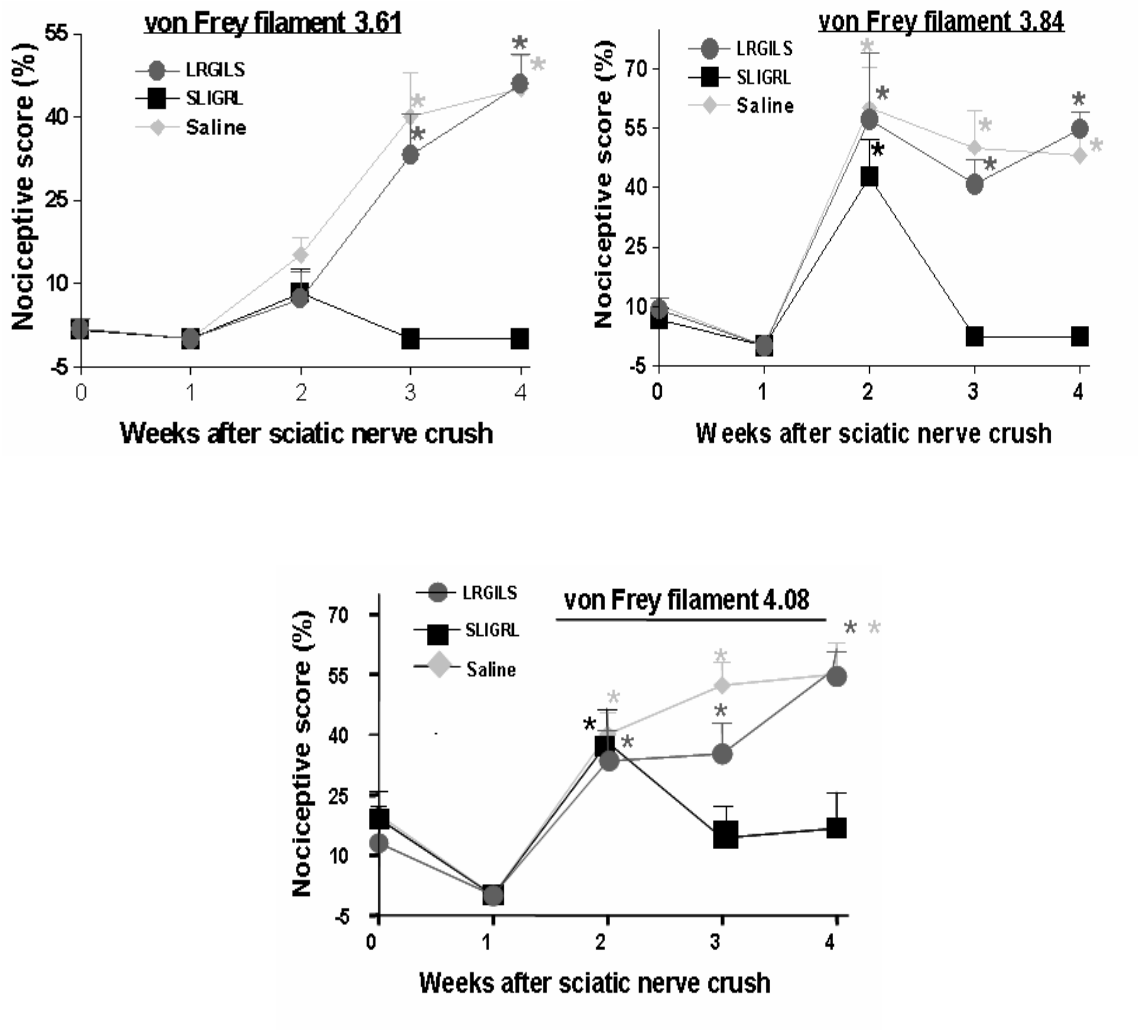

Figure 3-2. Mechanical Nociceptive Score Response Following a Sciatic Nerve Crush

Mechanical nociceptive response scores in wild-type mice following a sciatic nerve crush. Intramuscular (i.m.) injections of SLIGRL (1ng/mouse), LRGILS (1ng/mouse), or the vehicle saline were performed at the site of injury daily. Data were expressed as mean ± SEM; * means post-injury values were statistically different for $p < 0.05$ from basal values (week 0).

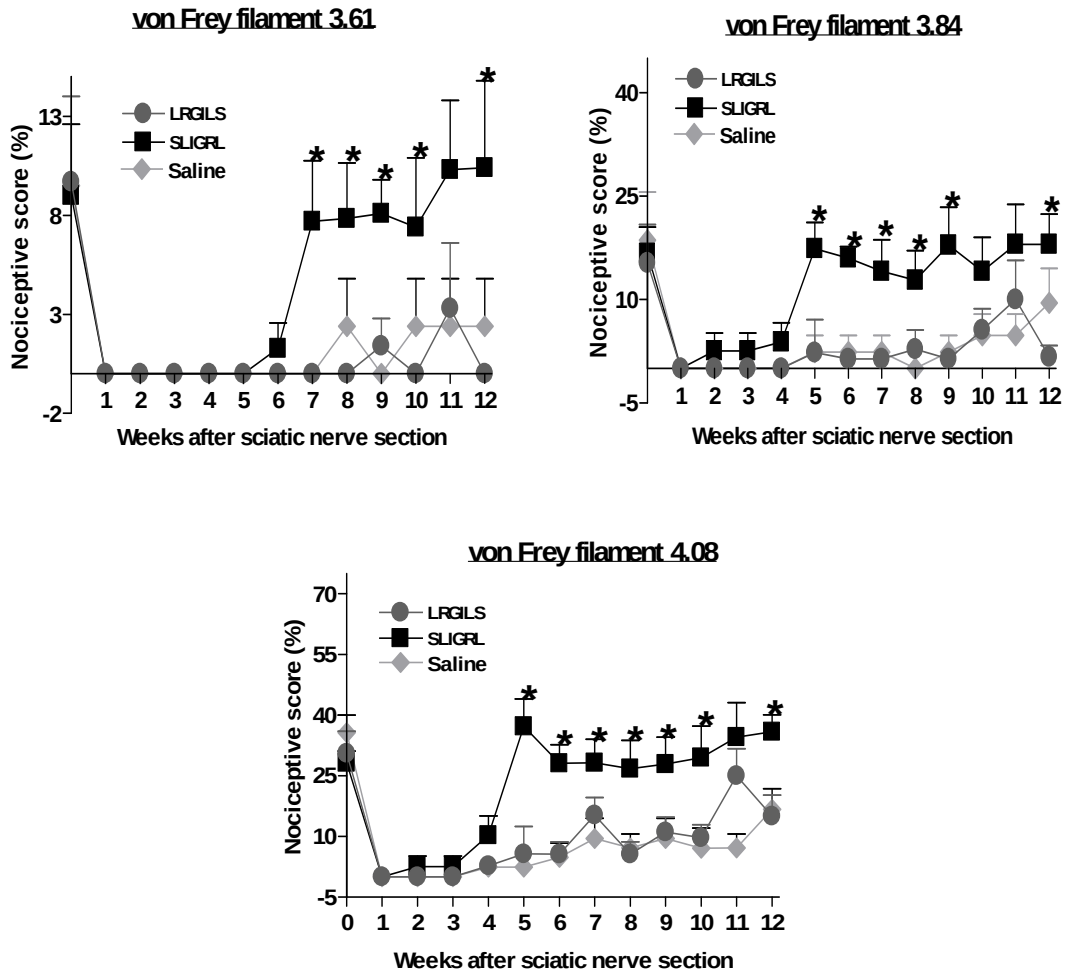

Figure 3-3. Mechanical Nociceptive Score Response Following a Sciatic Nerve Transection

Mechanical nociceptive response scores in mice following sciatic nerve transection. Intramuscular (i.m.) injections of SLIGRL (1ng/mouse), LRGILS (1ng/mouse), or the vehicle saline were performed at the site of injury daily. Data were expressed as mean ± SEM; * means post-injury values are considered significantly different for $p < 0.05$ when compared to control group values.

3.3.3 Effects of PAR_2 Agonist on Muscle Strength Following Nerve Injury

Crush: Evaluation of motor neuron regeneration was also assessed through muscle strength measurements. At the 2 weeks time-point following nerve crush, the group treated with the PAR_2-AP showed earlier muscle strength recovery compared to the two control groups. The SLIGRL-NH_2-treated group regained muscle strength values comparable to basal only 2 weeks after crush, while saline and LRGILS-NH_2-treated mice were back to normal (basal) muscle strength measurements, 4 weeks post-crush injury (Figure 3-4A). **Transection:** In contrast, in the sciatic nerve transection model, no difference in muscle strength recovery was observed between the groups treated with SLIGRL-NH_2 or LRGILS-NH_2 (Figure 3-4B).

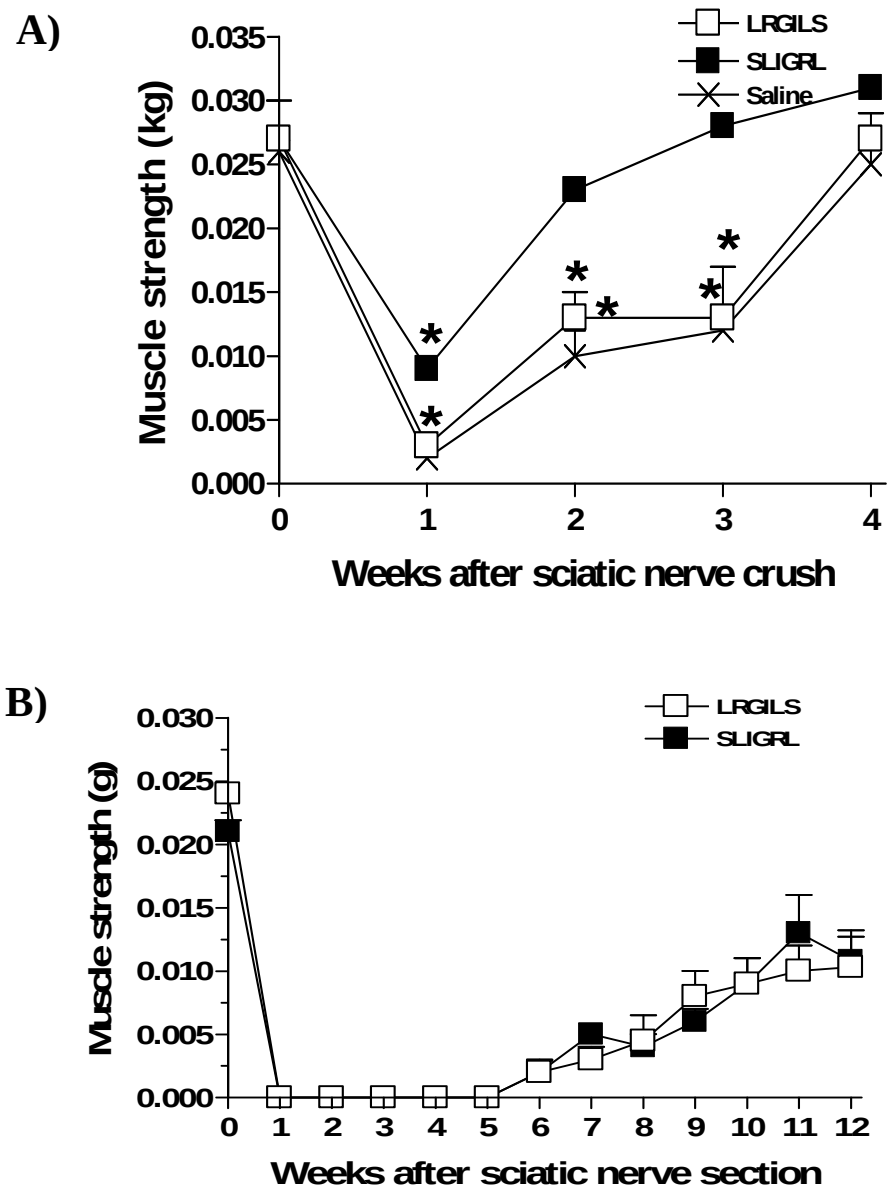

Figure 3-4. Muscle Strength Measurements Following a Sciatic Nerve Crush (A) or Transection (B)

Intramuscular (i.m.) injections at the site of injury of SLIGRL (1ng/mouse), LRGILS (1ng/mouse), or the vehicle saline were performed daily. Data were expressed as mean ± SEM; * means post-injury values were considered significantly different for $p < 0.05$ when compared to control group values.

3.3.4 Effects of PAR_2 Agonist on Sciatic Nerve Fibre Morphometry Following Nerve Injury

The results presented in this paragraph were generated by Dr. Valentine Brussee, in the laboratory of Dr. Zochodne. At the end of the sciatic nerve crush study, sciatic nerve tissues were collected at the site of injury and were embedded in epon. When the nerve tissues were assessed for morphometrical differences, there was no significant difference in the myelinated fibre calibre between the proximal stump of the PAR_2-AP treated group and the control peptide group (LRGILS-NH_2) (Figure 3-5). However, there was a significantly higher myelinated fibre calibre in the distal stump of mice that were treated with the PAR_2-AP, SLIGRL-NH_2 compared to mice treated with control peptide (LRGILS-NH_2) treated mice (Figure 3-5).

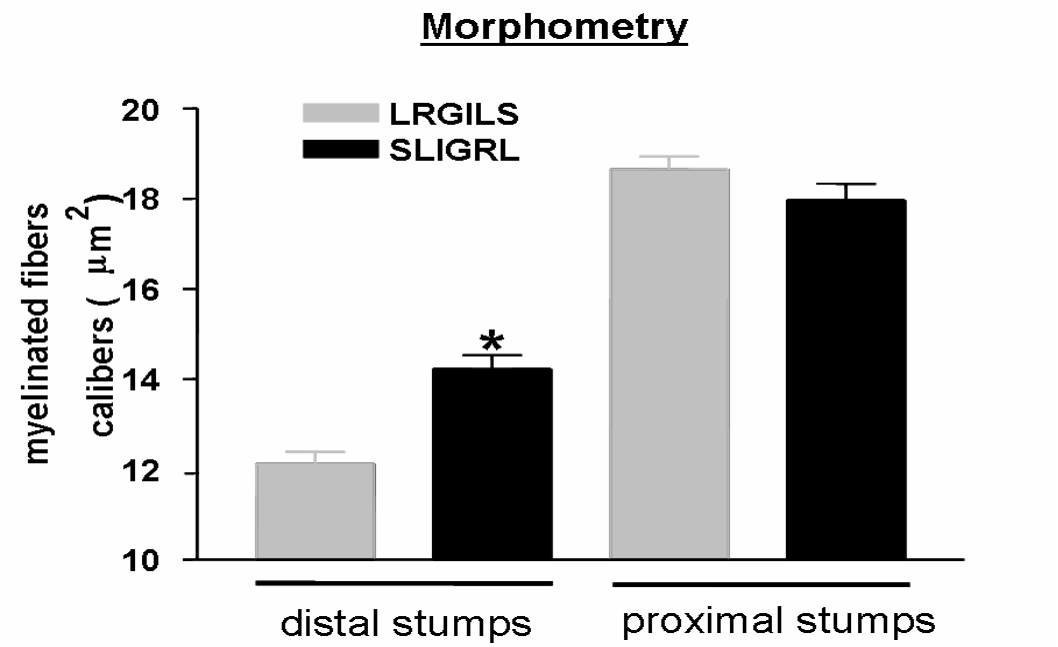

Figure 3-5. Evaluation of Sciatic Nerve Morphometry following Sciatic Nerve Crush

Sciatic nerve morphometry in C57Bl/6 mice at 4 weeks following sciatic nerve crush. (Courtesy of Dr. Brussee). Data were expressed as mean ± SEM; *SLIGRL myelinated fibre calibres were considered statistically significant for $p < 0.05$, when compared to the myelinated fibre calibers of the control (LRGILS) group.

3.3.5 Effect of PAR_2 Deficiency on Thermal Nociception Following Nerve Injury

Crush: Starting at day 7 post-crush, a significant delay in thermal withdrawal latency was seen in the $PAR_2^{(-/-)}$ mice when compared to the $PAR_2^{(+/+)}$ mice (Figure 3-6A). This significant difference in thermal withdrawal latency between $PAR_2^{(-/-)}$ mice and $PAR_2^{(+/+)}$ mice was observed up until day 20 post-crush at which point the $PAR_2^{(-/-)}$ mice withdrawal latencies have decreased to withdrawal latencies that were comparable to the $PAR_2^{(+/+)}$ mice. **Transection:** Differences in withdrawal latency responses to a thermal stimulation in between $PAR_2^{(+/+)}$ and $PAR_2^{(-/-)}$ following a sciatic nerve transection were observed at only one time-point: 5 weeks after sciatic nerve section (Figure 3-6B). At that time-point wild-type mice showed higher withdrawal latency compared to $PAR_2^{(-/-)}$ mice.

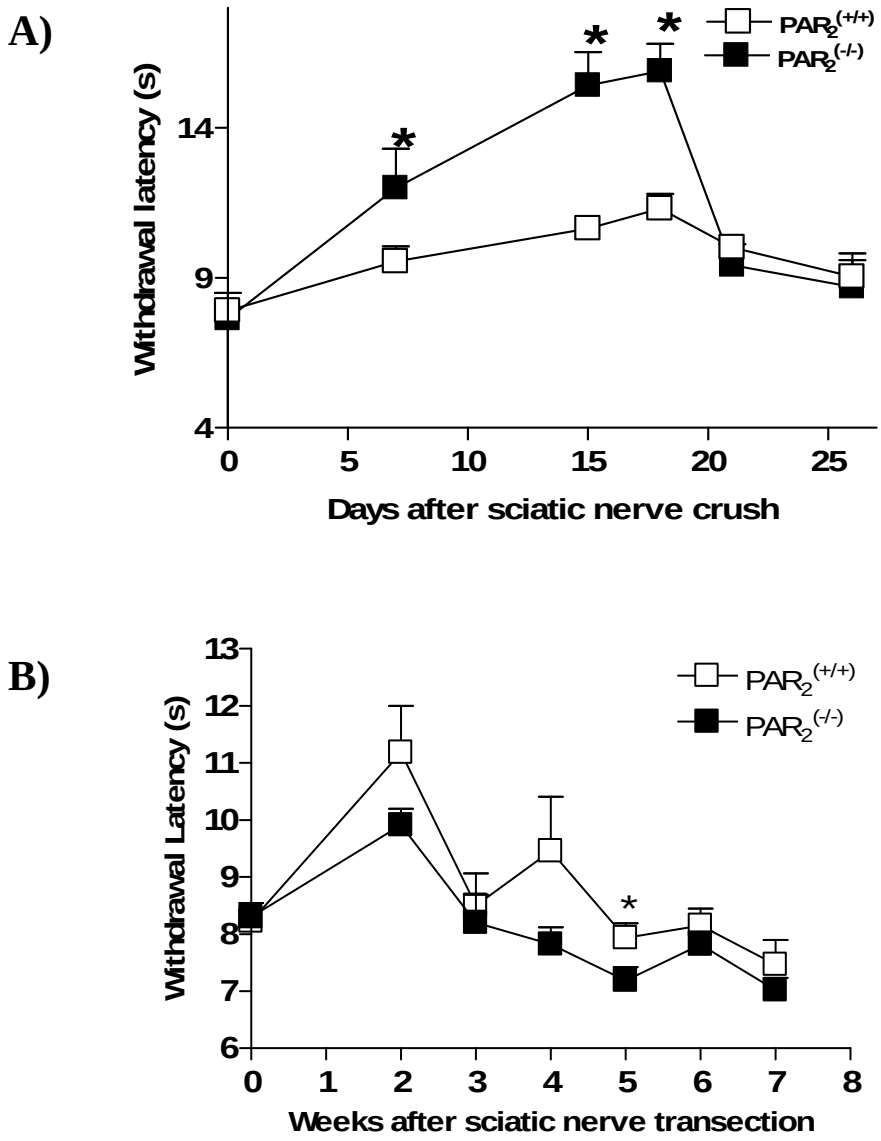

Figure 3-6. Comparison of Thermal Withdrawal Latencies between $PAR_2^{(+/+)}$ and $PAR_2^{(-/-)}$ Mice Following Sciatic Nerve Crush (A) or Sciatic Nerve Transection (B)

Thermal withdrawal latencies in $PAR_2^{(+/+)}$ and $PAR_2^{(-/-)}$ mice following sciatic nerve crush or sciatic nerve transection. Data were expressed as mean ± SEM; * means $PAR_2^{(+/+)}$ post-injury values were significantly different for $p < 0.05$ when compared to $PAR_2^{(-/-)}$ post-injury values.

3.3.6 Effects of PAR_2 Deficiency on Mechanical Nociception Following Nerve Injury

Crush: As shown in Figure 3-7, a decrease in mechanical nociceptive score was seen in both $PAR_2^{(+/+)}$ and $PAR_2^{(-/-)}$ at 7 days post-crush, which was indicative of the loss of mechanical nociceptive function. At 15 days post-crush an increase in nociceptive score is observed in both $PAR_2^{(+/+)}$ and $PAR_2^{(-/-)}$ mice. However, although the nociceptive score in both groups increased at day 15, the $PAR_2^{(-/-)}$ mice showed a significantly higher nociceptive score with the largest filament (4.08) in comparison to the $PAR_2^{(+/+)}$ mice. At day 18 post-crush, the nociceptive scores from all 3 filaments (3.61, 3.84, 4.08) of $PAR_2^{(-/-)}$ mice were significantly elevated in comparison to the $PAR_2^{(+/+)}$ mice. At day 21, the $PAR_2^{(-/-)}$ mice nociceptive scores are no longer significantly different from the $PAR_2^{(+/+)}$ nociceptive scores using the 3.61 filament. However, with the 3.84 and 4.08 filament sizes, the nociceptive scores of the $PAR_2^{(-/-)}$ mice continue to be significantly higher from the $PAR_2^{(+/+)}$ mice, up until day 25. **Transection:** In contrast, the only differences observed in nociceptive score between $PAR_2^{(+/+)}$ and $PAR_2^{(-/-)}$ mice after sciatic nerve transection was at the 5 weeks time-point using the finest filament, (3.61), and the 6 weeks time point using the 3.84 filament (Figure 3-8). In both cases, $PAR_2^{(-/-)}$ mice showed higher nociceptive score in comparison to the $PAR_2^{(+/+)}$ mice.

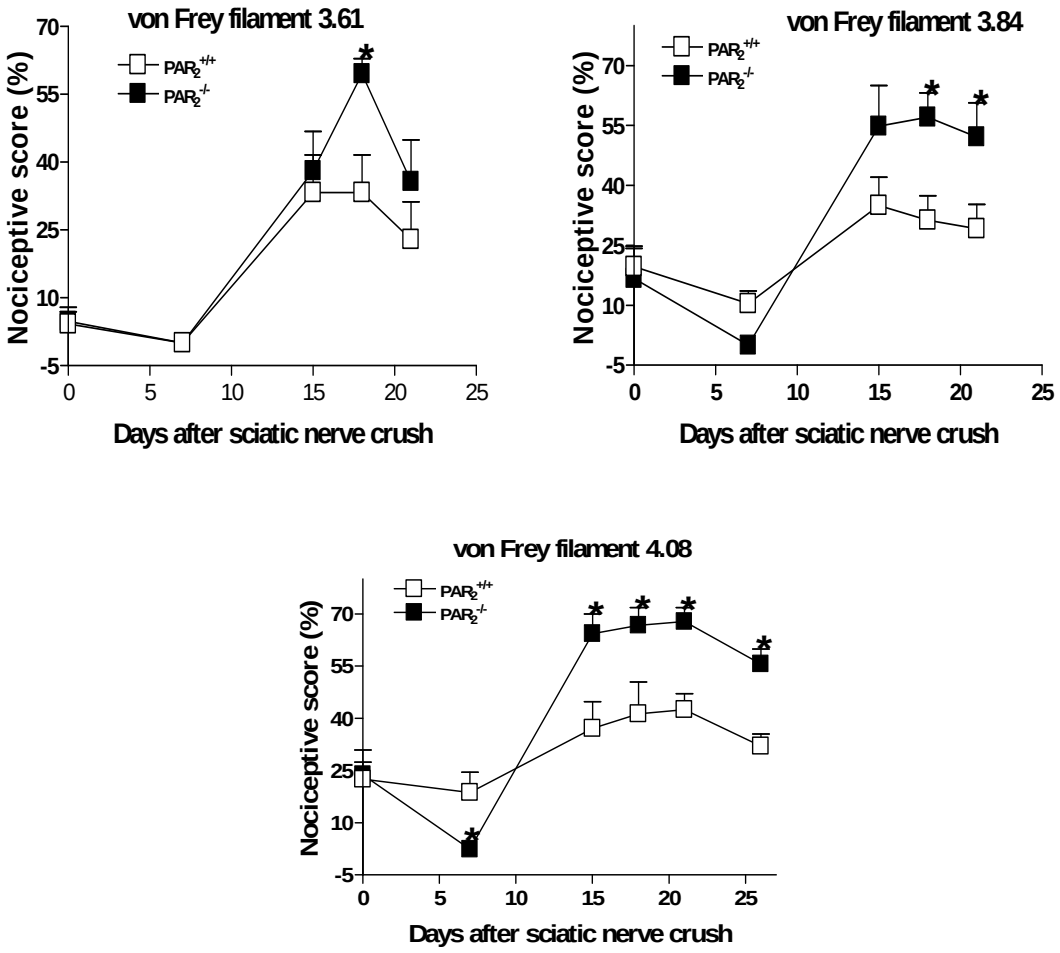

Figure 3-7. Comparison of Mechanical Nociceptive Score between $PAR_2^{(+/+)}$ and $PAR_2^{(-/-)}$ Mice Following Sciatic Nerve Crush

Mechanical nociception score in $PAR_2^{(+/+)}$ and $PAR_2^{(-/-)}$ mice following sciatic nerve crush. Data were expressed as mean ± SEM; * $PAR_2^{(+/+)}$ post-injury values were considered significantly different for $p < 0.05$ when compared to $PAR_2^{(-/-)}$ post-injury values.

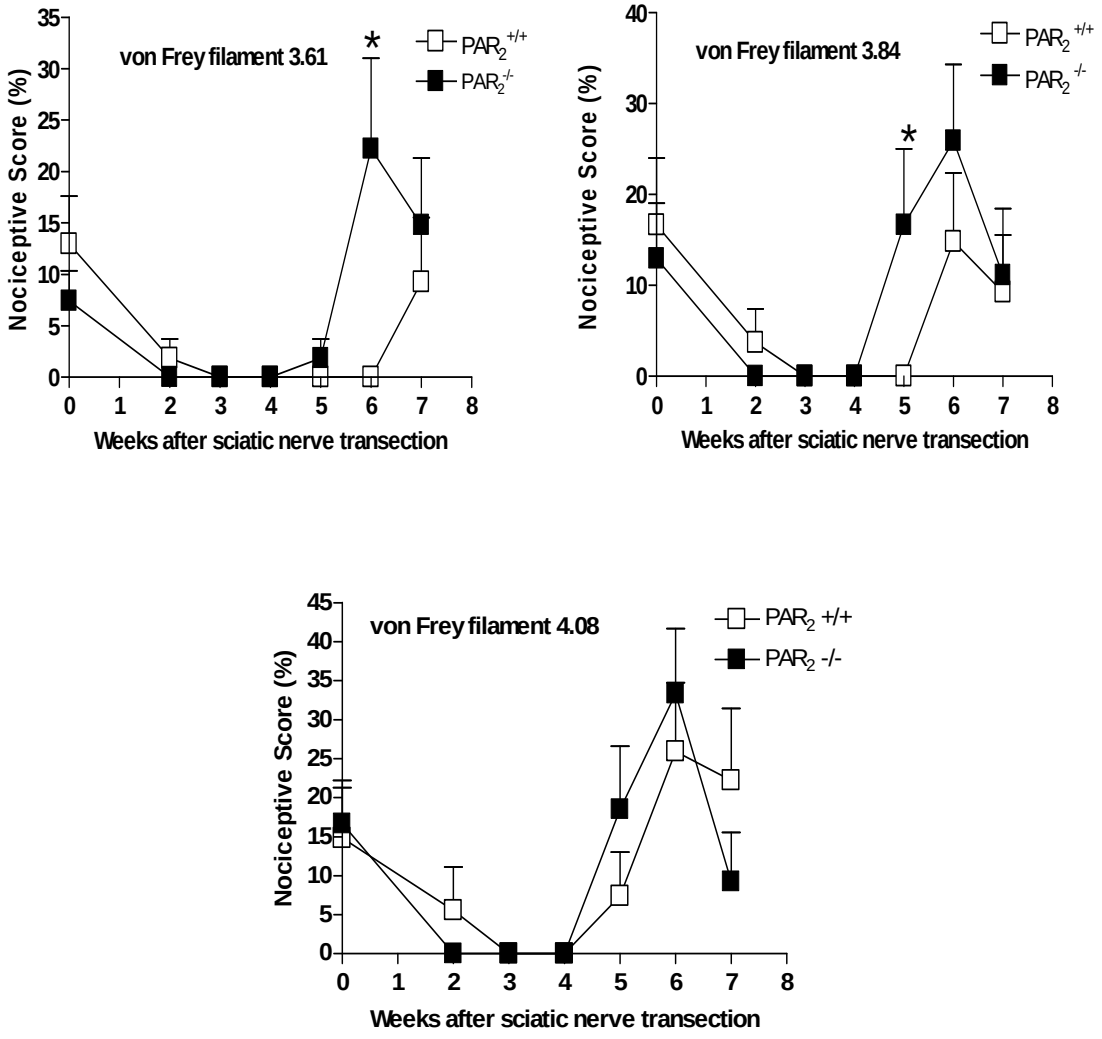

Figure 3-8. Comparison of Mechanical Nociceptive Score between $PAR_2^{(+/+)}$ and $PAR_2^{(-/-)}$ Mice Following Sciatic Nerve Transection

Mechanical nociception score in $PAR_2^{(+/+)}$ and $PAR_2^{(-/-)}$ mice following sciatic nerve transection. Data were expressed as mean ± SEM; * $PAR_2^{(+/+)}$ post-injury values were considered significantly different for $p < 0.05$ when compared to $PAR_2^{(-/-)}$ post-injury values.

3.3.7 Effect of PAR_2 Deficiency on Muscle Strength Following Nerve Injury

Crush: A decrease in muscle strength was seen at 7 days post-crush in both $PAR_2^{(+/+)}$ mice and $PAR_2^{(-/-)}$ mice, which reflected the loss of motor function. After 7 days muscle strength is seen to recover in both groups; however, no significant differences in muscle strength were seen between the $PAR_2^{(+/+)}$ mice and $PAR_2^{(-/-)}$ mice. **Transection:** Similarly, in the sciatic nerve transection mice, a decrease in muscle strength was seen at 2 weeks. Starting at approximately 4 weeks, muscle strength is seen to recover in both $PAR_2^{(+/+)}$ and $PAR_2^{(-/-)}$ mice, but no significant difference was seen between the groups.

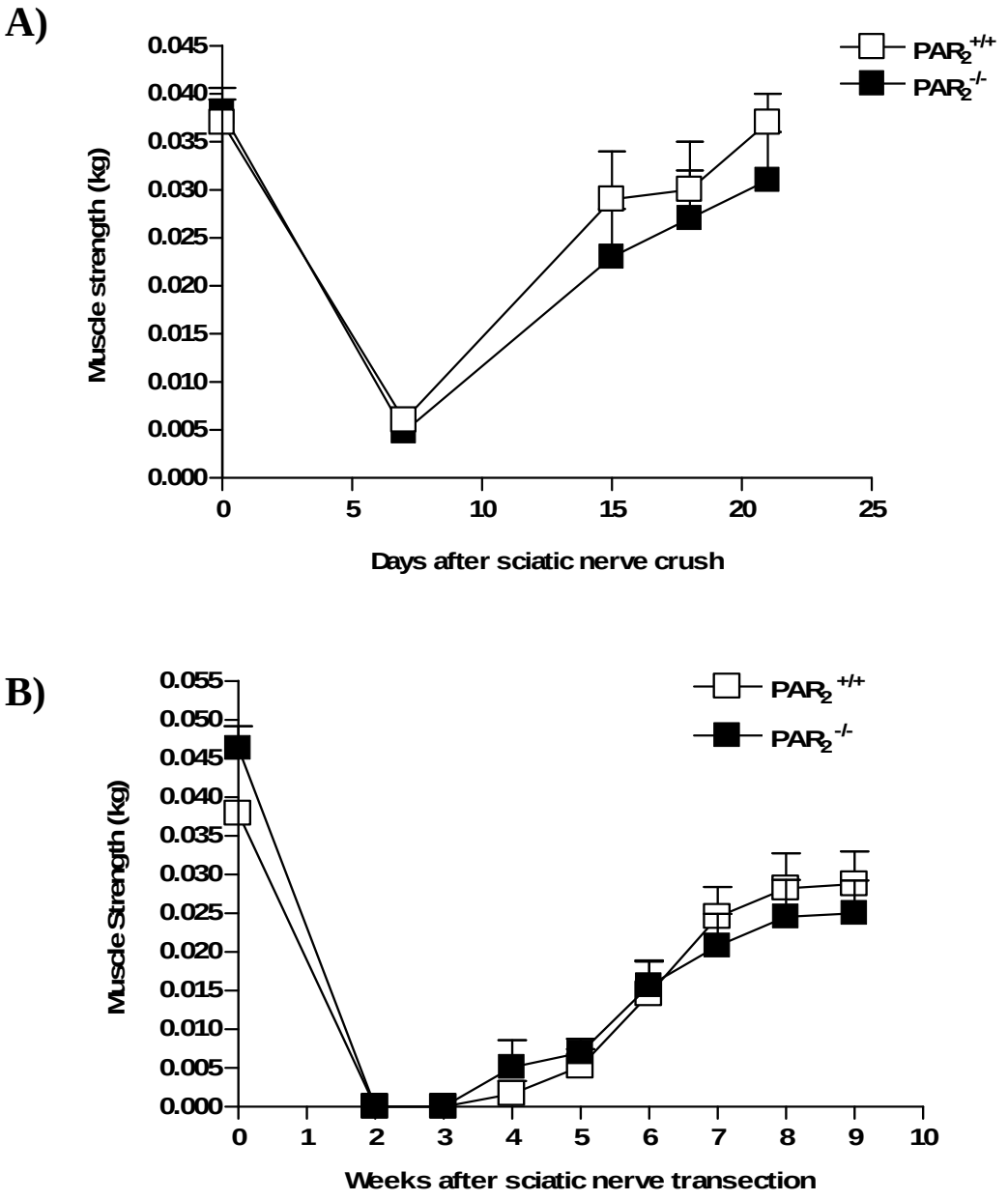

Figure 3-9. Comparison of Muscle Strength Measurements Between $PAR_2^{(+/+)}$ and $PAR_2^{(-/-)}$ Mice Following Sciatic Nerve Crush (A) or Transection (B)

Muscle Strength measurements in $PAR_2^{(+/+)}$ and $PAR_2^{(-/-)}$ mice following sciatic nerve crush or transection. Data were expressed as mean ± SEM.

3.4 Discussion

PAR_2 is generally recognized for its role in inflammation. Interestingly, it has been established in some tissue that PAR_2-mediated inflammation can be attributed to a neurogenic mechanism [61]. Knowing that PAR_2 has been detected on DRGs tissues sparked some interest into other potential functions of PAR_2 in the peripheral nervous system. Since the involvement of PAR_2 and peripheral nerve regeneration has not yet been documented, it was the aim of this study to examine the potential role of PAR_2 activation in peripheral nerve regeneration following nerve injury.

Two different peripheral nerve injury models were used to study the activation of PAR_2 *in vivo*, the sciatic nerve crush model and the sciatic nerve transection model. The main finding of this section of the study was that local injection of PAR_2 agonist at sub-inflammatory doses, results in an improvement in the rate of nerve regeneration as indicated by the behaviour nociceptive response tests, the motor nerve conduction amplitude measurements, and the increase in nerve fibre myelination.

In both nerve injury models (sciatic nerve crush and sciatic nerve transection), the thermal withdrawal latencies and mechanical nociception scores of mice treated with SLIGRL recovered faster to basal levels than the control group mice. This improvement in sensory nociceptive scores suggests that daily local treatment with PAR_2 agonist promotes sensory nerve fibre regeneration. Further support for the role of PAR_2 in peripheral nerve regeneration was seen in the muscle strength data. In the sciatic nerve

crush mice that were treated with the PAR_2-AP, SLIGRL-NH_2, muscle strength recovered back to baseline levels two weeks earlier than the control groups post-crush.

Sciatic nerve morphometry was used to examine the area of myelinated fibre calibre in the proximal and distal sciatic nerve stumps following the nerve injury. This technique illustrates the rate of nerve recovery as indicated by the increase in myelinated fibre calibre; the greater the fibre area the better the nerve recovery. In the sciatic nerve crush mice treated with SLIGRL-NH_2, the significant increase in myelinated fibre calibre area in the distal stumps confirmed that neurons have a better rate of recovery when treated with the PAR_2 agonist. This significant increase in myelinated fibre calibre area in the distal stump and the increase in the rate of nerve function recovery due to PAR_2 activation could be attributed to a variety of factors. Studies have suggested that Schwann cells serve as targets or guidance cues for sprouting neurons [83]. Thus, it is possible that PAR_2 activation may promote Schwann cell proliferation, which then could promote nerve fibre regeneration. Neurotrophic factors and their receptors have also been known to be upregulated in the dorsal root ganglion and Schwann cells following peripheral nerve injury [84, 85]. It is therefore possible that PAR_2 may contribute to the upregulation of these factors and/or receptors thereby promoting peripheral nerve regeneration. In addition to the potential promotion of Schwann cell proliferation and upregulation of neurotrophic factors, the known involvement of PAR_2 activation in promoting vasodilation [86] and vascular permeability[66] may also indirectly contribute to peripheral nerve regeneration. By increasing the blood flow to the area and providing easier access to the site for macrophages and other infiltrating cells, PAR_2 activation may

indirectly aid in peripheral nerve regeneration by promoting or advancing the degenerative and clearance process at the injury site. Alternatively, PAR_2 activation by PAR_2-AP has also been documented to exert anti-inflammatory activities [87] and therefore could aid in the regenerative process by lessening the deleterious effects of the inflammation induced by the injury.

The incorporation of PAR_2 deficient mice to the study was done for two reasons. The first was to see if the absence of PAR_2 had any effect on the rate of peripheral nerve regeneration following nerve injury. The second was to look at whether or not PAR_2 was being activated by potential endogenous proteases present in the microenvironment of the nerve injury site. The significant increase in hyperalgesic response to thermal and mechanical stimulation in the $PAR_2^{(-/-)}$ sciatic nerve crush mice compared to WT mice was quite unexpected because of the known effects of PAR_2 activation at inducing hyperalgesia and allodynia, and because of the decreased inflammatory pain symptoms observed in PAR_2 $^{(-/-)}$ mice [76]. The increased hyperalgesia associated to sciatic nerve crush in $PAR_2^{(-/-)}$ mice could perhaps be explained by a protective role of basal PAR_2 activation during situations involving peripheral nerve injury. Similarly, when tested with a more severe degree of peripheral nerve injury (sciatic nerve transection) hyperalgesic responses were also observed; however, the responses were not as prominent, and were not sustained over a lengthy period of time, unlike in the sciatic nerve crush mice. In terms of peripheral nerve regeneration, PAR_2 deficiency in mice did not appear to inhibit or promote peripheral regeneration. This observation would suggest that during the course of nerve injury, PAR_2 activation by endogenous proteases is not necessarily

involved in recovery and peripheral nerve regeneration. However, a knockout model is not a completely infallible model, as it is known that other compensatory mechanisms may counterbalance the deficiencies brought about by the absence of PAR_2.

Sciatic nerve crush or axonotmesis is a milder degree of nerve injury characterized by damage to the axoplasm and cells membrane in spite of preservation of the Schwann cells and connective tissue elements. Sciatic nerve transection or neurotomesis is the most severe degree of nerve injury characterized by the complete severance of the peripheral nerve trunk, which includes both the axon and the surrounding stromal tissue [3, 4]. Although the two nerve injury models demonstrated the pro-regenerative effects of exogenous PAR_2 activation following nerve injury, the differences noted between the two models could reflect the altered role of PAR_2 activation. This observation is most evident in the mechanical nociceptive scores of the wild-type mice. Following sciatic nerve transection and treatment with the PAR_2 agonist, peripheral nerve regeneration in wild-type mice was promoted whereas control mice did not show great improvement in mechanical nociceptive recovery. In contrast, with the sciatic nerve crush model, control mice experienced an extended hyperalgesic response whereas in the SLIGRL-NH_2 treated mice, a brief period of hyperalgesia was shortly followed by a return to basal levels. What this result suggests is that in milder cases of peripheral nerve injury, PAR_2 appears to aid in peripheral nerve regeneration by reducing the hyperalgesic response induced by the sciatic nerve crush.

Ultimately, the results suggest that PAR_2 has a pro-regenerative function following nerve injury as seen by the nociceptive, and morphometrical data presented. In summary, PAR_2 activation promotes peripheral nerve regeneration of thermal nociceptive fibres following sciatic nerve crush or transection as treatment with the PAR_2 agonist reduced the recovery time required for thermal withdrawal latency times to return back to basal levels. PAR_2 activation also appears to promote peripheral nerve regeneration of mechanical nociceptive fibres, but the method of promotion deemed to be dependent on the degree of nerve injury. More specifically, in sciatic nerve crush injuries, PAR_2 activation appeared to reduce the period of mechanical hyperalgesia that accompanied the peripheral nerve injury, thereby reducing the time need to recover back to normal (basal) mechanical nociceptive scores. In sciatic nerve transection injuries, PAR_2 activation simply appeared to promote peripheral nerve regeneration by reducing the time required to return back to baseline levels. Morphometrically, the significant increase in the fibre calibre confirms the pro-regenerative role of PAR_2 activation seen in the behavioural data collected *in vivo*. Lastly, from the PAR_2 knockout model, it can be suggested that PAR_2 has a protective role in lessening the nociceptive response, as a heightened nociceptive response in thermal and mechanical nociception was observed in the mice deficient in PAR_2.

Chapter Four: **Promotion of Neurite Outgrowth in Primary Sensory Neurons by PAR_2 Activation**

4.1 Study Introduction, and Objectives

Once it was identified that treatment with SLIGRL improved the rate of sciatic nerve regeneration *in vivo*, the next step in this study was to identify where PAR_2 is being activated. Various cell types have been identified in participating in the process of regeneration including Schwann cells, which are the main supporting cells of the peripheral nervous system, macrophages, which are the inflammatory cells known to infiltrate the area of injury to remove myelin and debris [7], and of course, the neuronal cell bodies located in the DRG, which undergo changes that are aimed at halting the synaptic function of the neuron and increasing the regeneration potential of the neuron [12-16]. To narrow the possibilities down from the sciatic nerve injury models, an *in vitro* approach was taken to study the effects of PAR_2 activation on nerve regeneration. Since PAR_2 has already been identified in the DRG neurons [61], it was decided to examine the effects of PAR_2 agonist on neurite outgrowth, using a primary neuronal culture model, isolating mice DRG.

Two parameters were used to examine to effects of PAR_2 activation on primary neuron cultures. First, the percentage of cells with neurite outgrowth was compared among groups. Our objective was to investigate whether a PAR_2 agonist could have an effect on promoting or initiating neurite outgrowth in primary cultures of sensory neurons. Second, neurite length was averaged among all groups. Our objective was to investigate whether

PAR_2 agonists had any effect on promoting neurite extension. Additionally, in order to ensure that the effects of SLIGRL on neurite outgrowth was due to the activation of PAR_2, the neurite outgrowth assays were also performed in neurons isolated from wild-type or PAR_2 deficient mice.

4.2 Experimental Methods

For techniques used in this chapter, see sections 2.4.1 and 2.10

Study Design

Neurons isolated from either wild-type or PAR_2 deficient mice DRGs were incubated for 48 hours in conditioned media. Cells were incubated in conditioned media immediately after isolation starting at day 0. Media conditions for the primary neurons in the neurite outgrowth study included SLIGRL 2μM, SLIGRL 20μM, SLIGRL 100μM, positive control NGF 100ng/mL, vehicle control (hepes buffer), or control peptide inactive on PAR_2 (LRGILS 100μM). Cells were immunostained for neurofilaments and evaluated for neurite outgrowth 48 hours after their isolation and incubation.

4.3 Results

4.3.1 Effects of PAR_2 Agonist on Neurite Outgrowth and Average Neurite Length in Primary Sensory Neurons Isolated from C57Bl/6 Mice

Over a 48 hours incubation period, the percentage of primary neurons incubated with SLIGRL (20μM, n=12) showed a significant ($p<0.05$) increase in neurite outgrowth, compared to the neurons treated with the reverse peptide, LRGILS (100μM, n=11)

(SLIGRL mean: 36.2 $\pm$ 4.7% vs. LRGILS mean 19.4 $\pm$ 2.6%) (Figure 4-1A). Moreover, the percentage of cells with neurite outgrowth seen in the SLIGRL incubation (20μM) (mean: 36.2 $\pm$ 4.7%) was comparable to the effects of nerve growth factor (NGF) (100ng/mL, n=12) (mean: 37.2 $\pm$ 3.5%). No significant difference was found between groups, on the average neurite length (B).

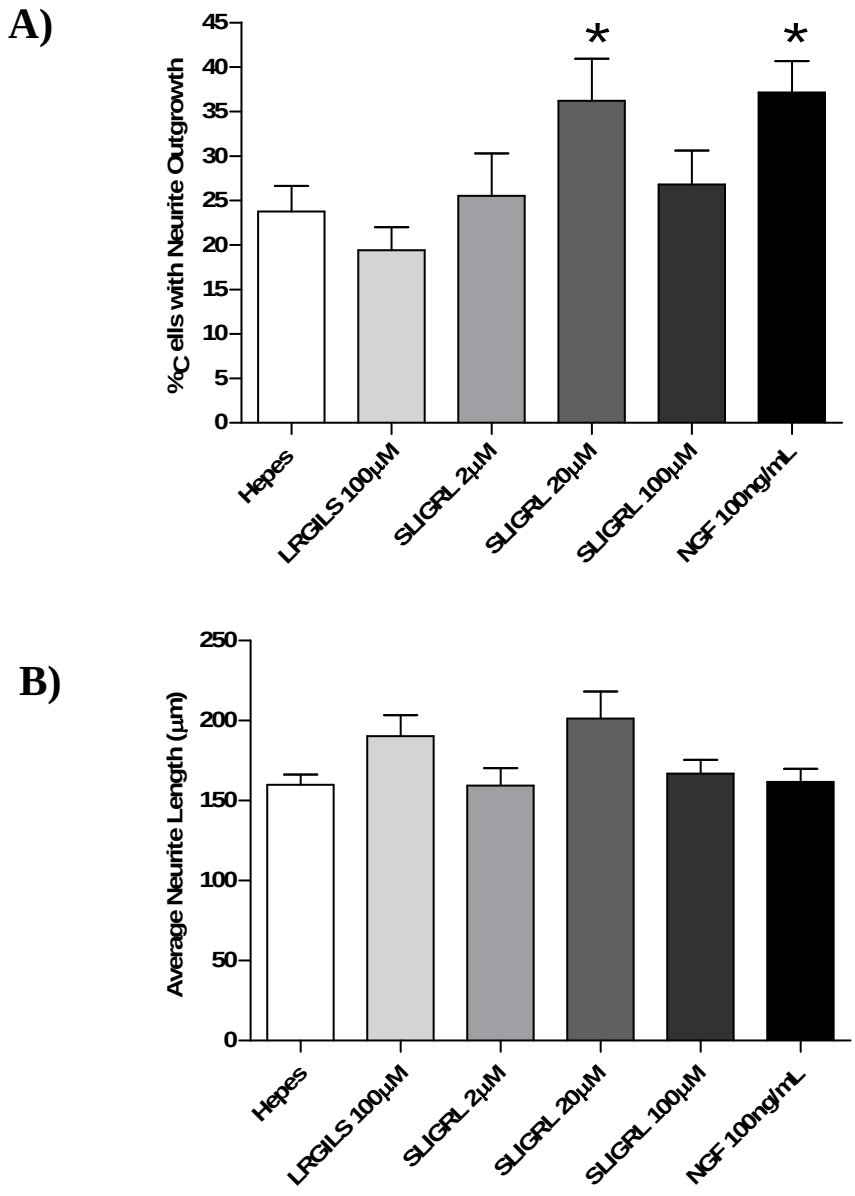

Figure 4-1. Measurement of Neurite Outgrowth on Primary Neurons Isolated from Wild-type Mice DRGs

Primary neurons isolated from 4-6 weeks old wild-type mice were incubated in conditioned media for 48 hours. Percentage of cells with neurite outgrowth (A) and average neurite length (B) were evaluated for the neurite outgrowth assay. Data were expressed as mean ± SEM; *means values were significantly different for $p < 0.05$ in comparison to the peptide control LRGILS (100µM).

4.3.2 Effects of SLIGRL on Neurite Outgrowth and Average Neurite Length in Primary Sensory Neurons Isolated from PAR_2 $^{(-/-)}$ Mice

The concentration of SLIGRL (20 μM), which exhibited significant neurite outgrowth in primary neurons isolated from wild-type mice, was used to evaluate neurite outgrowth and average neurite length in primary neurons isolated from PAR_2 $^{(-/-)}$ mice. There was no significant difference between PAR_2 agonist (n=6) and vehicle-treated neurons (n=6) both for neurite outgrowth (Figure 4-2A) and neurite length (Figure 4-2B). However, like in neurons isolated from wild-type mice, NGF (n=6) was able to significantly increase neurite-like outgrowth compared to the hepes-treated cells Figure 4-2A.

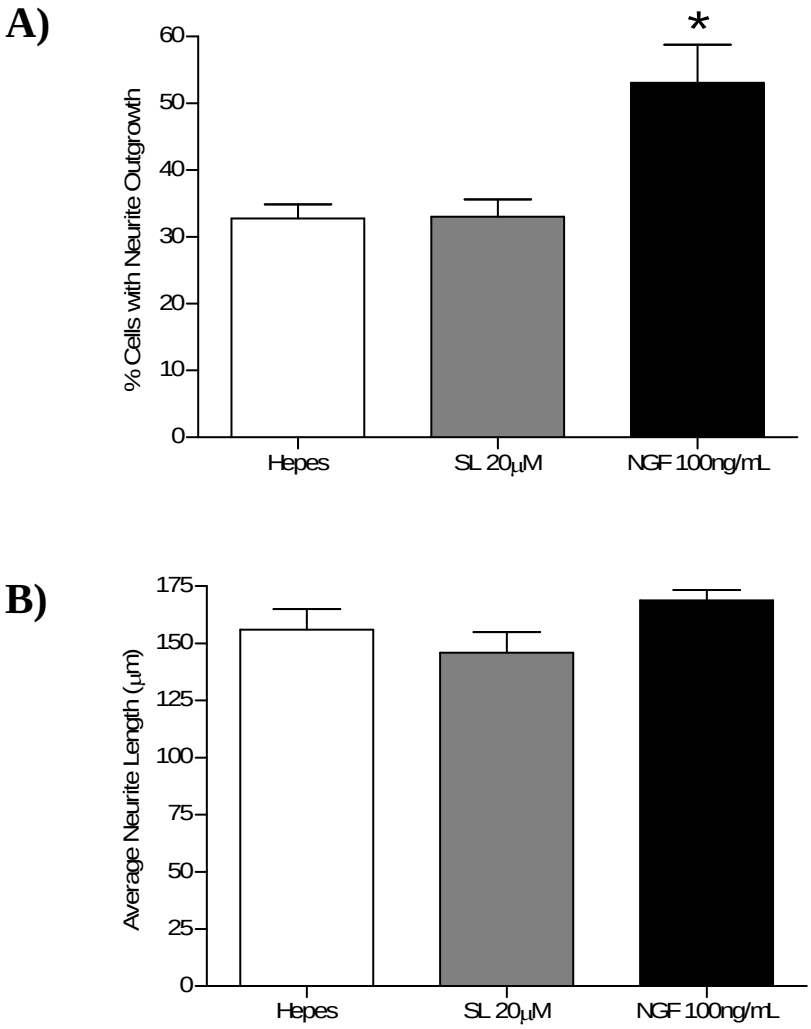

Figure 4-2. Measurement of Neurite Outgrowth in Primary Neurons Isolated from $PAR_2^{(-/-)}$ Deficient Mice DRGs

Primary neurons isolated from 4-6 weeks old $PAR_2^{(-/-)}$ deficient mice were incubated in conditioned media for 48 hours. Percentage of cells with neurite outgrowth (A) and average neurite length (B) were evaluated for the neurite outgrowth assay. Data were expressed as mean ± SEM; *means values were significantly different for $p < 0.05$ from control vehicle hepes.

4.4 Discussion

From the *in vivo* study discussed in the previous chapter, which examined the effects of PAR_2 agonist local treatment following the induction of nerve injury, it was suggested that PAR_2 had a pro-regenerative effect. The purpose of this section of the study was to examine the effects of PAR_2 activation on neurite outgrowth in primary neural cells isolated from mouse DRGs.

The main finding of this study was that addition of the PAR_2-AP did in fact promote neurite outgrowth and increased neurite length in primary neurons isolated from mouse DRGs. In order to ensure the effects of SLIGRL was specific of PAR_2 activation, two different controls were used, the vehicle Hepes, and the reverse peptide LRGILS and experiments were reproduced in PAR_2 deficient neurons. In order to ensure the cells were not damaged and neurite outgrowth was measurable using these primary cultured cells a NGF positive control was added to the assay. Additionally, three different concentrations of SLIGRL were assayed to find the most optimal concentration for the neurite outgrowth assay.

The most optimal SLIGRL concentration for this neurite outgrowth assay was 20μM. At this specific concentration, the percentage of cells with neurite outgrowth was significantly different from the reverse peptide negative control, LRGILS 100μM. The neurons that were cultured in 2μM and 100μM concentrations of SLIGRL did show an increase in the percentage of cells with neurite outgrowth, but the values were not significant from the negative control, LRGILS. Thus, it appeared that at low

concentrations of SLIGRL, PAR_2 is not effectively activated to significantly induce neurite outgrowth. At SLIGRL concentrations that were too high, there appeared to be an inhibitory effect, which impedes the neurite outgrowth. This phenomenon of neurite outgrowth inhibition with higher concentrations of SLIGRL is similar to a study, which has described similar effects with the addition of high concentrations of NGF to chick embryo dorsal root ganglia neurons [88]. Researchers observed neurite outgrowth in the chick dorsal root ganglia at low NGF concentrations, whereas at high NGF concentrations, growth cones and neurites collapsed and retracted towards the cell body. Similarities between NGF and the PAR_2-AP, SLIGRL (20μM) also extend to the values for the percentage of cells with neurite outgrowth. At the 20μM concentration, the mean of percentage of cells with neurite outgrowth was 36.2 $\pm$ 4.7%, which was extremely close to the NGF positive control, which had a mean of 37.2 $\pm$ 3.5%. In terms of average neurite length, no differences were observed among the SLIGRL group, the vehicle control, the reverse peptide control and the positive control NGF.

These results confirm the *in vivo* data observed with the sciatic nerve injury models. Activation of PAR_2 by SLIGRL promotes neurite outgrowth and ultimately nerve regeneration. Furthermore, these studies localize the activation of PAR_2 by SLIGRL to cell types located in the nervous system. However, although this primary culture has narrowed the activation of PAR_2 down to the nervous system, there are a number of other cell types that are present in the culture along with the neurons, which could be potential targets for PAR_2 activation. For instance, we cannot rule out an additional role for PAR_2 activation on macrophage infiltrated upon injury. However, our *in vitro* results showing a

role for PAR_2 activation on DRG cultures led us to further investigate *in vitro*, the potential target sites of PAR_2 activation to promote neurite outgrowth in neuronal cultures.

Chapter Five: **Characterization of PAR_2 in PC12 cells and Role of PAR_2 Agonist in PC12 Neurite Outgrowth**

5.1 Study Introduction, and Objectives

The PC12 cell line is an adrenal medullary cell line that was first established from transplantable rat adrenal pheochromocytoma and is presently the most widely used cell line to study neurite outgrowth. Its responsiveness to treatment with NGF has deemed it a suitable model to study the mechanisms underlying neuronal differentiation and signal transduction. Specifically, in the presence of NGF, PC12 cells have been shown to respond to NGF with reversible loss of mitotic activity and differentiation to a neuronal phenotype.

The goal of using this model was to see if PAR_2 activation could reproduce neurite outgrowth in the PC12 cell line similar to the action elicited by NGF, thereby evaluating whether or not PAR_2 could exert a direct growth factor like effect on neurons. However, before beginning the neurite outgrowth assay, it was considered important to characterize the PC12 cell line with respect to PAR_2. First, an RT-PCR was performed on the PC12 cell line to evaluate PAR_2 mRNA expression. Second, PAR_2 protein expression and function in the PC12 cell line was characterized using immunocytochemistry and Ca^{2+} signalling. Third, the PC12 cells were evaluated for PAR_2-induced neurite outgrowth with the neurite outgrowth assay.

5.2 Experimental Methods

For techniques used in this chapter, see sections 2.4.2, 2.6, 2.7, 2.9, and 2.10.

Study Design

PC12 cells cultured overnight were used for PAR_2 mRNA and protein detection. RT-PCR was used for PAR_2 mRNA detection. Rat colon was used as a PAR_2 positive control. Glyceraldehyde-3-phosphate dehydrogenase (GAPDH) was chosen as the internal positive control for mRNA. GADPH was used as an mRNA positive control because it is a well-characterized enzyme with a key role in glycolysis whose expression remains constant under a wide variety of physiological conditions.

Immunocytochemistry was used to detect PAR_2 protein expression in PC12 cells. Cells were cultured overnight, fixed, and immunostained for PAR_2. Two negative controls were used to eliminate the potential of false positive signals and included: 1) cell incubation with no primary, but with secondary antibody (1:5000), and 2) cell incubation with primary (1:500), but no secondary antibody.

PAR_2 protein detection was also evaluated in PC12 cells using a calcium mobilization assay. Calcium mobilization was tested with the PAR_2 agonist, SLIGRL (200μM). Bradykinin (2.5nM) was used as a positive control for calcium mobilization in PC12 cells.

PAR_2 induction of neurite outgrowth in PC12 cells was evaluated using the neurite outgrowth assay. Cells were incubated in conditioned media for 72 hours prior to fixation, neurofilament immunostaining and evaluation. Treatment conditions for the PC12 cells in the neurite outgrowth study were as follows: SLIGRL 20μM, positive control NGF 100ng/mL, vehicle (hepes buffer), or control peptide (LRGILS 20μM). In order to ensure that the most effective SLIGRL concentrations were being used in the neurite outgrowth assays, a PC12 dose response curve of SLIGRL was also performed. Cells were incubated in conditioned media for 72 hours and SLIGRL concentrations included 100μM, 50μM, 20μM, 10μM, 5μM, 1μM and 1nM. The control reverse peptide, LRGILS (100μM), was used at the concentration of 100μM.

5.3 Results

5.3.1 Detection of PAR_2 mRNA Expression in PC12 Cells

PAR_2 mRNA signal (502bp) was found in PC12 cells and rat colon samples were used as positive controls. GAPDH was the house-keeping gene used as an internal positive control and was located at the 306bp level.

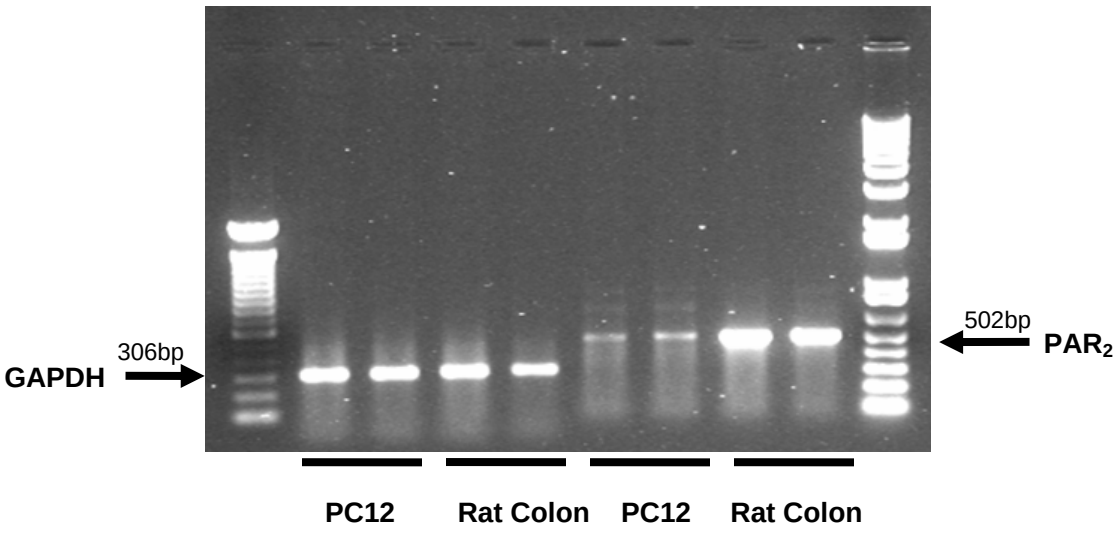

Figure 5-1. Detection of PAR_2 mRNA Expression in PC12 Cells Using RT-PCR and Gel Electrophoresis.

5.3.2 Detection of PAR_2 Protein Expression in PC12 Cells

PAR_2 protein expression was detected in the PC12 cells fixed on collagen coated plates using an A5 antibody, which is a polyclonal anti-PAR_2 antibody raised in rabbit (1:500) and a polyclonal donkey anti-rabbit conjugated to a Cy3 fluorescent label used as a secondary antibody (1:5000) (Figure 5-2). No emission signal was detected in the two negative control groups, where either the primary antibody or the secondary antibody was omitted from the immunostaining procedure.

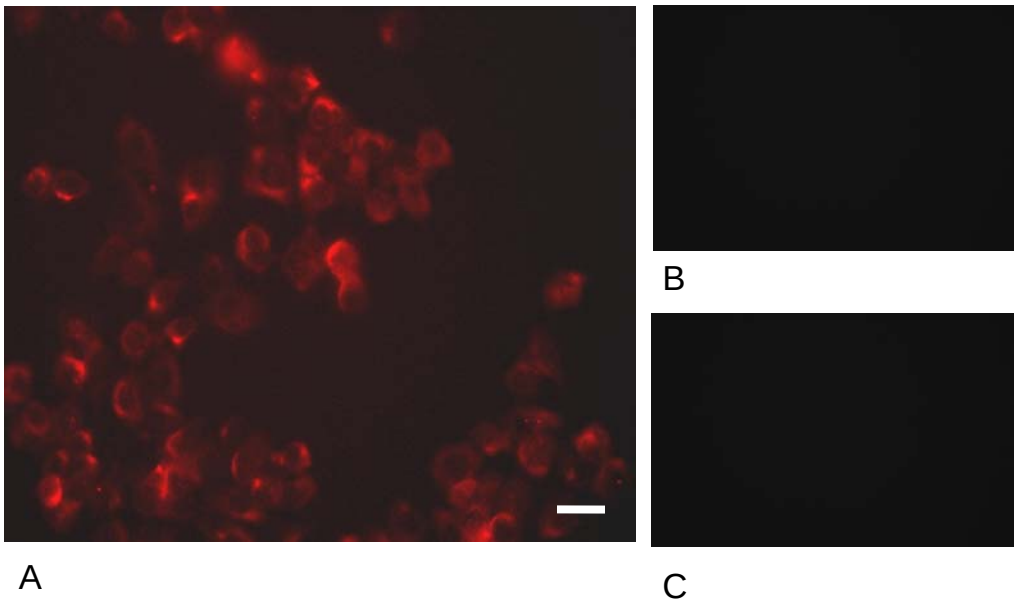

Figure 5-2. Immunocytodetection of PAR-2 Protein Expression in PC12 Cells

PC12 cells cultured overnight were immunostained for PAR_2 protein expression. A) PC12 cells (n =4) labeled with an anti-PAR_2 rabbit polyclonal primary antibody (1:500), scale bar 15μm; Cy3 labeled polyclonal donkey anti-rabbit secondary antibody (1:5000). B) PC12 negative control (n=4); no primary; Cy3 labeled polyclonal donkey anti-rabbit secondary antibody (1:5000). C) PC12 negative control (n=4); anti-PAR_2 rabbit polyclonal primary antibody (1:500); no secondary.

5.3.3 Ca^{2+} Signalling in PC12 cells

SLIGRL (200μM) added to the PC12 cells in suspension did not elicit a Ca^{2+} signal. In contrast, bradykinin (2.5nM) was able to induce Ca^{2+} mobilization when it was added moments later to the same cell suspension (Figure 5-3).

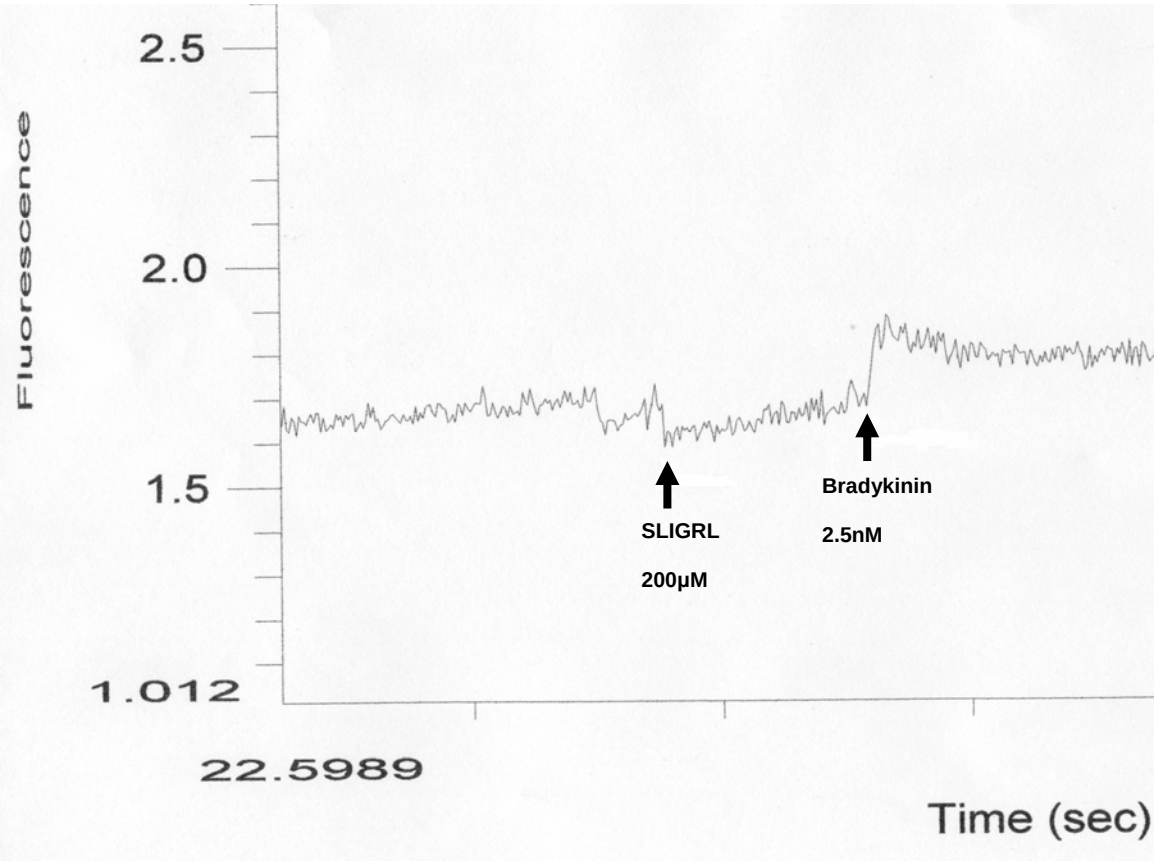

Figure 5-3. Representative Trace of Ca^{2+} Mobilization of PC12 cells in Suspension

Schematic trace showing the calcium response in PAR_2-expressing PC12 cells. Calcium response was tested with SLIGRL (200μM) and bradykinin (2.5nM).

5.3.4 Effects of PAR_2 Agonist on PC12 Neurite Outgrowth

The PC12 neurite outgrowth assay was followed for 7 days. At the end of the 7th day of incubation, cells were fixed, stained, and evaluated for neurite outgrowth. A significant ($p<0.001$) increase in the percentage of cells with neurite outgrowth was seen in the NGF-treated group (n = 6, mean: 84.4%, SE: $\pm$ 4.3), in comparison to the control groups with vehicle only (hepes) (n = 6, mean: 0.6%, SE: $\pm$ 0.2), or control peptide (LRGILS 20μM) (n = 6, mean: 1.4%, SE: $\pm$ 0.4) (Figure 5-4A). Cells incubated with SLIGRL (20μM) (n = 6, mean: 1.0%, SE: $\pm$ 0.2) did not show significant differences in the percentage of cells with neurite outgrowth when compared to hepes or LRGILS-treated cells. Similar results were observed for average neurite length. NGF-treated cells showed a significant ($p<0.001$) increase (n = 6, mean: 138μm, SE: $\pm$ 14) in average neurite length. However, the average neurite lengths of SLIGRL (20 μM)-treated cells (n = 6, mean: 12μm, SE: $\pm$ 2.8) were not significantly different when compared to the negative controls, hepes (n = 6, mean: 8.9, SE: $\pm$ 3.8) and LRGILS (20 μM) (n = 6, mean: 15.0%, SE: $\pm$ 5.4) (Figure 5-4B).

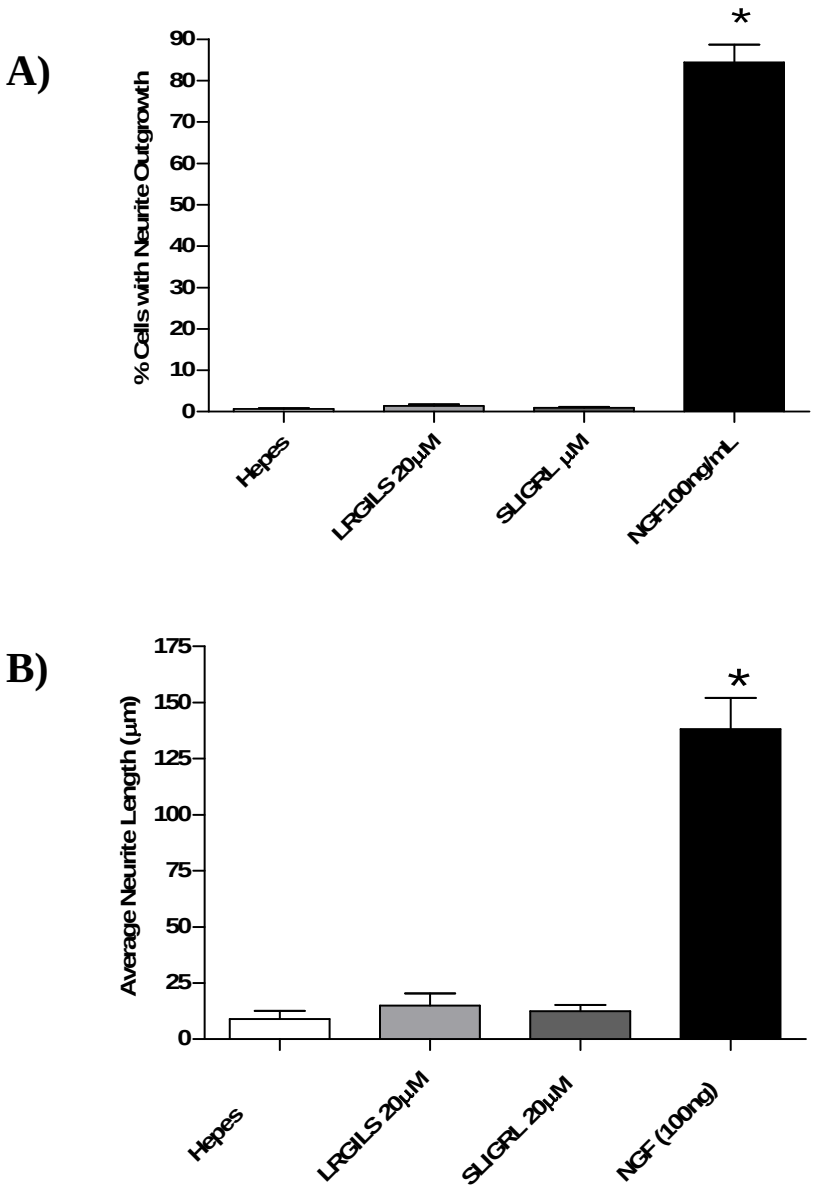

Figure 5-4. Measurement of Neurite Outgrowth in PC12 Cells Incubated with PAR_2 Agonist

PC12 cells incubated in conditioned media for 72 hours. Percentage of cells with neurite outgrowth (A) and average neurite length (B) were evaluated for the neurite outgrowth assay. Data were expressed as mean ± SEM; * means values were significantly different for $p < 0.05$ when compared to the vehicle control (hepes) or the peptide control (LRGILS 20µM).

5.3.5 Dose Response of PAR_2 Agonist on PC12 Neurite Outgrowth

In using only one concentration it was deemed important to see if other concentrations of SLIGRL would yield the same results as the 20μM concentration used in the previous neurite outgrowth assays. Therefore, a dose response curve was performed in PC12 cells exposed to SLIGRL and cell neurite outgrowth was evaluated. A very small portion of cells with neurite outgrowth was observed after exposure to SLIGRL or LRGILS (Figure 5-5A). Means of the groups ranged from a low of 0.3% $\pm$ SEM 0.2 (n=4) in the SLIGRL 5μM group to a high of 0.8% $\pm$ SEM 0.4 (n=4) in the LR 100μM group, but no significance difference was found among the SLIGRL-treated groups or the control reverse peptide control group, LRGILS. Similarly, with respect to average neurite length, no significant difference was found among the SLIGRL-treated groups or the control reverse peptide group (Figure 5-5B). Average neurite lengths ranged from 4.6μm $\pm$ SEM 2.0 (n=4) in the SLIGRL 50μM group to 1.2μm $\pm$ SEM 1.2 (n=4) in the SLIGRL 1μM group.

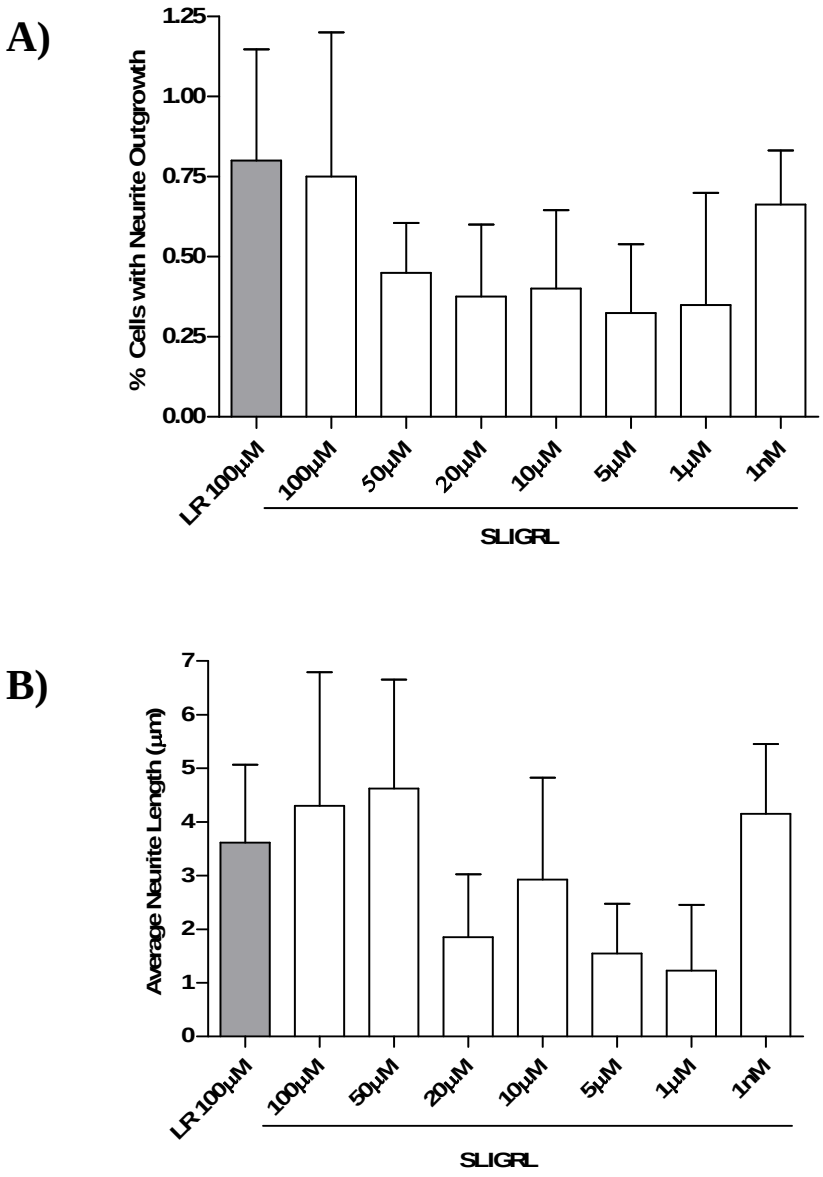

Figure 5-5. Dose Response of PAR_2 Agonist on PC12 Cell Neurite Outgrowth

PC12 cells incubated in media supplemented with the PAR_2-AP, SLIGRL-NH_2, or the control peptide, LRGILS-NH_2, for 72 hours. Percentage of cells with neurite outgrowth (A) and average neurite length (B) were evaluated for the neurite outgrowth assay. Data were expressed as mean ± SEM.

5.4 Discussion

Considering the primary neuronal culture indicated that PAR_2 activation was capable of inducing neurite outgrowth, it appeared promising to focus solely on the cells located in the peripheral nervous system as potential targets for PAR_2 activation. However, even though a primary neuronal culture was used, it would not be accurate to say that PAR_2 induced neurite outgrowth through a direct mechanism on sensory neurons. The reason for the caution stems from the fact that when the neurons were cultured from the dorsal root ganglions the culture was not purified to eliminate other cell types. Thus, other cells types including SCs and fibroblasts were most likely present and active in the culture.

As aforementioned, the PC12 cell line is a cell line that is extensively used to study the mechanisms of neurite outgrowth. Therefore the goal for using the PC12 cell line was to eliminate the other cell types and focus on the neurons. Prior to looking at neurite outgrowth, it was important to see if PAR_2 expression was present in the PC12 cell line. Finding both PAR_2 mRNA and protein expression on the PC12 cell line made it a favourable cell line to work with and thus, the neurite outgrowth assay was performed. However, when the SLIGRL 20μM was compared to the negative controls, hepes and LRGILS for neurite outgrowth and neurite length, no significant differences were observed. The functionality of PAR_2 could be questioned. From the Ca^{2+} signalling assay, it was observed that addition of SLIGRL to the cell in suspension did not produce a detectable Ca^{2+} signal, which could suggest that PAR_2 is not functional on these PC12 cells. However, there are a couple of considerations that needs to be taken with this set of data. First, the Ca^{2+}-signalling assay may not have worked due to the fact that some cells

need to be attached to an adherent surface such as collagen to function properly and in our assay, PC12 cells were used in suspension. However, the fact that PC12 cells in suspension responded by Ca^{2+} mobilization to bradykinin argues against this hypothesis. Another possibility that needs to be considered is the potential for SLIGRL to activate PAR_2 and signal intracellularly through a Ca^{2+} independent pathway such as the mitogen-activated protein kinase (MAPK) pathway, which includes extracellular-signal regulated kinase (ERK), the ERK kinase (MEK) and the ribosomal protein S6 kinase (RSK). Additionally, the 20μM SLIGRL concentration that was used on the PC12 cells for the neurite outgrowth assay may not be effective for this cell type. Just because the 20μM concentration of SLIGRL worked for the primary neurons, it does not mean that the same concentration of SLIGRL will work with the PC12 cells. Therefore, a dose response curve was performed on the PC12 cells using various concentrations of SLIGRL.

Comparing the various SLIGRL concentrations to the reverse peptide negative control, no significant differences were found in either of the neurite outgrowth parameters in the PC12 dose response assay. Although PAR_2 mRNA and protein was found to be expressed on PC12 cells, the data presented suggests that PAR_2 activation with SLIGRL does not promote neurite outgrowth through a direct mechanism of activation on neurons.

Chapter Six: **PAR_2 Activation and Inhibition of NGF Induced Neurite Outgrowth in PC12 Cells**

6.1 Study Introduction and Objectives

Discovered by Levi-Montalcini in the early fifties, NGF was the first neurotrophic factor described [20, 25, 89]. NGF belongs to a family of proteins termed the neurotrophins and is involved in neuronal, development, growth, maintenance, and survival. The active form of NGF exists as a 118 amino acid dimer and is more commonly known as β-NGF [90]. NGF has two distinct categories of receptors; the first is the low affinity receptor termed the p75 receptor, and the second are the family of tyrosine receptor kinase (trk) receptors of which there are three, trkA, trkB, and trkC.

NGF can interact independently with its receptors to elicit its effects, but NGF-receptor interaction does not have to be completely exclusive. Researchers have found that GPCRs and inflammatory molecules can act in conjunction with NGF or its receptors to enhance neurite outgrowth or differentiation. In 1996, a study was performed to examine the role of the inflammatory mediator, IL-6, in PC12 neuronal differentiation [91]. They proposed that the inflammatory mediator IL-6 potentiates NGF signaling rather than act as an autonomous inducer of neuronal differentiation. What they found was that IL-6 was not capable of inducing neurite outgrowth in PC12 cells alone, but required low levels of trk/NGF receptor activity. More recently, in 2005, another study was released documenting the activation of the GPCR, $P2Y_2$, by $ATP_\gamma S$ in the presence of NGF and its involvement in enhancing neuronal differentiation [92]. More specifically, they found that $ATP_\gamma S$ promotes phosphorylation of trkA, ERK1/2, and p38 thereby enhancing

sensitivity to NGF and accelerating neurite formation in both PC12 cells and neurons isolated from DRGs.

With these two studies in mind, it was deemed interesting to see if PAR_2, a known inflammatory mediator and GPCR, would have similar effects on PC12 cells neuronal differentiation. Thus, the objective of these set of experiments was to see if PAR_2 activation by SLIGRL could potentiate NGF-induced neurite outgrowth.

6.2 Experimental Methods

For techniques used in this chapter see sections 2.4.2 and 2.10.

Study Design

A NGF dose response curve was performed on PC12 cells in order to select the optimal NGF concentration for the PC12 cell NGF-SLIGRL co-incubation neurite outgrowth assay. PC12 cells were incubated in NGF conditioned media for 72 hours and NGF concentrations for the dose response curve included 100ng/mL, 50ng/mL, 25ng/mL, 10ng/mL, 1ng/mL, and 0.5ng/mL.

For the PC12 cell NGF-SLIGRL co-incubation neurite outgrowth assay, cells were incubated for 72 hours in conditioned media, which contained 1ng/mL NGF and one of the following SLIGRL concentrations: 100μM, 50μM, 20μM, 10μM, 5μM, 1μM and 1nM. For a negative peptide control, PC12 cells were incubated with the reverse peptide LRGILS (100μM) and NGF (1ng/mL).

6.3 Results

6.3.1 Effects of NGF on PC12 Neurite Outgrowth

PC12 cells were incubated with various concentrations of NGF ranging from 100ng/mL to 0.5ng/mL. No significant difference among the various concentrations was seen in the percentage of cells with neurite outgrowth (Figure 6-1A). The lowest percentage of cells with neurite outgrowth was observed at the 1ng/mL concentration of NGF with a value of 4.5% $\pm$ SEM 0.7 (n=8). At the 10ng/mL NGF concentration, the percentage of cells was the highest at 8.8%$\pm$ SEM 1.5 (n=8). No significant difference was seen in the average neurite length of the PC12 cells treated with NGF (Figure 6-1B). The mean average neurite lengths ranged from a minimum of 40.0μm $\pm$ SEM 6.9 (NGF 100ng/mL; n=16) to a maximum of 51.5μm $\pm$ SEM 6.8 (NGF 25ng/mL; n=8).

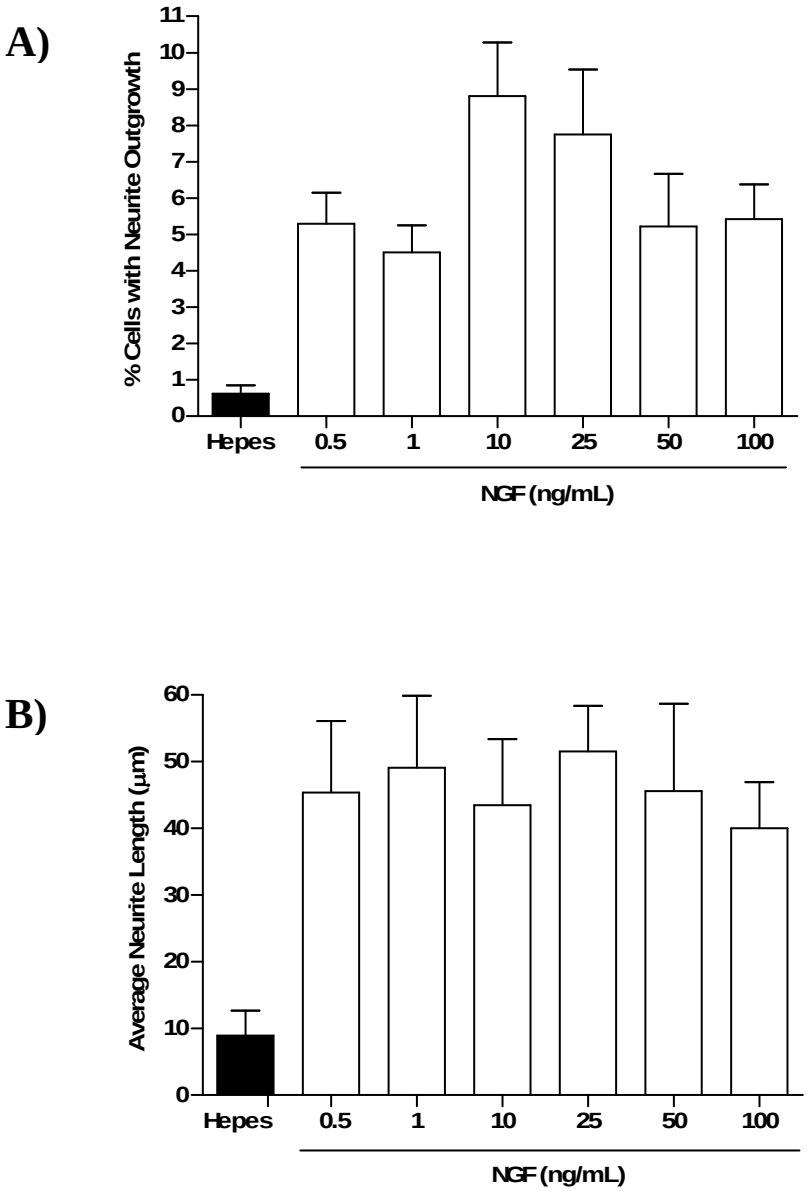

Figure 6-1. Dose Response of NGF-induced Neurite Outgrowth in PC12 Cells

PC12 cells incubated in conditioned media for 72 hours. Percentage of cells with neurite outgrowth (A) and average neurite length (B) were evaluated for the neurite outgrowth assay. Data were expressed as mean ± SEM.

6.3.2 . Inhibition of NGF Induced Neurite Outgrowth by SLIGRL in PC12 Cells

No significant difference was found in the percentage of cells with neurite outgrowth in any of the groups (Figure 6-2A). However, significant decreases in average neurite lengths were seen in the PC12 cells that were co-incubated with NGF (1ng/mL) and SLIGRL concentrations of 100μM ($p<0.05$; n=8), 50μM ($p<0.001$; n=8), 20μM ($p<0.05$; n=8), 10μM ($p<0.01$; n=8), 5μM ($p<0.05$; n=8), and 1μM ($p<0.001$; n=7) (Figure 6-2B). In cells treated with reverse peptide control, LRGILS (100μM; 40.5$\pm$ SEM 6.4; n=7), or very low concentrations of SLIGRL (1nM; 37.5$\pm$ SEM 7.4; n=8), no inhibitory effect was observed on average neurite length and values were comparable to NGF (1ng/mL) alone (55.3$\pm$ SEM 10.2; n=7).

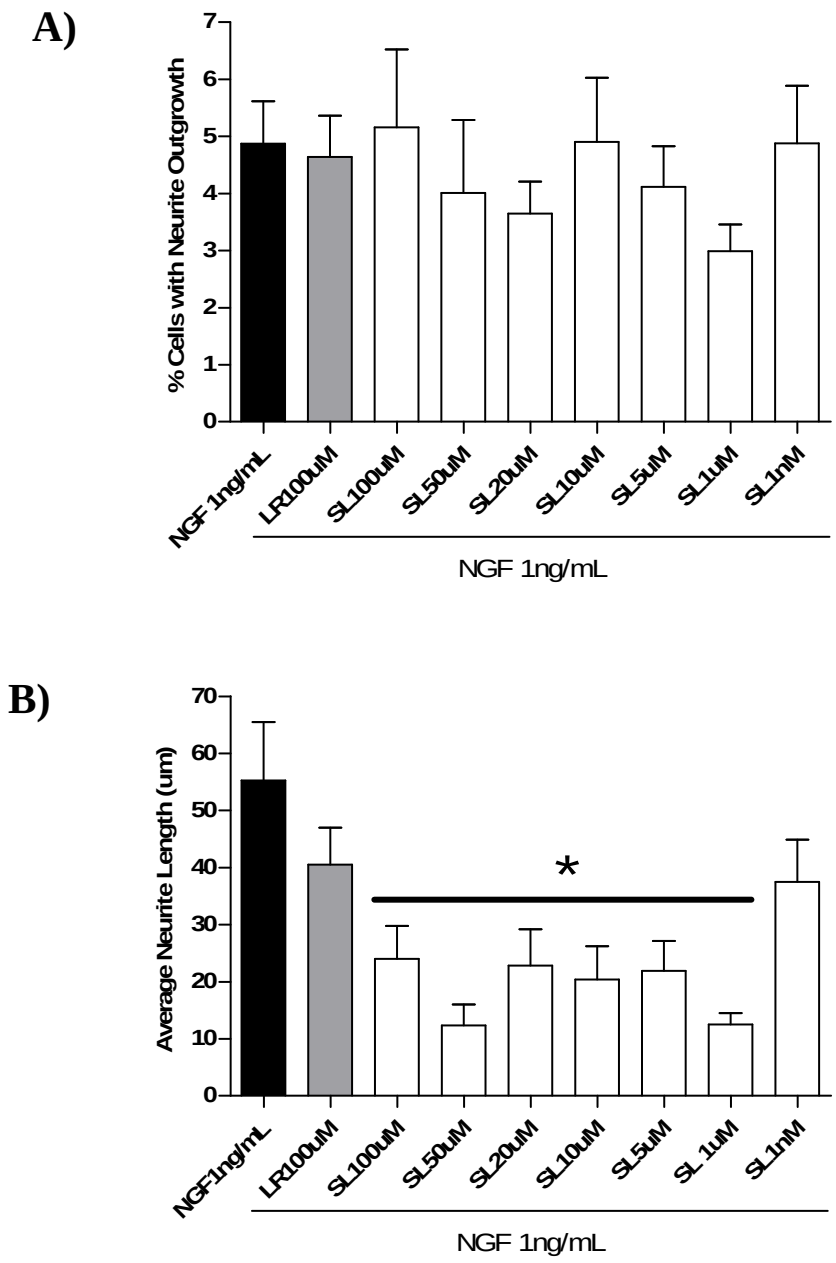

Figure 6-2. SLIGRL Inhibition of NGF-Induced Neurite Outgrowth in PC12 Cells
PC12 cells incubated in conditioned media for 72 hours. Percentage of cells with neurite outgrowth (A) and average neurite length (B) were evaluated for the neurite outgrowth assay. Data were expressed as mean ± SEM; * means values were significantly different for $p < 0.05$, when compared to NGF 1ng/mL.

6.4 Discussion

Since PAR_2 activation by SLIGRL alone did not appear to elicit any effects on PC12 cell neuronal differentiation in earlier studies, the objective of co-incubating the PC12 cells with SLIGRL and NGF was to see if SLIGRL was capable of potentiating neurite outgrowth induced by NGF. By initially doing an NGF dose response curve on the PC12 cells, the best NGF concentration could be determined. The dose of NGF that had the smallest effect on PC12 neurite outgrowth was chosen for the SLIGRL co-incubation experiments. This concentration was used to ensure that NGF was not overshadowing the potential effects of SLIGRL in the neurite outgrowth assay. At the dose 1ng/mL, NGF was still able to differentiate PC12 into neurons and promote neurite outgrowth compared to no NGF treatment; moreover, this concentration still left space for potential neurite outgrowth enhancement by PAR_2 activation.

PC12 co-incubation with SLIGRL and NGF did not appear to have any effect on the neurite outgrowth cell percentage. However, when the average neurite lengths were compared, an unforeseen observation was made. In contrast to what was expected, observations showed that activation of PAR_2 with SLIGRL in the presence of NGF (1ng/mL) in fact reduced average neurite lengths to at least half the size of the neurites in PC12 cells that were incubated in NGF (1ng/mL) alone. The control peptide LRGILS did not reproduce such an effect suggesting that the results observed with SLIGRL was specific of PAR_2 activation. What this result suggests is that PAR_2 is in fact functional in PC12 cells and furthermore, that PAR_2 activation in PC12 cells might be independent of Ca^{2+} mobilization. Unexpectedly, PAR_2 activation on PC12 cells was seen to inhibit

NGF-induced neurite outgrowth. Although unexpected, these observations could be explained by a potential toxic effect of PAR_2 activation in neurons. Earlier research into PAR_2 expression in the central nervous system has found PAR_2 to be neurotoxic in hippocampal cultures [60]. Furthermore, thrombin and synthetic peptide activators of PAR_1, the first member of the PAR family, has also been documented in inhibiting neurite outgrowth and causing neuronal cell death [93]. Lastly, the difficulties and the differences between using a cell line, in comparison to a primary neuronal culture, may explain or resolve the discrepancies between the two cell types. The lack of adherence to the tissue culture plates and immense cell clustering made it quite difficult to evaluate neurite outgrowth in individual PC12 cells. Studies have also shown that subclones of PC12 cells may demonstrate differing degrees of responsiveness to NGF stimulation due to varying degrees of cell heterogeneity [94], which is a common problem seen when establishing and maintaining certain cell lines. Furthermore, differences in PAR_2 protein expression and differences in intracellular signaling pathways may further contribute to the differing outcomes in neurite outgrowth between the two different cell types.

Albeit, interesting, these results do not explain the fact that neurite outgrowth was enhanced in the primary neuronal culture or the pro-regenerative effects of PAR_2 agonists *in vivo*. What these data suggested were that direct PAR_2 activation by SLIGRL did not promote or potentiate neurite outgrowth through direct activation on neurons. Thus, with the insight gained from the experiments performed with the PC12 cells, the next step was to look towards PAR_2 activation on other cell types in the nervous system such as SCs, which may indirectly promote neurite outgrowth in neurons.

Chapter Seven: **Promotion of PC12 Neurite Outgrowth with NGF-SLIGRL-Sciatic Nerve Conditioned Media and Expression of PAR_2 in Schwann Cells**

7.1 Study Introduction, and Objectives

Schwann cells (SCs) are extremely versatile cells that are considered to be essential contributors to nerve regeneration. As a rich source of neurotrophins including NGF [95], BDNF [9], and CNTF [96], studies have shown that SCs do participate in peripheral nerve regeneration [97] and CNS neurite outgrowth [98].

In 1995, a paper was published documenting the relationship between SCs and axons during nerve regrowth. What researchers discovered was that SCs have a very integral involvement in peripheral nerve regeneration [99]. More specifically, they discovered that (i) very few axons can significantly regrow without an intimate partnership with SC processes, (ii) SC migration and proliferation precede and are closely linked with axon growth, and (iii) considerable inhibition of SC proliferation reduces SC migration, axon regrowth, and repopulation of axonal myelination.

There has also been evidence demonstrating the capability of sciatic nerve conditioned media to increase neuronal survival, proliferation, and differentiation in cultured retinal cells [100]. What investigators found was that treatment with sciatic nerve conditioned media increases protein content of the culture three-fold in addition to, stimulating cytoplasmic processes from the retinal cells. In another study looking at PC12 cell neuronal differentiation and sciatic nerve conditioned media, researchers found that

sciatic nerve conditioned medium (SNCM) also promoted neuronal differentiation and neurite outgrowth on PC12 cells [101].

The studies aforementioned inspired the following section of the study. From the previous chapters it was suggested that PAR_2 could induce neurite outgrowth, but it did not appear to be through direct activation of PAR_2 on neurons. Therefore, it was decided that the next cells targeted to study would be SCs. Three main objectives were set out for the next set of experiments. First, we wanted to see if PAR_2 protein is in fact expressed in the proximal and distal stumps of the sciatic nerve tissue following injury. Therefore, sciatic nerve tissues from the sciatic nerve crush study were isolated to look at PAR_2 protein expression. Second, I wanted to see whether or not sciatic nerve conditioned media incubated with SLIGRL could induce PC12 differentiation and neurite outgrowth. Third, I wanted to see if PAR_2 expression could be detected at the cellular level using a primary SC culture.

7.2 Experimental Methods

For techniques used in this chapter, see sections 2.3.7, 2.5, 2.6, 2.8, and 2.11.

Study Design

Following the behavioural tests measurements for sciatic nerve crush experiment, tissue samples sent to Dr. M. D'Andrea from Johnson & Johnson were processed for PAR_2 expression. Both proximal and distal stumps were evaluated for PAR_2 expression using fluorescent immunohistochemistry. Three separate cell markers were used to localize the

PAR_2 protein expression to different cell types in both the proximal and distal stumps of the sciatic nerve tissue. The first marker was a S-100 antibody used to label SCs. The second marker was a GFAP antibody used to label activated SCs, and the last was a MAC-3 antibody used to label macrophages.

For the PC12 cell SLIGRL-SNCM neurite outgrowth assay sciatic nerve isolated from wild-type mice were rinsed, excised and placed in serum free media for 8 days. Media was change every 3 days during the 8 days. At the end of the eighth day media was removed and replaced with serum-free media containing one of the following conditions: PBS, reverse peptide control LRGILS 100 μM, SLIGRL 20μM, and SLIGRL 100μM. After 24 hours the media was removed, frozen at -70^{o}C, and replaced with fresh media containing one of the conditions. This procedure was repeated for another 2 days making a total of 3 media changes. Next, frozen media samples were thawed and PC12 cells were incubated in the conditioned media isolated from the sciatic nerves, which was then supplemented with serum. CM for the PC12 cells were changed every 24 hours for a total of 72 hours days. Additionally, another negative control was added to the assay, which consisted of unconditioned media. At the end of the 72 hours, PC12 cells were fixed, immunostained for neurofilaments, and evaluated for neurite outgrowth.

For the PC12 cell NGF-SLIGRL-SNCM neurite outgrowth assay, the study design is similar to the PC12 cell-SLIGRL-SNCM except for the media condition. In this experiment the serum free media conditions included NGF 1ng/mL, SLIGRL 20μM & NGF 1ng/mL, SLIGRL 100μM & NGF 1ng/mL, or LRGILS 100μM & NGF 1ng/mL.

PAR_2 mRNA and protein was then evaluated in primary SCs isolated from wild-type mice. RT-PCR was used for PAR_2 mRNA detection. NGF was used as a positive indicator of SCs. GAPDH mRNA was used as the internal positive control for reasons previously mentioned. PAR_2 protein expression in SCs was evaluated using immunocytochemistry. The negative control used to eliminate the potential of false positive signals consisted of incubating the cells without primary antibody and only secondary antibody (1:1000).

7.3 Results

7.3.1 Co-expression of PAR_2 and Schwann Cell Markers in the Proximal and Distal Stump of Sciatic Nerve Tissue Following Sciatic Nerve Crush

SCs in the proximal and distal stumps of sciatic nerve tissue were immunolocalized using the S-100 SC marker (green) 4 weeks post-crush injury (**Figure 7-1** A and B). Activated SCs were also immunolocalized using the GFAP activated SC marker (green) (**Figure 7-1** C and D). Macrophages tissue infiltration was detected using the MAC-3 antibody (green) (**Figure 7-1** E). To determine whether PAR_2 was co-localized with SC in the sciatic nerve tissues, PAR_2 expression was stained using an anti-PAR_2 antibody (red). Immunolocalization of PAR_2 (red) revealed a higher expression of the PAR_2 antibody (red) in distal sciatic nerve stump (**Figure 7-1** A-D). In the distal stump, PAR_2 protein was also co-localized with SCs (yellow) (**Figure 7-1** B). PAR_2 protein detection and co-localization was particularly strong in the distal stump immunostained for activated SCs

(yellow) (**Figure 7-1** D). When the distal sciatic nerve stump was evaluated for PAR_2 protein expression (red) and macrophage infiltration (green), both markers co-expressed (yellow) (**Figure 7-1** E).

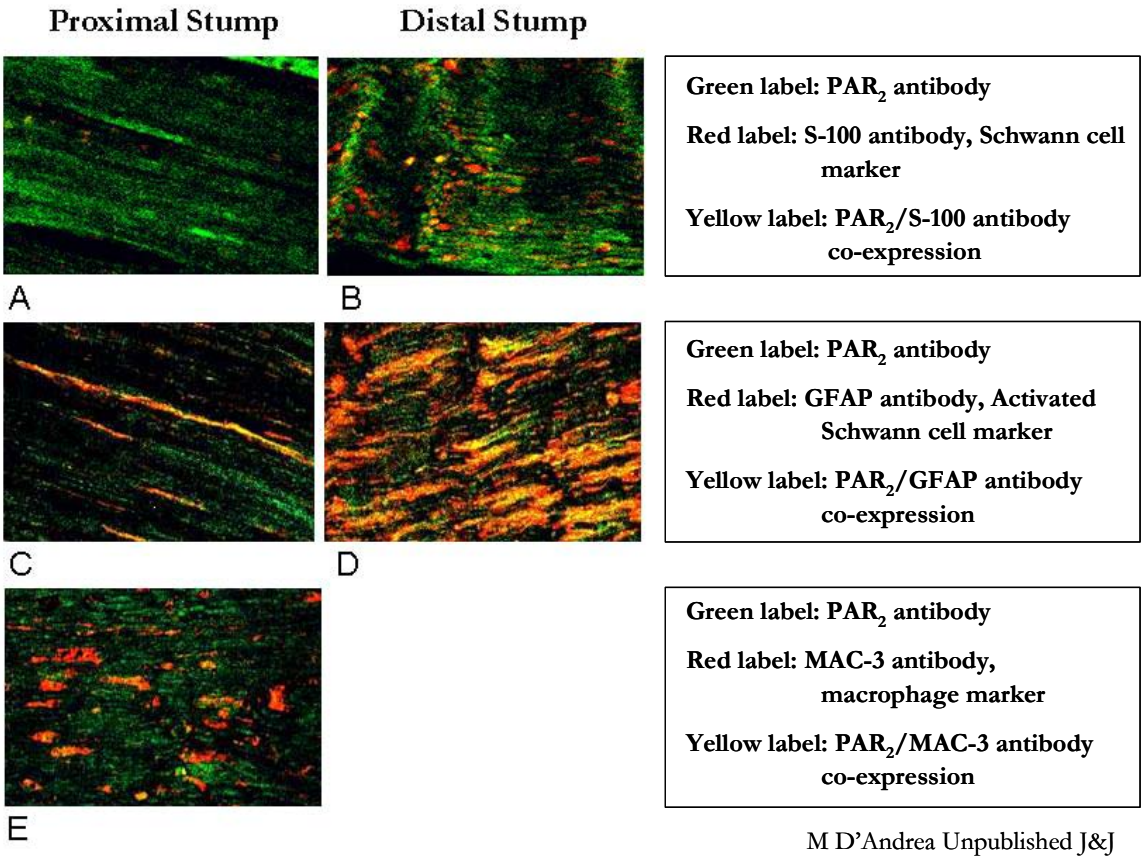

Figure 7-1. PAR_2 Expression in Proximal (A, C) and Distal (B, D, E) Sciatic Nerve Tissue Following a Sciatic Nerve Crush

Proximal (A,C) and distal (B,D,E) sciatic nerve tissues isolated from sciatic nerve crush mice, 4-weeks post-crush injury. Yellow-orange fluorescence indicates co-localization of PAR_2 antibody and one of the Schwann cell markers (S-100, or GFAP), or the macrophage marker (MAC-3).

7.3.2 Effects of SLIGRL-Sciatic Nerve Conditioned Media on PC12 Neurite Outgrowth

SLIGRL-SNCM (SLIGRL 100μM or SLIGRL 20μM) did not significantly increase the percentage of cells with neurite outgrowth when compared to conditioned media (CM) alone or when compared to the reverse peptide control, LRGILS-sciatic nerve conditioned media (Figure 7-2A). Similarly, no significant difference was seen in the average neurite lengths among the groups, non-CM, CM, LR100μM-CM, SL100μM, and SL100μM (Figure 7-2B). The percentage of cells with neurite outgrowth ranged from a minimum of 0.4% $\pm$ SEM 0.2 in PC12 cells treated with non-conditioned media to a maximum of 1.6% $\pm$ SEM 0.4 in PC12 cells treated with SNCM. Average neurite length ranged from a minimum of 3.9μm $\pm$ SEM 1.9 in PC12 cells treated with non-conditioned media to a maximum of 13.0μm $\pm$ SEM 2.7 in PC12 cells treated with LRGILS-conditioned media.

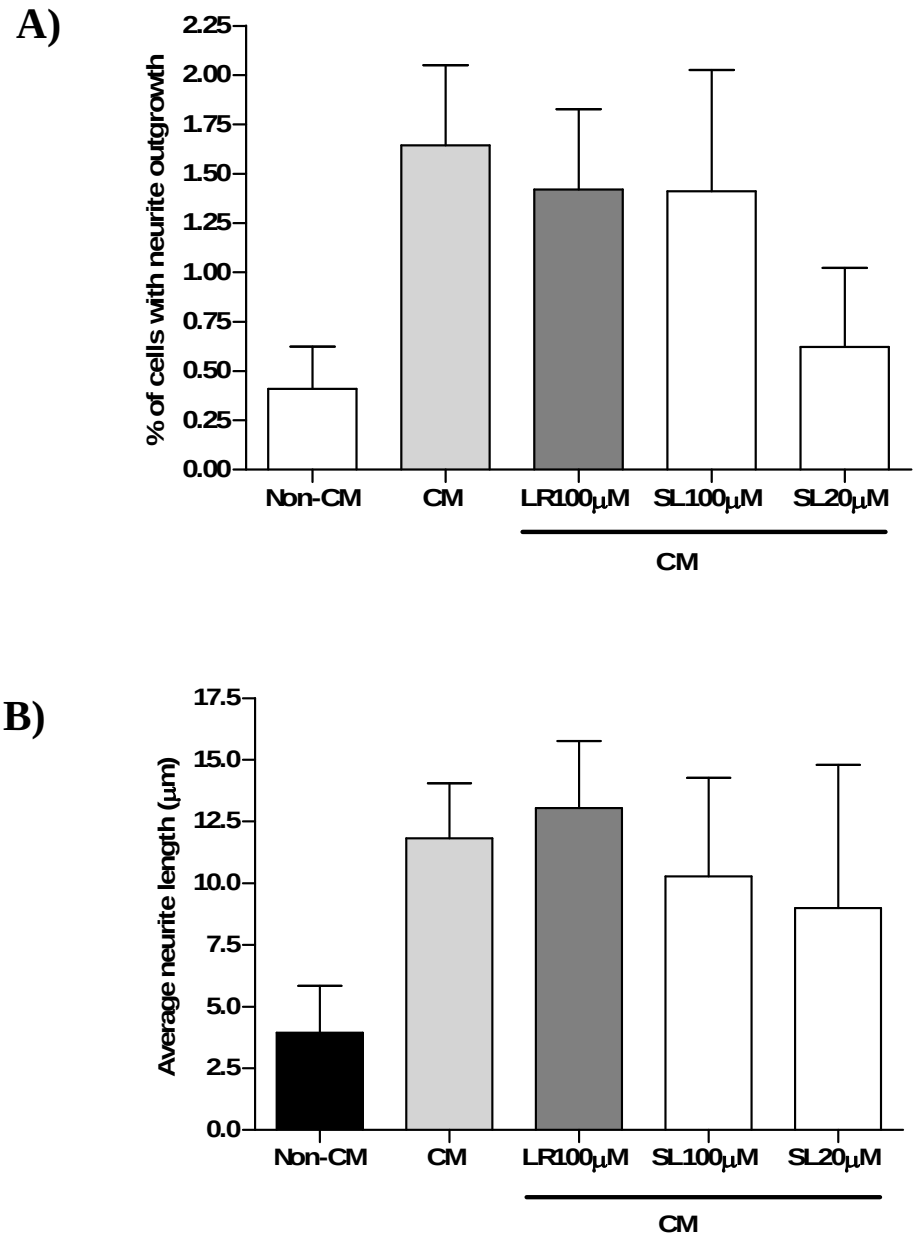

Figure 7-2. Measurement of Neurite Outgrowth in PC12 Cells Incubated with Sciatic Nerve Conditioned or Non-conditioned Media

PC12 cells incubated 72 hours in sciatic nerve conditioned media or non-conditioned media. Percentage of cells with neurite outgrowth (A) and average neurite length (B) were evaluated for the neurite outgrowth assay. Data were expressed as mean ± SEM.

7.3.3 Promotion of Neurite Outgrowth in PC12 by Sciatic Nerve Conditioned Media Co-incubated with NGF and PAR_2 Agonist

NGF-SLIGRL-SNCM did significantly increase the percentage of cells with neurite outgrowth at the 100μM SLIGRL concentration in comparison to the NGF-SCNM (17.5% ± SEM 2.3, n=10 vs. 27.7% ± SEM 4.1, n=9) (Figure 7-3A). However, when the PC12 cells were incubated with the NGF-SLIGRL-SNCM at a lower concentration of SLIGRL (20μM), the percentage of PC12 cell neurite outgrowth was not significantly different from the PC12 cell treated with NGF-SNCM alone. Similarly, in the PC12 cells treated with the control peptide LRGILS (100μM), there was no significant difference in the percentage of cells with neurite outgrowth when compared to the PC12 cells treated with NGF-SNCM (Figure 7-3A). When the average neurite lengths were compared among the groups, no significant differences were seen (Figure 7-3B).

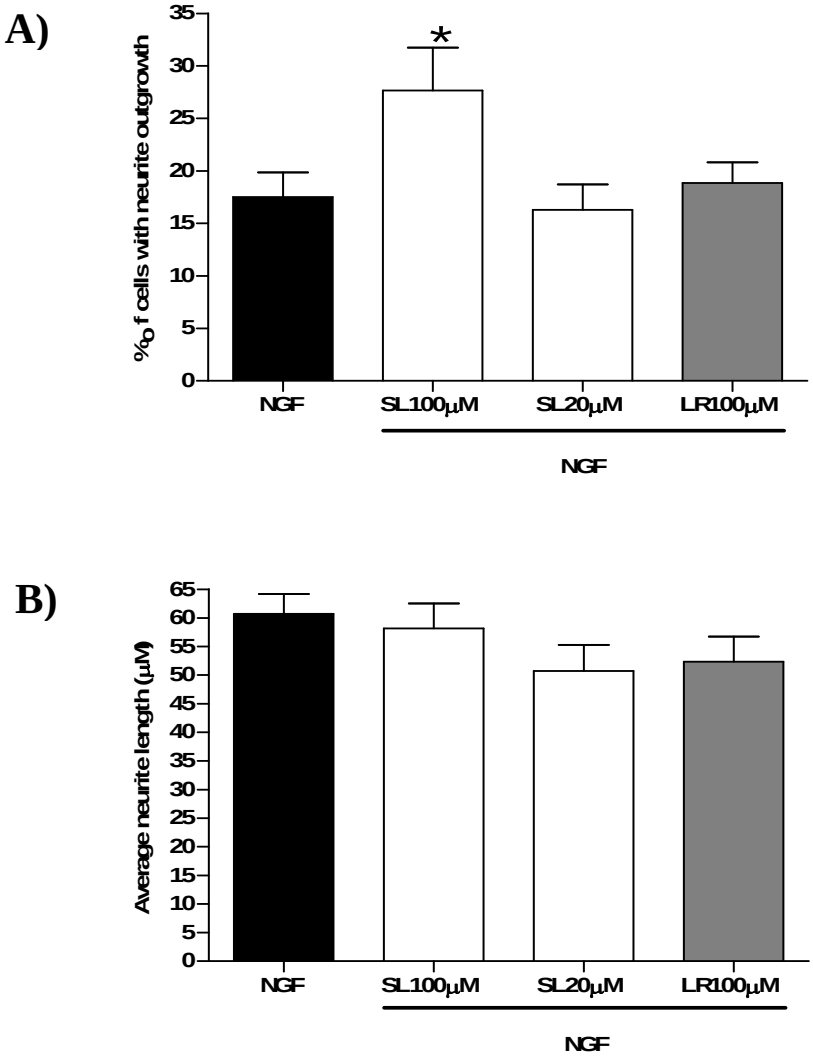

Figure 7-3. Measurement of Neurite Outgrowth in PC12 Cells Incubated with Sciatic Nerve Conditioned Media Treated with NGF alone or NGF in the presence of SLIGRL or LRGILS

PC12 cells incubated in conditioned media for 72 hours. Percentage of cells with neurite outgrowth (A) and average neurite length (B) were evaluated for the neurite outgrowth assay. Data were expressed as mean ± SEM; *means values were significantly different for $p < 0.05$, when compared to the NGF alone.

7.3.4 PAR_2 mRNA Expression in Schwann Cells

As seen in Figure 7-4, PAR_2 mRNA expression (549bp) was detected in SCs isolated from the sciatic nerve of the C57Bl/6 wild-type mice. NGF mRNA, used as a positive indicator of SCs was detected at 480bp. The housekeeping gene, GADPH, located at 306bp was used as the internal positive control. GAPDH was the house-keeping gene used as an internal positive control and was located at the 306bp level.

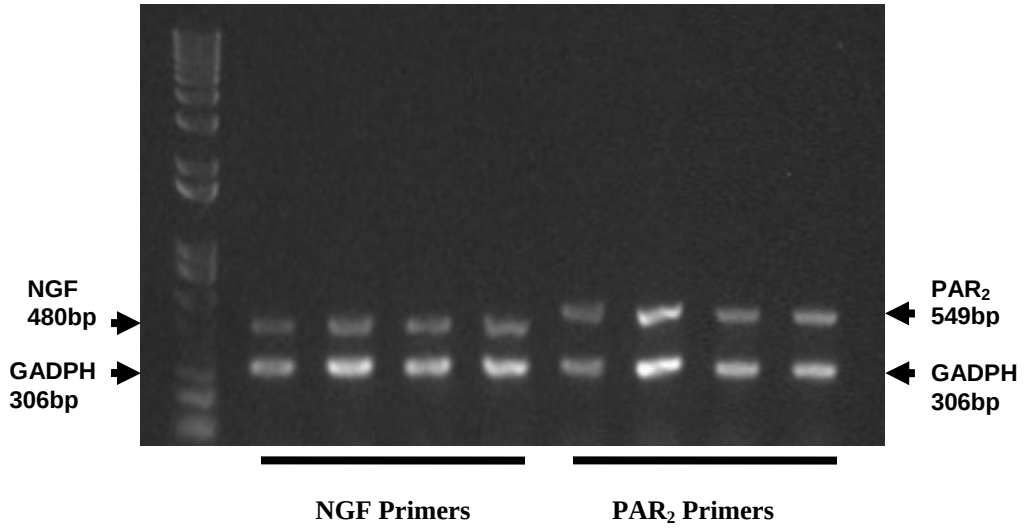

Figure 7-4. PAR_2 mRNA Expression in Isolated Mouse Schwann Cells

NGF mRNA expression was detected at 480bp (n = 4). PAR_2 mRNA expression was detected at 549bp (n = 4).

7.3.5 PAR_2 Protein Expression in Mouse Schwann Cells

PAR_2 protein expression was detected in isolated SCs fixed on collagen coated plates using a primary anti-PAR_2 goat polyclonal antibody (1:500) and a donkey anti-goat secondary antibody conjugated with an Alexa Fluor dye (1:5000) (Figure 7-5). No emission signal detected in the negative control group, which was not incubated with primary antibody.

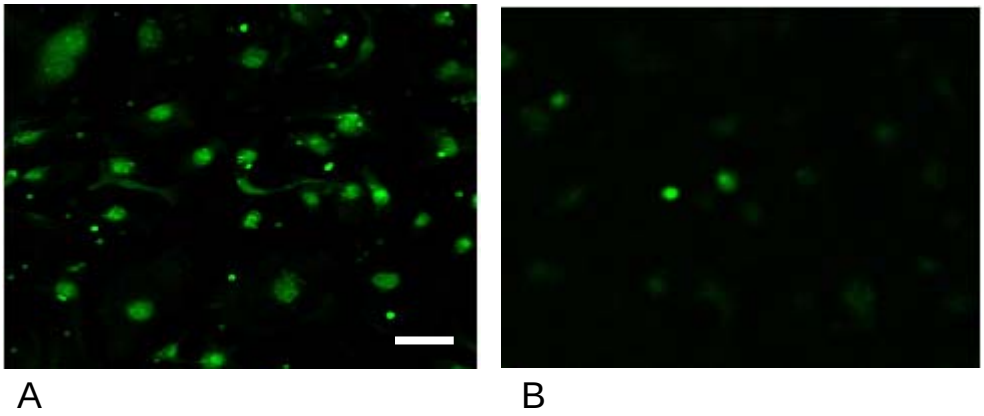

Figure 7-5. PAR_2 Protein Expression in Mouse Schwann Cells
(A) Detection of PAR_2 protein in SC (primary anti-PAR_2 antibody 1:500 (n=4); secondary anti goat antibody 1:5000), scale bar 20μm. (B) Negative control (no primary; secondary anti-goat antibody 1:5000) (n=4)

7.4 Discussion

From the *in vivo* studies, it was seen that local injection of the PAR_2-AP, SLIGRL promoted peripheral nerve regeneration. As PAR_2 activation by SLIGRL did not appear to have a direct role in neurite outgrowth, it was proposed that PAR_2 may have an indirect role in nerve regeneration and neurite outgrowth by signalling through another cell type. As mentioned in the study introduction, SCs are known to play an important

role in nerve regeneration and neurite outgrowth. As such, the present experiments attempted to investigate the potential relationship between PAR_2 protein activation and SCs.

Following the sciatic nerve crush experiments, tissue collected for PAR_2 protein expression studies showed that PAR_2 protein expression is most dominant in the distal stump and is strongly co-localized with activated SCs. What this result demonstrates is that following the induction of injury, activation of SCs in the distal stump correlates with an upregulation of PAR_2 protein expression. Additionally, the primary SC culture confirmed that PAR_2 was expressed in SCs. PAR_2 mRNA was detected using RT-PCR followed by gel electrophoresis and PAR_2 protein was also detected with fluorescent immunocytochemistry in mouse isolated SC primary cultures.

Prior to starting a long and in-depth investigation with SCs, it was deemed advantageous to take an initial approach looking at PAR_2 activation and sciatic nerve tissue, which is abundantly rich in SCs. Because SLIGRL alone did not appear to play a role in PC12 cell differentiation and neurite outgrowth, the PC12 cells were used as a neurite outgrowth indicator cell line for the media collected from the sciatic nerve tissue incubated in SLIGRL. SLIGRL-SNCM did not significantly increase the percentage of cells with neurite outgrowth and the average neurite length in comparison to the PC12 incubated with non-conditioned media. These observations are in contrast to the observations made in the Villegas study, which showed that SNCM increased PC12 cell neurite outgrowth in comparison to non-conditioned media. However, there are a variety of dissimilarities

between the Villegas study [101] and our experiments that may explain the differences. In the Villegas study, tissue was isolated from rat sciatic nerve and 8 sets of sciatic nerve were cultured in 6mLs of serum free-media. In contrast, this study used mouse sciatic nerve and 1 set of sciatic nerve was incubated in 1mL of serum-free media. Thus, in these experiments less tissue was aliquoted to each millilitre of media; thereby, most likely diluting the concentration of potential neurotrophic factors available to the PC12 cells.

Interestingly, in the presence of NGF-SLIGRL-SNCM, an increase in the percentage of cells with neurite outgrowth was seen in comparison to the PC12 cells that were treated with NGF-SNCM alone. Explanation for this phenomenon may lie in the data observed in earlier experiments. Recall that PAR_2 protein was detected in primary SC cultures and histological data collected from mice 4 weeks post-sciatic nerve crush revealed that PAR_2 protein was highly co-localized with activated SCs in the distal sciatic nerve stumps. Furthermore, although inhibiting neurite length in PC12 cells, data from the NGF-SLIGRL co-incubation PC12 neurite outgrowth assay demonstrated that PAR_2 activation can interact with NGF influencing PC12 neurite outgrowth. Therefore, an increase in the PC12 cell neurite outgrowth due to incubation in NGF-SLIGRL-SNCM suggests that in the presence of NGF, PAR_2 activation in cell-types located in the sciatic nerve can indirectly promote peripheral nerve regeneration. Additional support for PAR_2 activation in SCs to promote neurite outgrowth in PC12 cells and against activation on other cells types such as macrophages, resides in the sciatic nerve tissue isolation technique used for the SNCM. Specifically, in the media conditioned with sciatic nerve, tissue was immediately excised from the mice in the absence of nerve injury. Therefore, it is highly

unlikely that macrophages could have infiltrated the tissue prior to excision and thus, macrophages would not likely be present in the conditioned media.

However, the complex relationship and differences between PAR_2 activation on neurons and PAR_2 activation on supporting cells, such as Schwann cells should be addressed. Recall the data observed in the PC12 neurite outgrowth assay with NGF and SLIGRL in chapter 6, section 6.3.2. In this set of experiments, the NGF-induced PC12 neuronal differentiation is seen to be inhibited in the presence of the PAR_2-AP, SLIGRL. It has been previously documented that NGF degradation is a slow process strictly determined by receptor-mediated binding and uptake [102]. According to radio-labeled NGF protein degradation studies in PC12 cells, extensive NGF proteolytic degradation is a slow process; over a 24 hour period, less than 10% of the radio-labeled NGF present was degraded to a trichloroacetic acid soluble form and over a 7 day period, less than 50% degradation occurred. Therefore, it can speculated that if there was still PAR_2 agonist and NGF present in the media when the media was collected after the 24 hour sciatic nerve incubation period, the inhibitory effect of SLIGRL on NGF-induced PC12 neuronal differentiation could have still affected the pro-regenerative effects of PAR_2 activation on supporting cells present in the sciatic nerve tissue.

Nonetheless, a significant increase in the percentage of cell with neurite outgrowth was seen in the PC12 incubated with SLIGRL-NGF-sciatic nerve media, which confirms the *in vivo* data collected from previous studies (Chapter 3), which demonstrated that local PAR_2 activation can promote peripheral nerve regeneration following nerve injury.

Therefore, overall in a complex system such as the whole animal, PAR_2 activation promotes peripheral nerve regeneration.

Chapter 8: Major Findings, Conclusions and Future Directions

8.1 Major Findings and Conclusions

I. *In vivo* PAR_2 activation by local daily injection of SLIGRL was observed to have a pro-regenerative function, which was indicated by the faster rate of recovery in nociceptive function, motor function and increased myelinated fibre calibre using two murine models of peripheral nerve injury.

II. The role of PAR_2 activation is dependent on the severity of the peripheral nerve injury. In sciatic nerve crush injuries, PAR_2 activation reduced the duration of the hyperalgesic response that accompanied the peripheral nerve injury, thereby reducing the time need to recover back to normal (basal) mechanical nociceptive scores. In sciatic nerve transection injuries, PAR_2 activation simply appeared to promote peripheral nerve regeneration by reducing the time required to return back to baseline levels.

III. In $PAR_2^{(-/-)}$ mice, the absence of PAR_2 resulted in a heightened nociceptive response in thermal and mechanical nociception suggesting that PAR_2 may have a protective role in reducing nerve injury-induced nociceptive responses.

IV. PAR_2 activation by SLIGRL in a primary neuronal culture isolated from murine DRG, exhibited a significant increase in the percentage of cells with neurite outgrowth compared to the negative control groups, thereby confirming the pro-regenerative function seen with the with *vivo* observations.

V. Specific PAR_2 activation by the PAR_2 agonist, SLIGRL, in the primary neuronal culture was confirmed by the using neurons isolated from DRGs of PAR_2-deficient mice.

VI. PAR_2 mRNA and protein expression was detected in the PC12 neuronal cell line. However, PAR_2 activation in PC12 cells does not appear to promote PC12 neuronal differentiation and neurite outgrowth.

VII. PAR_2 activation by SLIGRL in the presence of low concentrations of NGF inhibits PC12 cell neurite outgrowth. Micromolar concentrations of SLIGRL ranging from 100μM to 1μM significantly decreased average neurite length compared to control peptide-treated cells.

VIII. PAR_2 protein expression was found to be co-localized with activated SCs in the murine sciatic nerve distal stump following sciatic nerve injury. PAR_2 mRNA and protein expression was detected in primary SCs isolated from murine sciatic nerve.

IX. PAR_2 activation in sciatic nerve culture media in the presence of NGF, significantly increases the percentage of PC12 neurite outgrowth, suggesting that PAR_2 activation can promote peripheral nerve regeneration indirectly by activating cells in the sciatic nerve, apart from the neurons itself.

Although much more research needs to be dedicated to this topic, our studies have demonstrated that PAR_2 activation in the peripheral nervous system does participate in nerve regeneration and repair following nerve injury. Evidence for this claim is strongly

supported by both the *in vivo* and *in vitro* murine models of nerve injury and neurite outgrowth.

The relationship between all of the components of the peripheral nervous system proves to be very important to the balance and beauty of the PAR_2 receptor's participation in peripheral nerve regeneration. As it was reflected in the last few sets of experiments, deciphering the ability for PAR_2 to aid in peripheral nerve regeneration is complicated when the components of the peripheral nervous system are separated. As such, this delicate balance between the different components of the peripheral nervous system combined with this multifunctional receptor proves this topic to be even more challenging and intriguing to investigate.

8.2 Future Directions

The contrasting neuronal responses due to activation of PAR_2 on different cell types and conditions are quite quintessential of this particular receptor. In studies examining the role of PAR_2 in TNBS colitis, researchers have documented the dual role of the PAR_2 receptor; in some conditions the receptor is pro-inflammatory and in other conditions the receptor is anti-inflammatory. Similarly, researchers studying the role of PAR_2 in the central nervous system have identified the receptor to be both neurodegenerative [103] and neuroprotective [72, 104].

Nevertheless, if the role of PAR_2 is to be fully understood in the context of peripheral nerve regeneration, it is absolutely necessary to carry out further experiments. The most

interesting, but also the most puzzling observation was the contrast in PAR_2 activation and response of different cell types under different conditions. From this study PAR_2 is proposed to be pro-regenerative due to PAR_2 activation on the supporting cells of the nervous system. However, it has yet to be proven where exactly PAR_2 activation is occurring and what signaling mechanism is being activated to elicit these effects. First, it is recommended that future studies investigate the PAR_2 functionality in SCs, by testing Ca^{2+} signaling responses for instance, but also activation of other signaling pathways, which may involve PKC, or MAPK. Second, it would be advantageous to attempt to identify potential molecules or mechanisms that would contribute to peripheral nerve regeneration and neurite outgrowth. Some direct mechanisms that may be involved in PAR_2 induced neurite outgrowth may include upregulation and secretion of neurotrophins such as NGF, BDNF, or CNTF. On the other hand, indirect signaling pathways triggered by the PAR_2 receptor may be involved in promoting neurite outgrowth by potentiating other signals through receptor phosphorylation such as the NGF-trkA receptor interaction. Finally, once the SCs are more clearly characterized, it would be useful to see if PAR_2 activation on SCs could promote neurite outgrowth in purified primary neurons through the signaling of one of these identified mechanisms. Further studies into the role of PAR_2 activation and peripheral nerve regeneration may give us a better understanding into the unknown mechanisms and signaling pathways of nerve regeneration. With this new found knowledge into the role of PAR_2 activation and peripheral nerve regeneration, future studies may provide us with new insights and novel resources for studying central nervous system injuries.

References

1. *National Trauma Registry. Injury statistics in Canada 2005 Report*. 2006, Canadian Institute for Health Information Ottawa, Ontario. p. 123.
2. Matsuyama, T., Mackay M, Midha R. , *Peripheral nerve repair and grafting techniques: a review.* Neurol Med Chir (Tokyo). 2000. **40**(4): p. 187-99.
3. Seddon, H., *Three types of nerve injury*. Brain 1943. **66**: p. 237-288.
4. Lundborg, G., *Nerve injury and repair* 1988, New York: Churchill Livingstone.
5. Raffe, M., *Biology of Nerve Repair and Regeneration.* Text book of Small Animal Orthopaedics, ed. C.N.a.D. Nunamaker. 1985, Ithaca, New York, USA: International Veterinary Information Service.
6. Levy, D., P. Kubes, and D.W. Zochodne, *Delayed peripheral nerve degeneration, regeneration, and pain in mice lacking inducible nitric oxide synthase.* J Neuropathol Exp Neurol, 2001. **60**(5): p. 411-21.
7. Reichert, F., A. Saada, and S. Rotshenker, *Peripheral-Nerve Injury Induces Schwann-Cells to Express 2 Macrophage Phenotypes - Phagocytosis and the Galactose-Specific Lectin Mac-2.* Journal of Neuroscience, 1994. **14**(5): p. 3231-3245.
8. Perry, V.H., M.C. Brown, and S. Gordon, *The Macrophage Response to Central and Peripheral-Nerve Injury - a Possible Role for Macrophages in Regeneration.* Journal of Experimental Medicine, 1987. **165**(4): p. 1218-1223.
9. Acheson, A., et al., *Detection of brain-derived neurotrophic factor-like activity in fibroblasts and Schwann cells: inhibition by antibodies to NGF*. Neuron, 1991. **7**(2): p. 265-75.
10. Heumann, R., et al., *Changes of Nerve Growth-Factor Synthesis in Nonneuronal Cells in Response to Sciatic-Nerve Transection.* Journal of Cell Biology, 1987. **104**(6): p. 1623-1631.
11. Sendtner, M., K.A. Stockli, and H. Thoenen, *Synthesis and localization of ciliary neurotrophic factor in the sciatic nerve of the adult rat after lesion and during regeneration.* J Cell Biol, 1992. **118**(1): p. 139-48.
12. Bixby, J.L., J. Lilien, and L.F. Reichardt, *Identification of the major proteins that promote neuronal process outgrowth on Schwann cells in vitro.* J Cell Biol, 1988. **107**(1): p. 353-61.
13. Wong, B.J. and D.E. Mattox, *Experimental nerve regeneration. A review.* Otolaryngol Clin North Am, 1991. **24**(3): p. 739-52.
14. Rutishauser, U., *Adhesion molecules of the nervous system.* Curr Opin Neurobiol, 1993. **3**(5): p. 709-15.
15. Grafstein, B., *The nerve cell body response to axotomy.* Exp Neurol, 1975. **48**(3 pt. 2): p. 32-51.
16. Lieberman, A.R., *The axon reaction: a review of the principal features of perikaryal responses to axonal injury.* Int Rev Neurobiol, 1971. **14**: p. 99-124.
17. Varon, S. and R. Adler, *Nerve growth factors and control of nerve growth.* Curr Top Dev Biol, 1980. **16**: p. 207-252.

18. Varon, S. and S.D. Skaper, *In vitro responses of sympathetic neurons to nerve growth factor and other macromolecular agents.* Ciba Found Symp, 1981. **83**: p. 151-76.
19. Harper, G.P. and H. Thoenen, *Nerve Growth-Factor - Biological Significance, Measurement, and Distribution.* Journal of Neurochemistry, 1980. **34**(1): p. 5-16.
20. Levi-Montalcini, R., *Effects of mouse tumor transplantation on the nervous system.* Annals of the New York Academy of Sciences, 1952. **55**: p. 330-348.
21. Shooter, E.M., et al., *Biosynthesis and mechanism of action of nerve growth factor.* Recent Prog Horm Res, 1981. **37**: p. 417-46.
22. Purves, D. and A. Nja, *Effect of Nerve Growth-Factor on Synaptic Depression after Axotomy.* Nature, 1976. **260**(5551): p. 535-536.
23. Saika, T., et al., *Effects of nerve crush and transection on mRNA levels for nerve growth factor receptor in the rat facial motoneurons.* Brain Res Mol Brain Res, 1991. **9**(1-2): p. 157-60.
24. Meyer, M., et al., *Enhanced synthesis of brain-derived neurotrophic factor in the lesioned peripheral nerve: different mechanisms are responsible for the regulation of BDNF and NGF mRNA.* J Cell Biol, 1992. **119**(1): p. 45-54.
25. Levi-Montalcini, R. and V. Hamburger, *A diffusable agent of mouse sarcoma producing hyperplasia of sympathetic ganglia and hypernemotization of viscera in the chick embryo.* J Exp Zool, 1953. **123**: p. 233-278.
26. Rende, M., et al., *Immunolocalization of Ciliary Neuronotrophic Factor in Adult-Rat Sciatic-Nerve.* Glia, 1992. **5**(1): p. 25-32.
27. Hansson, H.A., et al., *Evidence indicating trophic importance of IGF-I in regenerating peripheral nerves.* Acta Physiol Scand, 1986. **126**(4): p. 609-14.
28. Dery, O., et al., *Proteinase-activated receptors: novel mechanisms of signaling by serine proteases.* Am J Physiol, 1998. **274**(6 Pt 1): p. C1429-52.
29. Vergnolle, N., M.D. Hollenberg, and J.L. Wallace, *Pro- and anti-inflammatory actions of thrombin: a distinct role for proteinase-activated receptor-1 (PAR1).* Br J Pharmacol, 1999. **126**(5): p. 1262-8.
30. Vergnolle, N., et al., *Protease-activated receptors in inflammation, neuronal signaling and pain.* Trends Pharmacol Sci, 2001. **22**(3): p. 146-52.
31. Carney, D.H., et al., *Enhancement of incisional wound healing and neovascularization in normal rats by thrombin and synthetic thrombin receptor-activating peptides.* J Clin Invest, 1992. **89**(5): p. 1469-77.
32. Stiernberg, J., et al., *The role of thrombin and thrombin receptor activating peptide (TRAP-508) in initiation of tissue repair.* Thromb Haemost, 1993. **70**(1): p. 158-62.
33. Chambers, R.C., et al., *Thrombin is a potent inducer of connective tissue growth factor production via proteolytic activation of protease-activated receptor-1.* J Biol Chem, 2000. **275**(45): p. 35584-91.
34. Vu, T.K., et al., *Molecular cloning of a functional thrombin receptor reveals a novel proteolytic mechanism of receptor activation.* Cell, 1991. **64**(6): p. 1057-68.
35. Hollenberg, M., Laniyonu AA, Saifeddine M, Moore GJ., *Role of the amino- and carboxyl-terminal domains of thrombin receptor-derived polypeptides in*

biological activity in vascular endothelium and gastric smooth muscle: evidence for receptor subtypes. Mol Pharmacol, 1993. **43**(6): p. 921-30.

36. Nystedt, S., et al., *Molecular-Cloning of a Potential Proteinase Activated Receptor.* Proceedings of the National Academy of Sciences of the United States of America, 1994. **91**(20): p. 9208-9212.
37. Barnes, J., Singh, S, Gomes, AV, *Protease activated receptors in cardiovascular function and disease.* Molecular and Cellular Biochemistry 2004. **263**: p. 227–239.
38. Molino, M., et al., *Interactions of mast cell tryptase with thrombin receptors and PAR-2.* Journal of Biological Chemistry, 1997. **272**(7): p. 4043-4049.
39. Uehara, A., Sugawara, S, Muramoto, K, Takada, H., *Activation of human oral epithelial cells by neutrophil proteinase 3 through protease-activated receptor-2.* J Immunol., 2002. **169**(8): p. 4594-603.
40. Camerer, E., W. Huang, and S.R. Coughlin, *Tissue factor- and factor X-dependent activation of protease-activated receptor 2 by factor VIIa.* Proc Natl Acad Sci U S A, 2000. **97**(10): p. 5255-60.
41. Takeuchi, T., Harris, JL, Huang, W, Yan, KW, Coughlin, SR, Craik, CS., *Cellular localization of membrane-type serine protease 1 and identification of protease-activated receptor-2 and single-chain urokinase-type plasminogen activator as substrates.* J Biol Chem, 2000. **275(**34): p. 26333-42.
42. Corvera, C., Dery O, McConalogue K, Bohm SK, Khitin LM, Caughey GH, Payan DG, Bunnett NW., *Mast cell tryptase regulates rat colonic myocytes through proteinase-activated receptor 2.* J Clin Invest., 1997. **100**(6): p. 1383-93.
43. Kong, W., K. McConalogue, L.M. Khitin, M.D. Hollenberg, D.G. Payan, S.K. Bohm, and N.W. Bunnett, *Luminal trypsin may regulate enterocytes through proteinase-activated receptor 2.* Proc. Natl. Acad. Sci. USA, 1997. **Vol. 94**: p. 8884-8889
44. DeFea, K., Zalevsky, J, Thoma, MS, Dery, O, Mullins, RD, Bunnett, NW., *beta-arrestin-dependent endocytosis of proteinase-activated receptor 2 is required for intracellular targeting of activated ERK1/2.* J Cell Biol, 2000. **148**(6): p. 1267-81.
45. Sawada, K., Nishibori M, Nakaya N, Wang Z, Saeki K. , *Purification and Characterization of a Trypsin-Like Serine Proteinase from Rat Brain Slices that Degrades Laminin and Type IV Collagen and Stimulates Protease-Activated Receptor-2.* J Neurochem, 2000. **74**(4): p. 1731-8.
46. Sun, G., Stacey MA, Schmidt M, Mori L, Mattoli S., *Interaction of mite allergens Der p3 and Der p9 with protease-activated recptor-2 expressed by lung epithelial cells.* . J Immunol., 2001. **167**(2): p. 1014-21.
47. Lourbakos, A., Chinni C, Thompson P, Potempa J, Travis J, Mackie EJ, Pike RN., *Cleavage and activation of proteinase-activated receptor-2 on human neutrophils by gingipain-R from Porphyromonas gingivalis.* FEBS Lett., 1998. **435**(1): p. 45-8.
48. Miki, M., Nakamura Y, Takahashi A, Nakaya Y, Eguchi H, Masegi T, Yoneda K, Yasuoka S, Sone S. , *Effect of human airway trypsin-like protease on intracellular free Ca2+ concentration in human bronchial epithelial cells.* J Med Invest, 2003. **50**(1-2): p. 95-107.

49. Angelo, P., Lima AR, Alves FM, Blaber SI, Scarisbrick IA, Blaber M, Juliano L, Juliano MA. , *Substrate specificity of human kallikrein 6: salt and glycosaminoglycan activation effects.* J Biol Chem, 2006. **281**(6): p. 3116-26.
50. Oikonomopoulou, K., Hansen KK, Saifeddine M, Vergnolle N, Tea I, Blaber M, Blaber SI, Scarisbrick I, Diamandis EP, Hollenberg MD. , *Kallikrein-mediated cell signalling: targeting proteinase-activated receptors (PARs).* Biol Chem 2006. **387**(6): p. 817-24.
51. Nystedt, S., et al., *The Mouse Proteinase-Activated Receptor-2 Cdna and Gene - Molecular-Cloning and Functional Expression.* Journal of Biological Chemistry, 1995. **270**(11): p. 5950-5955.
52. Smith, R., Jenkins A, Lourbakos A, Thompson P, Ramakrishnan V, Tomlinson J, Deshpande U, Johnson DA, Jones R, Mackie EJ, Pike RN. , *Evidence for the activation of PAR-2 by the sperm protease, acrosin: expression of the receptor on oocytes.* FEBS Lett., 2000. **484**(3): p. 285-90.
53. Alm, A., Gagnemo-Persson R, Sorsa T, Sundelin J., *Extrapancreatic trypsin-2 cleaves proteinase-activated receptor-2.* Biochem Biophys Res Commun, 2000. **275**(1): p. 77-83.
54. Cottrell, G., Amadesi, S, Grady, EF, Bunnett, NW., *Trypsin IV, a Novel Agonist of Protease-Activated Receptors 2 and 4.* The Journal of Biological Chemistry 2004. **279**(14): p. 13532-13539.
55. McGuire, J.J., et al., *2-Furoyl-LIGRLO-amide: A potent and selective proteinase-activated receptor 2 agonist.* Journal of Pharmacology and Experimental Therapeutics, 2004. **309**(3): p. 1124-1131.
56. Hollenberg, M.D., *Physiology and pathophysiology of proteinase-activated receptors (PARs): proteinases as hormone-like signal messengers: PARs and more.* J Pharmacol Sci, 2005. **97**(1): p. 8-13.
57. Bohm, S.K., et al., *Molecular cloning, expression and potential functions of the human proteinase-activated receptor-2.* Biochem J, 1996. **314 (Pt 3)**: p. 1009-16.
58. Rickard, A., and J. McHowat, *Phospholipid metabolite production in human urothelial cells after protease-activated receptor cleavage.* Am J Physiol Renal Physiol, 2002. **52**: p. F944-F951.
59. Steinhoff, M., et al., *Proteinase-activated receptor-2 in human skin: tissue distribution and activation of keratinocytes by mast cell tryptase.* Exp Dermatol, 1999. **8**(4): p. 282-94.
60. Smith-Swintosky, V.L., et al., *Protease-activated receptor-2 (PAR-2) is present in the rat hippocampus and is associated with neurodegeneration.* J Neurochem, 1997. **69**(5): p. 1890-6.
61. Steinhoff, M., et al., *Agonists of proteinase-activated receptor 2 induce inflammation by a neurogenic mechanism.* Nature Medicine, 2000. **6**(2): p. 151-158.
62. Nystedt, S., V. Ramakrishnan, and J. Sundelin, *The proteinase-activated receptor 2 is induced by inflammatory mediators in human endothelial cells - Comparison with the thrombin receptor.* Journal of Biological Chemistry, 1996. **271**(25): p. 14910-14915.

63. Vergnolle, N., *Proteinase-activated receptor-2-activating peptides induce leukocyte rolling, adhesion, and extravasation in vivo.* J Immunol, 1999. **163**(9): p. 5064-9.
64. Vergnolle, N., et al., *Characterization of the inflammatory response to proteinase-activated receptor-2 (PAR2)-activating peptides in the rat paw.* Br J Pharmacol, 1999. **127**(5): p. 1083-90.
65. Cenac, N., et al., *Induction of intestinal inflammation in mouse by activation of proteinase-activated receptor-2.* Am J Pathol, 2002. **161**(5): p. 1903-15.
66. Kawabata, A., Kuroda, R, Minami, T, Kataoka, K, Taneda, M, *Increased vascular permeability by a specific agonist of protease-activated receptor-2 in rat hindpaw* Br J Pharmacol, 1998. **125**(3): p. 419-22.
67. Glusa, E., Saft, A., Prasa, D., Sturzebecher, J., *Trypsin- and SLIGRL-induced vascular relaxation and the inhibition by benzamidine derivatives.* Thrombosis and haemostasis, 1997. **78**(5): p. 1399-403.
68. Nguyen, C., et al., *Colitis induced by proteinase-activated receptor-2 agonists is mediated by a neurogenic mechanism.* Can J Physiol Pharmacol, 2003. **81**(9): p. 920-7.
69. Striggow, F., et al., *Four different types of protease-activated receptors are widely expressed in the brain and are up-regulated in hippocampus by severe ischemia.* Eur J Neurosci, 2001. **14**(4): p. 595-608.
70. Takahashi, M., Liou, SY, Kunihara, M., *Ca(2+)- and Cl(-)-dependent, NMDA receptor-mediated neuronal death induced by depolarization in rat hippocampal organotypic cultures.* Brain Res., 1995. **675**(1-2): p. 249-56.
71. Siesjo, B.K., et al., *Calcium, excitotoxins, and neuronal death in the brain.* Ann N Y Acad Sci, 1989. **568**: p. 234-51.
72. Noorbakhsh, F., et al., *Proteinase-activated receptor-2 induction by neuroinflammation prevents neuronal death during HIV infection.* J Immunol, 2005. **174**(11): p. 7320-9.
73. Corvera, C.U., et al., *Thrombin and mast cell tryptase regulate guinea-pig myenteric neurons through proteinase-activated receptors-1 and-2.* Journal of Physiology-London, 1999. **517**(3): p. 741-756.
74. Reed, D.E., et al., *Mast cell tryptase and proteinase-activated receptor 2 induce hyperexcitability of guinea-pig submucosal neurons.* Journal of Physiology-London, 2003. **547**(2): p. 531-542.
75. Cenac, N., et al., *Proteinase-activated receptor-2-induced colonic inflammation in mice: possible involvement of afferent neurons, nitric oxide, and paracellular permeability.* J Immunol, 2003. **170**(8): p. 4296-300.
76. Vergnolle, N., et al., *Proteinase-activated receptor-2 and hyperalgesia: A novel pain pathway.* Nat Med, 2001. **7**(7): p. 821-6.
77. Coelho, A.M., et al., *Proteinases and proteinase-activated receptor 2: a possible role to promote visceral hyperalgesia in rats.* Gastroenterology, 2002. **122**(4): p. 1035-47.
78. Kirkup, A.J., et al., *Stimulation of proteinase-activated receptor 2 excites jejunal afferent nerves in anaesthetised rats.* J Physiol, 2003. **552**(Pt 2): p. 589-601.

79. Streit, W., Hurley, SD, McGraw, TS, Semple-Rowland, SL., *Comparative evaluation of cytokine profiles and reactive gliosis supports a critical role for interleukin-6 in neuron-glia signaling during regeneration.* J Neurosci Res., 2000. **61**(1): p. 10-20.
80. Schwartz, M., Solomon, A, Lavie, V, Ben-Bassat, S, Belkin, M, Cohen, A., *Tumor necrosis factor facilitates regeneration of injured central nervous system axons.* Brain Res, 1991. **545**(1-2): p. 334-8.
81. Mason, J., Suzuki, K, Chaplin, DD, Matsushima, GK., *Interleukin-1beta promotes repair of the CNS.* J Neurosci., 2001 **21**(18): p. 7046-52.
82. Keilhoff, G., Fansa, H, Wolf, G., *Differences in peripheral nerve degeneration/regeneration between wild-type and neuronal nitric oxide synthase knockout mice.* J Neurosci Res, 2002. **68**(4): p. 432-431.
83. Thompson, D., Buettner HM. , *Neurite outgrowth is directed by schwann cell alignment in the absence of other guidance cues.* Annals of Biomedical Engineering,, 2006. **34**(1): p. 161-8.
84. Sebert, M., Shooter EM, *Expression of mRNA for neurotrophic factors and their receptors in the rat dorsal root ganglion and sciatic nerve following nerve injury.* J Neurosci Res, 1993. **36**(4): p. 357-67.
85. Taniuchi, M., Clark HB, Johnson EM Jr. , *Induction of nerve growth factor receptor in Schwann cells after axotomy.* Proc Natl Acad Sci U S A. , 1986. **83**(11): p. 4094-8.
86. Emilsson, K., et al., *Vascular effects of proteinase-activated receptor 2 agonist peptide.* Journal of Vascular Research, 1997. **34**(4): p. 267-272.
87. Fiorucci, S., Mencarelli A, Palazzetti B, Distrutti E, Vergnolle N, Hollenberg MD, Wallace JL, Morelli A, Cirino G, *Proteinase-activated receptor 2 is an anti-inflammatory signal for colonic lamina propria lymphocytes in a mouse model of colitis.* Proc Natl Acad Sci U S A, 2001. **98**(24): p. 13936-41.
88. Griffin, C., Letourneau, PC. , *Rapid retraction of neurites by sensory neurons in response to increased concentrations of nerve growth factor.* J. Cell Biol., 1980. **86**(1): p. 156-61.
89. Levi-Montalcini R, H.V., *Selective growth stimulating effects of mouse sarcoma on the sensory and sympathetic nervous system of the chick embryo.* Journal of Experimental Zoology, 1951. **116**: p. 321-362.
90. Brain, A., and PK Moore, *Pain and Neurogenic Inflammation* Progress in Inflammation Research, ed. M. Parnham. 1999, Germany: Birkhauser
91. Sterneck, E., Kaplan, DR, Johnson, PF. , *Interleukin-6 induces expression of peripherin and cooperates with Trk receptor signaling to promote neuronal differentiation in PC12 cells.* J Neurochem, 1996. **67**(4): p. 1365-74.
92. Arthur, D., Akassoglou, K, Insel, PA, *P2Y2 receptor activates nerve growth factor/TrkA signaling to enhance neuronal differentiation.* Proc Natl Acad Sci USA, 2005. **102**(52): p. 19138-43.
93. Turgeon, V., Lloyd, ED, Wang, S, Festoff, BW, Houenou, LJ. , *Thrombin perturbs neurite outgrowth and induces apoptotic cell death in enriched chick spinal motoneuron cultures through caspase activation.* J Neurosci, 1998. **18**(17): p. 6882-91.

94. Hatanaka, H., *Nerve growth factor-mediated stimulation of tyrosine hydroxylase activity in a clonal rat pheochromocytoma cell line.* Brain Res, 1981. **222**: p. 225-233.
95. Bandtlow, C., Heumann, R, Schwab, M, and Thoenen, H, *Cellular localization of nerve growth factor synthesis by insitu hybridization.* Eur Mol Biol J, 1987. **6**: p. 891-899.
96. Friedman, B., Scherer, SS, Rudge, JS, *Regulation of ciliary neurotrophic factor expression in myelin related Schwann cells in vivo.* Neuron 1992. **9**: p. 295-305.
97. Hall, S., *Regeneration in cellular and acellular autografts in the peripheral nervous system.* Neuropathol Appl Neurobiol, 1986. **12**: p. 27-46.
98. Richardson, P., McGuinness, U and Aguayo, AJ *Axons from CNS neurons regenerate into PNS grafts.* Nature, 1980. **284**: p. 264-265.
99. Chen, Y., McDonald, D, Cheng, C, Magnowski, B, Durand, J, Zochodne, DW. , *Axon and Schwann cell partnership during nerve regrowth.* J Neuropathol Exp Neurol, 2005. **64**(7): p. 613-22.
100. Torres, P., Guilarducci, CV, Franco, AS, de Araujo, EG. , *Sciatic conditioned medium increases survival, proliferation and differentiation of retinal cells in culture.* Int J Dev Neurosci, 2002. **20**(1): p. 11-20.
101. Villegas, G.M., A.T. Haustein, and R. Villegas, *Neuronal differentiation of PC12 and chick embryo ganglion cells induced by a sciatic nerve conditioned medium: characterization of the neurotrophic activity.* Brain Res, 1995. **685**(1-2): p. 77-90.
102. Vroegop, S., Decker, D, Hinzmann, J, Poorman, R, Buxser, S., *Probing the structure-function relationship of nerve growth factor.* Journal of Protein Chemistry, 1992. **11**(1): p. 71-82.
103. Noorbakhsh, F., et al., *Proteinase-activated receptor 2 modulates neuroinflammation in experimental autoimmune encephalomyelitis and multiple sclerosis.* J Exp Med, 2006. **203**(2): p. 425-35.
104. Noorbakhsh, F., et al., *Proteinase-activated receptor-2 expression is neuroprotective in lentivirus-induced neuroinflammation.* Journal of Neuroimmunology, 2004. **154**(1-2): p. 201-201.